PHENOTYPIC AND MOLECULAR CHARACTERIZATION OF CATARACT IN THE TDRD7 KNOCKOUT MOUSE MUTANT

by

Carrie E. Barnum

A thesis submitted to the Faculty of the University of Delaware in partial fulfillment of the requirements for the degree of Master of Science in Biological Sciences

Spring 2015

PHENOTYPIC AND MOLECULAR CHARACTERIZATION OF CATARACT IN THE TDRD7 KNOCKOUT MOUSE MUTANT

by

Carrie E. Barnum

Approved: _____
Salil A. Lachke, Ph.D.
Professor in charge of thesis on behalf of the Advisory Committee

Approved: _____
Robin W. Morgan, Ph.D.
Chair of the Department of Biological Sciences

Approved: _____
George H. Watson, Ph.D.
Dean of the College of Arts and Sciences

Approved: _____
James G. Richards, Ph.D.
Vice Provost for Graduate and Professional Education

ACKNOWLEDGMENTS

I would like to thank my advisor Dr. Salil Lachke, he has been patient, helpful, understanding, critical when needed, and has always been there for me whether I knew it or not. He is a true friend as well as a true mentor and I will never forget that or stop appreciating it. I am so lucky that I was able to work with him. I know I am a better scientist because of it and he has fostered my appreciation of this field. I would like to thank my committee members, Dr. Melinda Duncan and Dr. Shawn Polson, I am sure they thought I would never graduate but they have been there for me with ideas and help throughout this process. I would like to especially thank Dr. Duncan for all her intellectual input and guidance in my times of need. I would like to thank my lab members, past and present, especially, Archana and Soma, they are the backbone of our lab and they have helped me keep focused and balanced, even when times are rocky. I would like to thank my family; they have been unwavering in their support and never stopped believing in me. I would like to thank my friends, especially Katie and Megan (I love you both). I would like to thank my dogs Pork and Beans, they are little lights that always shine in my life. Lastly, I would like to thank all of the animals used for this thesis.

TABLE OF CONTENTS

Appendix

LIST OF TABLES

LIST OF FIGURES

ABSTRACT

Although there are an estimated fifteen hundred genes encoding RNA binding proteins (RBPs) in the human and mouse genomes - accounting for nearly seven percent of all protein coding genes - their significance to development and disease is poorly understood. It was recently demonstrated that deficiency of Tdrd7, an RBP that is also a component of cytoplasmic RNA granules, causes cataracts in human, mouse and chicken, suggesting that this protein has a critical function in lens development that is conserved in vertebrates. Tdrd7 contains three OST-HTH (Oskar-Tdrd7-Helix-Turn-Helix)/LOTUS domains and three Tudor domains that are predicted to bind RNA and methylated arginine residues within other proteins, respectively. My M.S. thesis research focuses on the detailed characterization of cataracts in *Tdrd7* targeted germline knockout (*Tdrd7-/-*) mouse mutants, which closely phenocopy the human cataract and therefore serve as a model to investigate the molecular function of this protein in the lens.

I have applied diverse approaches at the phenotypic, cellular, molecular and the systems-level to study *Tdrd7-/-* mouse mutants. I first carried out phenotypic characterization of *Tdrd7-/-* mouse mutant lenses at various stages by grid imaging under light and dark field microscopy, and histological analysis. I find that *Tdrd7-/-* mutant and control lenses are indistinguishable by these analytical methods at stage postnatal day 18 (P18). In contrast, just four days later at stage P22, 100% of the

Tdrd7-/- mutant animals tested ($n > 50$) exhibit severe lens defects and a distinct flattened iris phenotype. To gain further insight into the lens phenotype, I performed high-resolution imaging by Scanning Electron Microscopy (SEM) on mutant and control lenses. Surprisingly, P18 *Tdrd7*-/- mutant lenses that appear completely transparent and devoid of any visible defects by light microscopic or histological analyses, exhibit severe fiber cell membrane protrusion defects as revealed by SEM analysis. Together these data lead to the important conclusion that transparent mutant lenses cannot be considered normal unless subjected to high-resolution phenotypic analysis like SEM. Furthermore, these data also indicate that *Tdrd7*-/- mouse mutants exhibit lens defects at stage much earlier than was previously anticipated.

Next, I sought to gain insight into the molecular changes that result due to *Tdrd7* deficiency in mouse lens by performing next generation RNA sequencing (RNA-Seq) on P4 *Tdrd7*-/- and control lenses. I selected stage P4 for this analysis because it is prior to the earliest stage (P18) wherein lens defects are detectable by SEM in *Tdrd7*-/- mutants, and therefore would increase the possibility for detecting primary changes while minimizing the number of secondary changes detected. RNA-Seq led to the identification of 193 differentially regulated genes (DRGs) at 1.5 fold cut-offs at 2 counts per million (counts of the transcript for every million reads of sequencing) values in *Tdrd7*-/- mouse mutant lenses. Out of these DRGs, 84 are up-regulated and 109 are down-regulated in the mutant lens. To prioritize promising candidates for further analysis, I next carried out an integrated analysis on the RNA-Seq data to identify the DRGs that are linked to Tdrd7 in a protein-protein interaction

(PPI) network, and also exhibited lens expression or enrichment according to *iSyTE*. This analysis identified a regulatory cluster of candidates that is connected to Tdrd7 in the nearest neighbor analysis, and importantly 7 of these genes exhibit significantly enriched lens-expression in *iSyTE*. Interestingly, this cluster is connected to Tdrd7 through Atxn2, a known cytoplasmic RNA granule protein. Further, the cluster analysis identifies Actn2, an F-actin crosslinking protein, as a protein-protein binding partner of Atxn2 and I find *Actn2* transcripts to be significantly down-regulated in *Tdrd7-/-* mutant lens. Thus, this analysis reveals interesting interactions between two RNA granule component proteins that are highly expressed in the lens, Tdrd7 and Atxn2, with Actn2 at both the RNA and protein levels. This indicated a complex regulatory relationship between these proteins, perhaps suggestive of the importance of their function in the lens. I next analyzed lens and whole body embryonic tissue (WB) microarray datasets in *iSyTE* to gain insights into expression of the genes *Atxn2* and *Actn2* in embryonic and postnatal lens. Both genes are significantly expressed in the lens at these stages. In particular, *Actn2* expression in wild type lens is found to be sharply up-regulated between P4 and P12 stages, before being down-regulated at P20 and later stages.

These findings lead to the hypothesis that up-regulation of *Actn2* expression in early postnatal stages is critical for normal lens development, and disruption of *Actn2* up-regulation as a result of *Tdrd7* deficiency may contribute to the lens defects in *Tdrd7-/-* mutants. Because Actn2 protein is described to function in deposition of F-actin, I next tested the hypothesis that Tdrd7 deficiency results in defective F-actin

distribution and abnormal fiber cell architecture within mutant lens. I performed whole mount staining of the lens by Phallodin, which allows observation of the spatial localization of F-actin. This analysis demonstrates that F-actin distribution in lens fiber cells was abnormal, exhibiting aggregates, compared to control lens wherein fiber cells had uniform F-actin distribution. Furthermore, I next analyzed the phenotype at individual cell resolution by staining lenses with wheat germ agglutinin (WGA), a marker that allows examination of cell membranes by staining sialic acid and N-acetylglucosaminyl sugar residues. WGA staining exhibits a hexagonal pattern of fiber cells in saggital sections of normal lens tissue. In *Tdrd7-/-* lenses, the hexagonal pattern is disrupted, providing further evidence supporting a defect in fiber cell architecture.

Finally, I hypothesized that the molecular mechanism of Tdrd7-mediated regulation in the lens involves its direct binding to *Actn2* transcripts. I tested this hypothesis by performing RNA-immunoprecipitation (RIP) by Tdrd7 antibody followed by qRT-PCR for *Actn2* transcripts. Tdrd7-pulldown complexes exhibit high enrichment of *Actn2* transcripts in lens tissue. Thus, RIP experiments demonstrate that Tdrd7 functions by directly interacting with *Actn2* transcripts perhaps by stabilizing them in turn ensuring the build-up of a critical amount of Actn2 protein necessary for F-actin deposition in fiber cells.

To gain insight into which proteins are differentially expressed in *Tdrd7-/-* mutant lens, I undertook a proteomics screen and performed 2-D gel analysis followed by Mass Spectrometry (MS). This analysis identified a heat shock protein, Hspb1

(Hsp27), to be significantly down-regulated in the mutant lens. Interestingly, Hspb1 transcript is identified by RNA-Seq to be down-regulated in *Tdrd7-/-* mutant lenses. Further RIP analysis by Tdrd7 antibody indicates enrichment of Hspb1 in pulldowns, suggesting that it interacts with Tdrd7 complexes. Interestingly, Hspb1 protein in addition to being a component of RNA granules is linked to actin cytoskeletal dynamics.

Thus, my research proposes a model wherein disruption of Tdrd7 function results in reduction of Actn2 and Hspb1 and consequently in abnormal deposition of F-actin and membrane protrusion defects in fiber cells, which contribute to lens defects and cataracts.

In summary, my M.S. research provides significant new insights into the mechanism of Tdrd7 function in the mammalian lens. It achieves this through the careful characterization of the ocular phenotype coupled with the identification of molecular changes in the *Tdrd7-/-* mutant lens, which together serve to identify alterations in the fiber cell cytoskeleton that contribute to formation of cataracts. Thus, this research highlights that an integrated multi-disciplinary approach based on mouse gene-knockout mutants, high-resolution phenotypic characterization, cell biological methods, and state-of-the-art molecular analyses involving RNA-sequencing, in combination with existing information from large databases such as protein-protein interaction networks and *iSyTE*, is exceptionally effective in providing novel insights into regulatory mechanisms in tissue development. Importantly, by contributing to our understanding of the molecular mechanism of a novel RNA binding protein and RNA

granule component Tdrd7 in the lens, this research not only elucidates the various mechanistic layers in gene regulation during cell differentiation, which may find general applicability in other tissues, but also provides unique insights into the pathophysiology of the most prevalent eye disease, cataract.

INTRODUCTION

1.1 Development of the Ocular Lens

The lens of the eye is a transparent tissue that functions with the cornea to refract and focus light on the retina (Bassnett et al., 2011; Mathias et al., 2007). Photons from the focused light are then detected by specialized cells called photoreceptors within the retina and converted into signals that are replayed and interpreted by the brain as visual information, rendering us with the critical sense of sight (Bassnett et al., 2011). The lens is located in the anterior portion of the eye, behind the cornea and iris, and is supported by a clear semi-solid gel termed the vitreous body, which is located in the posterior portion of the eye along with the retina (Bassnett et al., 2011; Mathias et al., 2007).

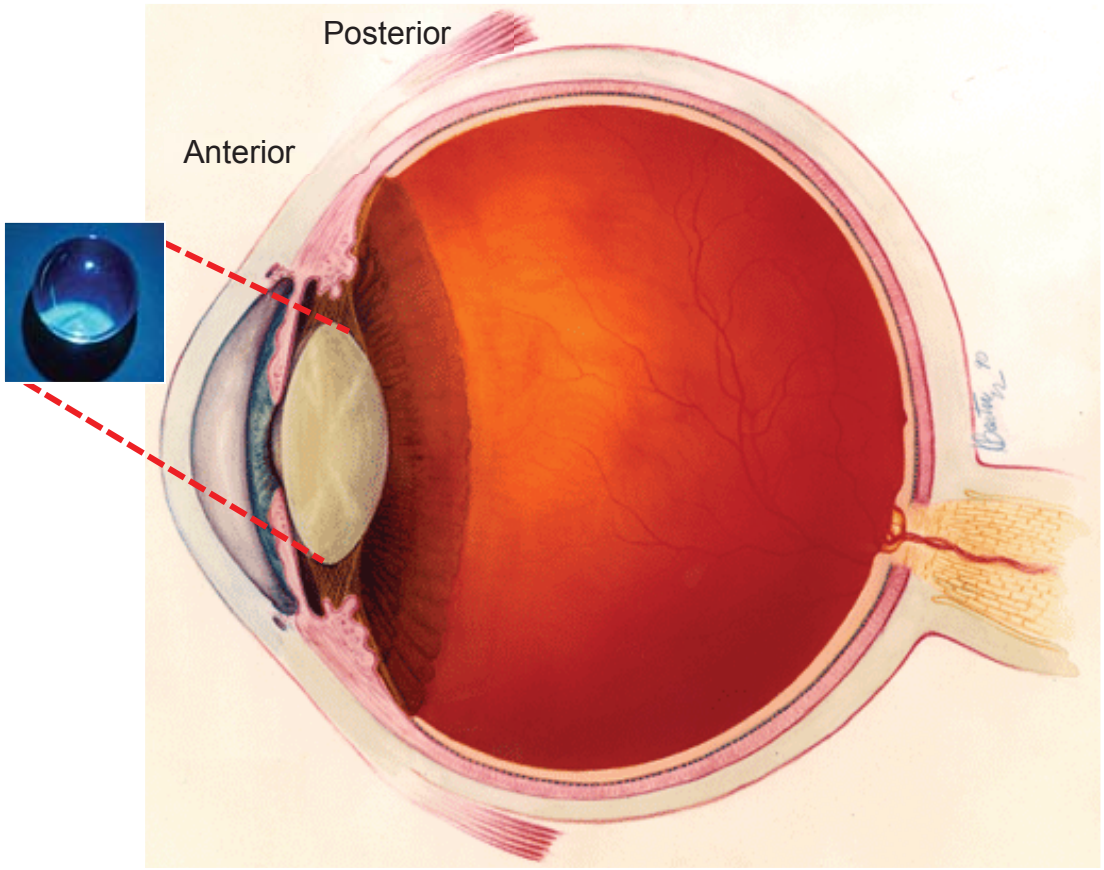

Figure 1. Anatomy of the eye. The lens is a transparent tissue located in the anterior portion of the eye called the anterior segment. The lens is situated just behind the cornea and the iris and in front of the retina, which is located in the posterior portion of the eye. The lens, together with the cornea, functions to refract and focus light onto the retina. The lens must maintain its transparency in order to sustain clear vision. (Duncan, MK 2011). NEI, (Eye)).

Eye development in mammals begins early, during late stages of gastrulation, when the ectoderm is specified into four regions that form the neural plate, neural

crest, pre-placodal region and epidermis. After the formation of neural tube, neural ectodermal tissue from either side of the forebrain forms optic vesicles – each of which later develop into the retina. Each optic vesicle extends through the surrounding mesenchyme until it contacts the surface ectoderm that will form the lens (Lovicu and Robinson 2004, Lachke Maas 2010). The optic vesicle induces the overlying (surface) ectoderm to thicken and form a structure termed the lens placode (Donner, Lachke, Maas 2006). In a classic example of co-ordinate signaling between developing tissue, the pre-lens ectoderm in turn is required for the optic vesicle to develop into the optic cup (Ashery-Padan Genes Dev 2000, Hyer J, Kuhlman J et al 2003 Dev Biol). The thickened lens placode invaginates along with the optic vesicle to forms the lens vesicle. During this process, anteriorly localized cells of the resulting lens vesicle get inverted in their orientation to the overlying surface ectoderm. At this stage, the lens vesicle is composed of anteriorly localized epithelial cells and posteriorly localized cells that will begin to differentiate into primary fiber cells (Cvekl and Piatigorsky, 1996). Also at this stage in development, lens cells begin to form a basement membrane called the lens capsule that encloses the lens tissue and is made up of laminin, Type IV collagen and fibronectin proteins (Cammarata et al., 1986, Danysh and Duncan, 2009; Yurchenco and Schittny, 1990). As lens developments proceeds, primary fiber cells elongate and fill the lens vesicle. Later during development and indeed throughout the life of the organism, cells from the anterior epithelium continue to proliferate, exit the cell cycle and differentiate into secondary fiber cells.

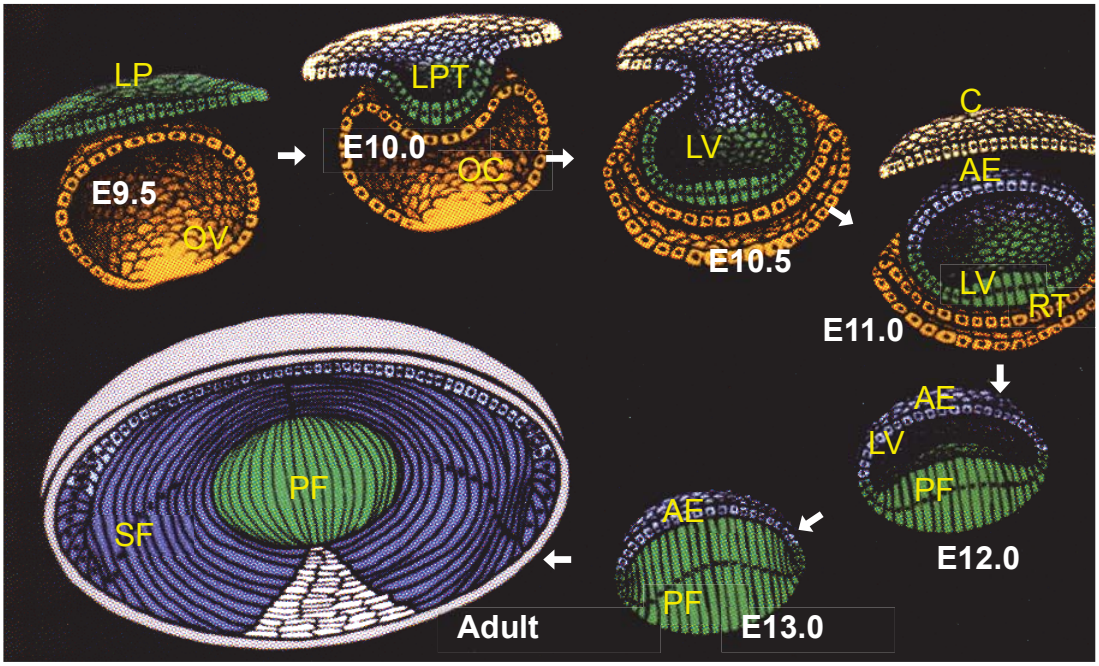

Figure 2. Eye Development in Mammals. The schematic shows the major morphological events that occur during mammalian lens development. The schematic begins from the top left and continues clockwise. Specific stages of a developing mouse embryo are indicated as follows: embryonic (E) day 9.5 represents 9 and half days after conception. These developmental events are similar among different mammals, although the exact time/day of each stage varies between different species. The process begins with the induction of the surface ectoderm by the optic vesicle (OV) into a thickened of lens placode (LP). The LP and the OV coordinately develop to form the lens pit (LPT) and optic cup (OC), respectively. Between stages E10.5-E12.0, the LPT develops into the lens vesicle (LV) in which the anteriorly localized cells and the posterior localized cells can be differentiated as anterior epithelial (AE) or primary fiber (PF) cells, respectively. Primary fiber cells elongate and differentiate to fill the vesicle (E13.0). In adult lens, cells of the anterior epithelium located near the transition zone exit the cell cycle and differentiate into secondary fiber cells (SF), a process that continues throughout the life of the animal. (Figure modified from Kuszak & Brown, 1994)

1.2 Cataract

Figure 3. Cataract: Disease of the Lens. A cataract is a clouding of the lens in the eye that affects vision. The image above serves to illustrate normal vision (left) or impaired vision due to cataract (right).

Cataract, or the opacification of the lens, is the major cause of blindness worldwide (Javitt et al., 1996; Petrash, 2013; Shichi, 2004). Based on the 2012 World Health Organization report, it is estimated that cataract is responsible for about 50% of the 39 million individuals that are blind worldwide (Petrash, 2013; Rao & Perry, 2011). Although cataract is treatable, access to the corrective surgery, especially in developing countries, is not feasible for many cataract patients (WHO, 2014). Moreover, as the age of the population continues to increase, it is expected that the

number of aged-related cataract cases will rise. For example, in the U.S., by the age of 80, majority of Americans have either had cataract or have had cataract surgery (NEI 2013).

Cataract in name is one disease, however it presents with a spectrum of clinical presentation. The clinical features of different cataract types vary depending mainly on the anatomical location of the opacity, as well as its severity. Some of the cataract classifications are as follows: Polar cataracts (anterior and posterior), nuclear, lamellar, pulverulent, cerulean, total, cortical, polymorphic, and structural (Ionides, A. et al., 1999). Some, but not other, of these cataract types are commonly associated with inherited mutations. However with all types of cataract, early diagnosis is key for the best treatment outcome.

Depending on their onset, cataracts can be classified as either pediatric (or early onset) or age-related (late-onset). Congenital cataract is the most common cause of treatable visual impairment in children (Evans et al., 1996). Although congenital or pediatric cataracts occur in frequencies of approximately 1 in 10,000 live births, they account for one-tenth of childhood blindness worldwide (Francis et al., 2000). Mutations in several genes that cause congenital or pediatric cataract have been identified. These genes also represent candidate gene variations that may influence the onset of age-related cataracts (Francis et al., 2000). Depending on population and social structure, between a quarter to half of congenital cataract cases are estimated to have a genetic basis (Rahi and Dezateux 2000). Interestingly, a study described that

~56% of children with bilateral isolated congenital cataract had a genetic basis, compared to only six percent of unilateral cases (Rahi and Dezateux 2000).

Although cataract is a treatable disease, its treatment costs are substantial. Depending on the severity of the cataract, its treatment may vary; minimal treatment includes simple fixes such as: brighter lighting or even sunglasses (NEI 2014). However if these treatments are not sufficient, surgery is the only effective treatment option. Indeed, cataract removal is one of the most common surgeries performed in the United States (NEI 2014).

For around ninety percent of patients, cataract surgery improves vision (NEI 2014). Cataract surgery is a procedure in which the natural lens of the eye is removed and in most cases replaced by an artificial lens called an intraocular lens (IOL) implant (Mayo Clinic 2014). There are two different types of cataract surgeries available: phacoemulsification (phaco) and extracapsular. Between the two, phaco involves a smaller incision at the side of the cornea, followed with the insertion of a small probe emitting ultra sound waves that function to fracture the cataractous lens into pieces that may be removed by suction (NEI 2014). Phaco is the currently the most commonly preformed procedure in developed countries (NEI 2014). Extracapsular cataract surgery differs from phaco in that a larger incision on the side of the cornea is made in order to remove the core of the lens in one piece, which is followed by eradicating the rest of the lens via suction. In both procedures, after the ocular lens is removed, it is replaced by the IOL (NEI 2014).

An IOL is a plastic implant that requires no maintenance from patients and can significantly improve vision. The IOL becomes part of the eye and functions to focus light onto the retina. There are two main types of IOLs, monofocal and multifocal lenses. Monofocal lenses are the most commonly implanted lenses. They harness the same focusing power for all areas of the lens. Conversely, multifocal lenses are akin to bifocal glasses, they have areas of the lens with different focusing power (American Optometric Association 2014).

In the United States, cataract surgery is relatively common, but it is also expensive. Annually in the US, upwards of 1.4 million cataract operations are performed which account for over two percent of the total Medicare budget (Babizhayev et al., 2004). As the average population age within the US and the world continues to increase, the number of cataract cases is expected to rise as well. Thus, cataract surgery-related costs are predicted to increase in the U.S., and may not be sufficiently offset by a decline in the total cost per surgery (Babizhayev et al., 2004).

Presently at least 35 independent loci are shown to be correlated with non-syndromic or isolated cataract classically segregating as an autosomal dominant or recessive trait with high penetrance worldwide (Rees et al. 2000; Sheils, A., Bennett, T.M., and Hejtmancik, J.F., 2010). Historically, mapping and identification of mutations that cause cataract has been a formidable challenge. Indeed, prior to 1997, mutations in specific genes causing inherited human cataract had not been identified (Reddy et al. 2004). However, with advances in genomics, including the completion of the human genome project, several cataract-associated genes have now been

identified. Identification of genes associated with inherited cataract involves karyotyping, linkage analysis, mapping and positional cloning of candidate gene or mutation screening of candidate genes (Reddy et al. 2004).

Determining which mutations cause phenotypic variation is the fundamental theme of genetic research (Reddy et al. 2004). Previously, traditional Sanger sequencing, as well as using PCR products to detect rare variants are some of the earlier methods utilized in genetic disease based studies. More recently microarray capture technology has made large sequencing more efficient; however this type of approach has limitations, specifically it depends on the specificity of primer design for all capture probes (Mardis, E.R., 2008).

Whole genome sequencing has become more feasible due to the advent of next generation sequencing technology. Whole genome sequencing for variant discovery is faster and less expensive than using next generation sequencers with conventional approaches (Mardis, E.R., 2008).

As the efficiency of these technologies increases, the massive data generated by these high throughput technologies are accompanied by the challenge of the interpretation of this data to establish genotype-phenotype correlations. Sequencing analysis of personal human genomes has revealed that individuals differ from the human genome reference sequence at 3.5 million SNPs on average. Furthermore establishing the pathology of a sequencing variant can also be difficult since at times single patients are used to try to establish a disease causing gene, but even within families multiple variants will be present leaving several candidates for gene discovery

(Tang, N.L.S and Poon, T., 2014). This technology is accompanied by a high false positive rate and this technique is unable to distinguish between a homologous genomic regions or pseudogenes as well as large rearrangements and deletions. These difficulties need to be addressed and resolved before this approach can be fully implemented (Tang, N.L.S and Poon, T., 2014). Nevertheless, exome sequencing has already impacted cataract gene discovery and has led to the identification of *TRPM3* as a new human non-syndromic cataract gene as well new mutations in established cataract genes *GJA8* and *CRYGD* (Bennett, TM 2014; Mackay, DS 2014). As more of the genome gets functionally characterized, it will lead to a greater understanding of genetic variation and will allow the effective interpretation of genomic data and its correlation to human diseases such as cataract (Mardis, E.R., 2008).

1.3 Cell Types in the Lens

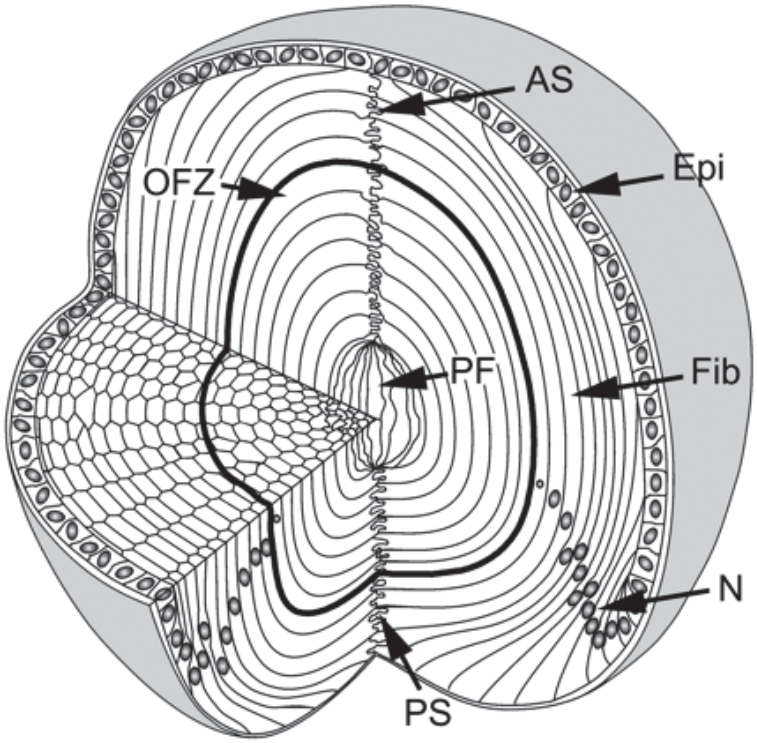

Figure 4. Anatomy of the Adult Mammalian Lens. The mature lens contains three main components, the epithelial cells, the fiber cells, and the capsule. The epithelial cells (Epi) are found at the anterior portion of the lens while fiber cells (Fib) found in the posterior portion account for the bulk of the lens tissue. Epithelial cells proliferate in an area termed the germinative zone and cells displaced below the equatorial region get located in the transition zone where they respond to signals such as Fgfs to differentiate into fiber cells. The elastic structural basement membrane surrounding the lens is the capsule (gray), which encloses the epithelium and the fibers. Fiber cells from apposing ends meet to form the anterior- and posterior sutures (AS and PS). During fiber cell differentiation nuclei (N) as well as other cellular structures are degraded. This process forms the organelle free zone (OFZ). This zone consists of both primary fiber cells (PF) as well as secondary fiber cells. (Figure acquired from Shi, Y., et al. 2009)

The lens contains two types of cells: (a) epithelial cells localized in the anterior part, and (b) fiber cells localized in the posterior part of the lens (Bassnett et al., 2011; Bassnett and Mataic, 1997). During embryonic development, cells within the posterior portion of the lens vesicle begin to differentiate and elongate to fill the vesicle and become primary fiber cells, while the anterior cells of the vesicle are the epithelium of the lens (Lachke et al., 2011). Cells of the anterior epithelium serve as a reservoir of cells that proliferate, and exit the cell cycle for differentiation of new fiber cells, termed secondary fiber cells (Bassnett et al., 2011). Although during early lens development proliferation occurs throughout the anterior epithelium of the lens, it is increasingly restricted to a region of cells known as the germinative zone that is located just above the lens equator, (Figure 4). As a result of the proliferative activity in this zone, cells that get located below the equator are placed what is called as the transition zone (Bassnett et al., 2011). In the transition zone, cells of the epithelium are induced by signaling cues such as Fgfs to exit the cell cycle and begin differentiation into secondary fiber cells (Zhao, HT et al. 2008).

As they differentiate, fiber cells assume an orientation in which their apical regions face the apical portion of the anterior epithelium, and thus "invert" in orientation (Cvekl, A and Ashery-Padan, R., 2014). As newer epithelial cells continue to terminally differentiate into fiber cells, earlier differentiating fiber cells progressively migrate toward the center of the lens. This differentiation processes involves extensive cellular lengthening and eventually results in the apical-apical and basal-basal regions of apposing cells to form coaxial rings in the center of the lens

(Cvekl, A and Ashery-Padan, R., 2014). Furthermore, this unique differentiation program involves the degradation of all cellular organelles and nuclei in terminally differentiated fiber cells, an essential feature for lens transparency (Bassnett and Mataic, 1997, Mathias et al., 2007).

Both lens anterior epithelial cells and differentiated fiber cells are polarized cell types that have their basal membranes attached to the basement membrane. The lens capsule, the biochemical matrix surrounding the lens and representing its outer most layer, is smooth and transparent, and functions as the basement membrane. The capsule is formed by epithelial cells of the lens and is essential for maintaining its shape (Bassnett et al., 1999, Zampighi et al., 2000). The capsule is maintained by membrane complexes and is critical for cell survival, differentiation, and the homeostasis of the lens (Coulombre and Coulombre, 1963, Greenburg and Hay, 1982, Bassnett et al., 1999)

1.4 Cellular Biology of the Ocular Lens

The characteristic cellular morphology of lens fiber cells is important not only for the overall shape of the lens, but also its unique cell biology is essential for its function to enable light to pass with minimum loss of photons as well as focus. During their differentiation from epithelial cells, lens fiber cells undergo elongation, migration, and extensive cellular remodeling. A genetic circuitry coordinates the various molecular and cellular events that generate these profound changes in cellular shape and length. These cellular events are precisely orchestrated through actin

cytoskeletal reorganization, the generation of contractile forces, and cellular adhesive interactions (Minko, A., 2002; Lee, A., et al., 2000; Nowak, RB et al., 2009).

Actin is a highly conserved cytoskeletal protein expressed as one of the most abundant proteins within eukaryotic cells. In most cells, it comprises of around five to ten percent of all cellular proteins and plays a central role in forming cytoskeletal structures. There are two major forms of actin in the cell: Filamentous (F) and globular (G) actin; however only filamentous actin is a major component of the cytoskeleton as well as mediates internal motility. One of the hallmark transitions that denote fiber cell differentiation is the increase in the ratio of F-actin to G-actin as the cytoskeleton begins to form a discrete organizational pattern. Furthermore, actin is a major component of stress fibers or complexes found in non-muscle cells, which consist of actin filaments, crosslinking proteins, and myosin II motors, these fibers have been found to play a critical role in cell adhesion as well as morphogenesis (Tojkander S. Gateva, G and Lappalainen, P. 2012). Actin content as well as stress fiber formation increases in cells along the elongating epithelium where fiber cell differentiation begins, when compared to cells within the central epithelium where differentiation has not been initiated (Ramaekers, FCS; Boomkens, TR; Bloemendal, H; 1981; Ramaekers, F; Jap, P; Mungyer, G; 1982; Mousa, GY and Trevithick, JR; 1979).

Actin filaments affect cells by influencing the re-organization of cell shape. Actin has been shown to localize to the plasma membrane within elongating lens fiber cells. Furthermore studies have shown that when actin localization is disrupted, epithelial cells express fiber cell differentiation markers and therefore disrupt

differentiation; indicating a critical role actin plays in fiber cell differentiation (Mousa, GY and Trevithick, JR.; 1977). Previous research has shown that disruption of the actin cytoskeleton disturbs the epithelial elongation essential for fiber cell differentiation; reiterating the significance of actin filaments for a reliable fiber cell transition. This evidence supports the importance of actin cytoskeletal interactions with adhesive connections to influence fiber cell differentiation (Mousa, GY and Trevithick, JR., 1977; Iwig, M; Glaesser, D; Bethge, M; 1981). For instance, previous research has shown that Src, Cortactin, EphA2, and F-actin function together in the formation of the hexagonal shapes the form within fiber cells of the lens (Cheng, C, et al. 2013). Furthermore, adherens junctions are particularly prominent at intersections where fiber cells meet. These junctions have been shown previously to usually correlate with the distribution of N-cadherin (Bassnett, S et al. 2011).

Actin function is regulated by its interaction with myosin II resulting in actin: myosin complexes. These complexes are the main influence that direct cellular fate between contractile ability of muscle cells to the formation of cell adhesions and junctions. Myosin II forms bipolar filaments, which are able to contract with actin-filament networks in the cytoplasm affecting membrane tension. This tension is critical in the cellular shape and therefore its function (Bresnick, AR; 1999).

Some molecules including spectrin, actin, and tropomyosin have been shown to be constitutively expressed as well as assembled onto the plasma membrane of both undifferentiated and differentiated fiber cells (Woo, M. K et al.; 2000). However other molecules including tropomodulin has shown to be expressed only after fiber cell

differentiation begins. Both tropomodulin and tropomyosin, as well as other actin-binding proteins stabilize tropomyosin–actin filaments by capping their pointed ends. Capping proteins have been shown to function within the ends of actin filaments in order to either stabilize the filaments or increase disassembly. Capping proteins such as tropomodulin have also been hypothesized to affect the lengths actin filament. (Rao, VP and Maddala, R 2006). These proteins are also associated with the spectrin-actin membrane skeleton of lens fiber cells (Fowler, VM, 1994).

While some proteins including microtubules and intermediate filaments undergo proteolysis during fiber cell differentiation, others proteins such as actin and tropomysoin remain associated with the membrane and are not degraded during this process. It is proposed that modifications of actin filament capping; which bind to the fast-growing ends of actin filaments (barbed end), to inhibit the exchange of subunits at these ends; are essential for remodeling of the lens membrane skeleton to maintain plasma membrane integrity and transparency within the lens (Lee, A; Fischer, RS; Fowler, VM; 2000; Woo, MK; Fowler, VM; 1994; Sussman, MA; McAvoy, JW; Rudisill, M; et al; 2006). (Rao, PV and Maddala, R 2009).

1.5 Transcriptional Control of Lens Development

Functional analysis of several transcription regulator proteins that are expressed in the presumptive eye region and called as eye-field transcription factors (EFTFs) have shown these to be essential for eye formation in vertebrates (Cvekl and Mitton, 2010; McCabe, KL and Bronner-Graser, M, 2009; Cvekl, A and Ashery-

Padan, R 2014). These transcription factor gene families are present during eye development and include: Pax, Six, Sox, Eya, Msx, Prox, and Pitx/Rieg. Specifically for the lens, some of the highly conserved transcription factors (TFs) include *Pax6*, *Rax*, *Six3*, and *Lhx2* (Donner, A; Lachke SA, and Maas RL 2006; Heavner and Pevny 2012; Cvekl, A and Ashery-Padan, R 2014). These TFs participate in a regulatory network operational within ectodermal cells to define and establish eye tissue development. Beginning with their expression in the presumptive retinal ectoderm (PRE), these transcription factors coordinately function with each other and signaling molecules like Sonic hedgehog (Shh) to establish eye formation. Furthermore, human mutations of many of these EFTFs have been shown to cause a spectrum of eye malformation phenotypes, and mutations of these factors in mouse knockout models result in animals with abnormal or no eyes (Lachke SA and Maas RL, 2010; Zuber et. al. 2003; McCabe, KL and Bronner-Graser, M, 2009; Cvekl, A and Ashery-Padan, R 2014). EFTFs are critical for inducing the expression of downstream transcription factors that operate within the lens development gene regulatory network (GRN) (Donner et al. 2006; Lachke and Maas 2010; Cvekl, A and Ashery-Padan, R 2014). EFTFs also function in the major signaling pathways that direct lens development.

Known as the "master regulator" of the eye development, *Pax6* (*Paired box 6*) encodes a highly conserved paired homeodomain transcription factor essential for eye development in metazoans, and its deficiency in fruit fly, mouse or human results in profound eye defects or the complete absence of eyes (Halder, G et al. 1995; Glaser, T et al. 1994; Hill, RE et al. 1991; Cvekl, A and Ashery-Padan, R 2014). Ectopic

expression of Pax6 in fly or vertebrate species results in the induction of ectopic eyes (Halder, G et al. 1995; Chow, RL et al. 1999; Shaham, O et al. 2012). Heterozygous mutations in *Pax6* cause profound eye defects including aniridia (absence of iris) and cataract in human, and "small eye" and cataract in mouse and rat (Hill et al., 1991; Hogan et al., 1986; Matsuo et al., 1993). *Pax6* homozygous null mutations in human results in complete absence of eyes (anophthalmia) (Glaser, T et al. 1994), and in mice cause an early onset defect in lens initiation that results in the absence of lens (Hill, RE et al. 1991; Ashery-Padan et al., 2000). Pax6 is cooperatively regulated by members of TALE transcription factors (TFs) including Meis1 and Pknox1 (Rowan et al., 2010; Zhang et al., 2002) as well as Six3, Sox2/Oct1 or by directly binding to its own enhancer in a feedback loop (Donner et al., 2007; Liu et al., 2006; Cvekl, A and Ashery-Padan, R 2014).

Conditional deletion of *Pax6* from mouse lens tissue after lens vesicle stage causes failure of lens epithelial cells to exit cell cycle and initiate fiber cell differentiation. In addition to induction of lens fate, these findings are indicative of Pax6 function in lens fiber cell differentiation (Huang et al., 2011; Shaham et al., 2009). Pax6 interacts with other significant lens-enriched TFs including c-Maf, AP2α and Sox2, as well as with non-lens specific TFs including pRb and TFIID (Cvekl & Piatigorsky, 1996). These interactions partially explain Pax6 function in the lens that ranges from regulation of other transcriptional regulators including Six3, c-Maf, Prox1, transmembrane receptor molecules like α5β1 integrins, as well as structural

proteins such as crystallins (Cvekl and Piatigorsky, 1996, Ashery-Padan et al., 2000; Goudreau et al., 2002; Sakai et al., 2001, Duncan et al., 2000).

Pax6 regulates other transcriptional factors including Sox11 and AP-2a that are essential for lens placode invagination and lens vesicle separation (Pontoriero et al 2008, Wurm et al. 2008) as well as Pitx3, which is essential for the maintenance of the anterior epithelium of the lens (AEL) (Ho et al. 2009). Additionally Pax6 controls yet another transcription factor Mab21l1, which regulates Foxe3 that in turn negatively controls expression of a fiber cell-enriched transcription factor Prox1 (Blixt et al. 2000, Yamada et al, 2003).

Another critical transcription factor that assists in lens fiber cell differentiation; Prox1 is expressed in the lens placode and eventually the lens vesicle early on during lens development. Prox1 regulates transcription of gamma-crystallins as well as cell cycle inhibitors p27KIP1 and p57KIP2, both of which inhibit cell cycle kinase proteins to promote fiber cell differentiation (Duncan et al. 2002). *Prox1* germline knockout mouse mutants exhibit lens fiber cell elongation defect (Wigle et al., 1999).

Similar to Prox1, Sox1 also regulates transcription of gamma-crystallins (Nishiguchi, S et al. 1998). Sox1 belongs to the Sox-family of transcription factors and when deleted in mouse models, Sox1 null mutants exhibit lens defects including mis-expression of Pax6 in fiber cells (Donner et al. 2007). Further, mutations in the large *Maf* family transcription factor gene *MAF (c-Maf)* are associated with human juvenile cataracts (Jamieson, RV et al. 2002) and mouse mutants exhibit profound lens defects with mis-regulation of gamma-crystallin genes (Kim, JI et al. 1999). Finally, another

transcription factor Hsf4 has been shown to control γ-crystallin expression in lens and null mouse mutants exhibit down-regulation of *Dlad* (*Dnase2b*), which encodes a DNase that is essential for degradation of fiber cell nuclei during fiber cell differentiation (Shi, X. et al. 2009; Cui, X. et al., 2013; Lv, H. et al., 2014). These findings indicate Hsf4 functions in fiber cell differentiation and homeostasis. Indeed, mutations in human *HSF4* cause congenital cataract, as do *Hsf4* null mouse mutants (Cui et al., 2012; Yi et al., 2011).

Together, *Pax6*, *Six3, Sox2/Oct1*, *Meis1*, *Pknox1*, *Mab21l1*, *Foxe3*, *Pitx3*, *c-Maf*, *Prox1*, *Sox1*, and *Hsf4* have critical functions in lens development and homeostasis (Cvekl, A et al. 2004; Lv, H. et al., 2014; Cvekl, A and Ashery-Padan, R 2014). Thus, while function of signaling molecules and transcription factors are well defined, the significance of a different functional class of regulatory molecules, which participate in post-transcriptional control of gene expression, remains relatively uncharacterized in the eye and lens development (Taube, JR et al. 2002; (Harocopos GJ et al. 1998).

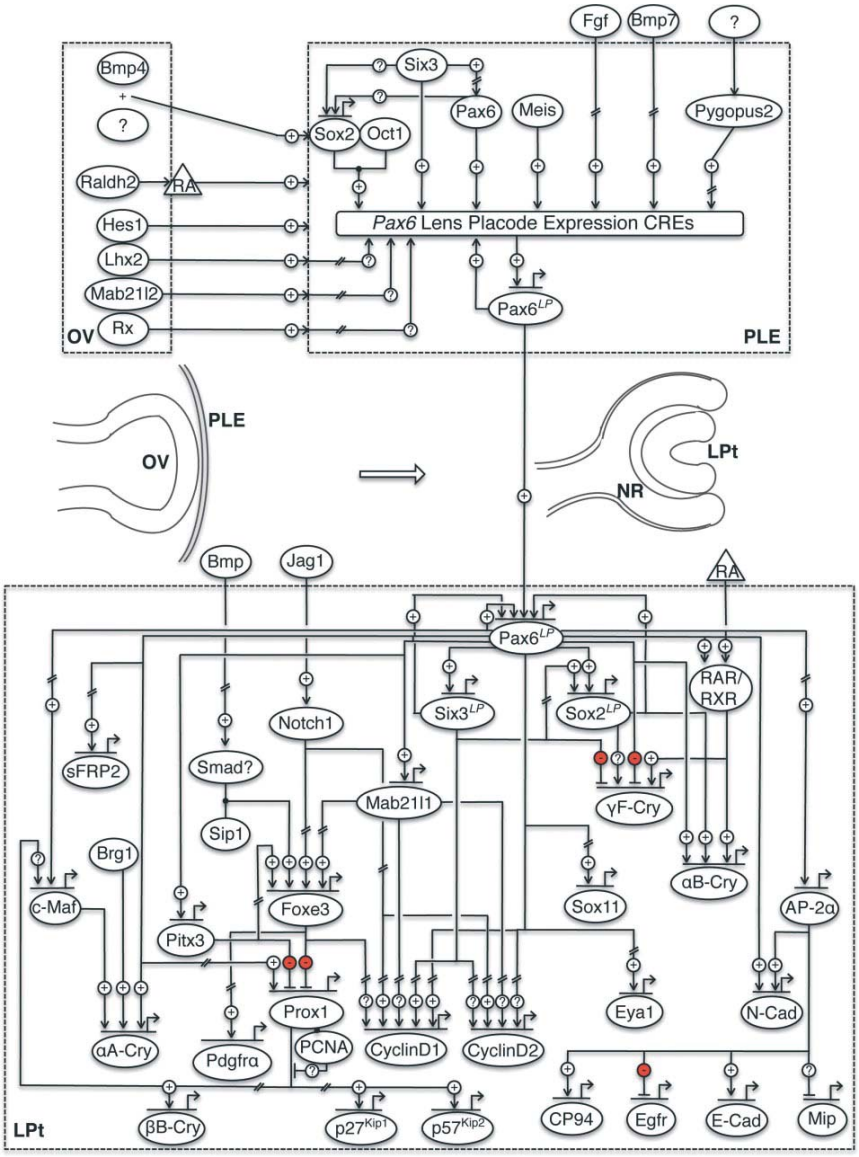

Figure 5. Circuitry of Early Mammalian Lens Development. Signals from the optic vesicle (OV) induce other regulatory molecules in the presumptive lens ectoderm (PLE), which then bind to multiple *cis*-regulatory elements (CREs) to induce the placodal expression of Pax6 (Pax6LP). As the PLE develops into the lens pit (LPt), Pax6LP turns on the necessary transcription factor cascade and circuitry required for lens formation. Pax6LP, Six3LP, and Sox2LP indicate the expression of these genes in stages following lens placode induction. Hatches in lines are to indicate the interaction may have more intermediate steps. Figure modified from Lachke and Maas 2010.

1.6 Post-Transcriptional Control in the Lens

Our understanding of the molecular biology of eye development has grown immensely in the past twenty years (Cvekl A and Ashery-Padan R, 2014). This is largely due to use of various model organisms to investigate gene function and the application of genomics-level technologies such as microarrays and high-throughput sequencing. From these studies, it does not come as a surprise that several transcriptional regulators associated with ocular disease have been shown to function in orchestrating the development of this complex multi-component sensory organ (Lachke & Maas 2010). Through these efforts, we have gained a detailed understanding of transcription factor proteins that initiate gene transcription. Excitingly, breakthroughs within the past decade are now beginning to point to a previously underappreciated role for non-coding RNA and RNA binding proteins (RBPs) in mediating post-transcriptional control (PTC) mechanisms for controlling gene expression (Eddy 2001; Sanchez-Diaz, P and Penalva, LOF 2006; Keene, JD 2007; Gliaovic, T et al. 2008; Licatolosi, DD and Darnell RB 2010; Cirillo, D et al. 2014).

In eukaryotic cells, several different types of RNA (mRNA, miRNA, tRNA, rRNA) molecules are transcribed in the nucleus and undergo extensive modifications by molecular mechanistic events that offer opportunities for mediating regulatory control (Figure 6). For example, generation of mature mRNA involves diverse and

multiple regulatory mechanisms that include 5'-end capping, splicing, RNA modification, and 3' cleavage and polyadenylation before their exit from the nucleus and being available for translation. Exit of mature mRNAs from the nucleus through the nuclear pores involves the binding of RNA-binding proteins. Once transported out of the nucleus these mRNAs are directed to specific cellular locations where they are translated. These events as well as inherent *cis*-sequences in the 5' and 3' untranslated region (UTR) of mRNAs influence the timing and extent of their translation into protein, as well as their stability. These diverse molecular events are representative of opportunities where post-transcriptional control (PTC) functions to produce a diverse and dynamic pool of proteins, thus generating complexity in the proteome of a cell (Figure 6). Thus PTC mechanisms give an additional means for cellular gene regulation, beyond transcriptional control, and need to be investigated in as much detail as transcriptional mechanisms.

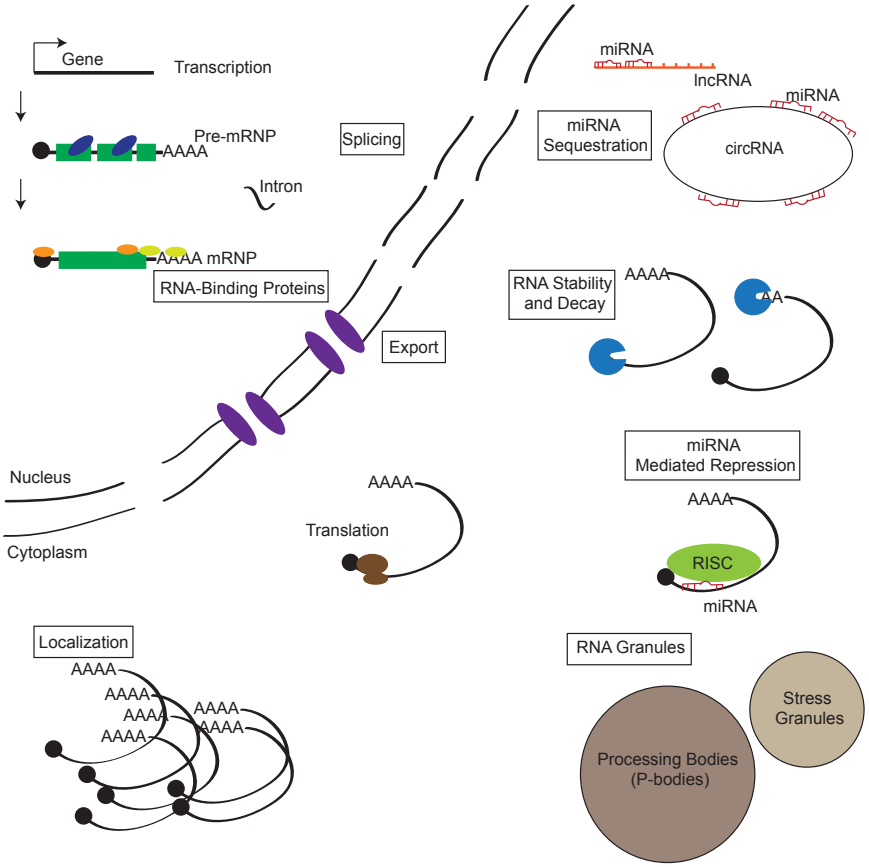

Figure 6. Post-Transcriptional Gene Control. As RNA is transcribed in the nucleus, the resulting transcripts are processed and modified in distinct steps. For simplicity, I focus on the life of mRNA molecules. During transcription, small RNAs and RNA binding proteins bind to the pre-mRNA molecules to facilitate proper splicing events, as well as in cleavage and polyadenylation. A mature mRNA molecule must contain a 5'-cap, correct splicing signals, a poly-A tail, as well as polyA-binding proteins, and other RNA-binding proteins, in order to be successfully transported out of the nucleus. RNA-binding proteins also function in the correct localization of the mRNA within the cell. Furthermore, RNA-binding proteins can also influence the rate of translation of mRNA molecules by regulating both the stability as well as the degradation of mRNAs within the cell.

1.6.1 Alternative Splicing in the Lens

More than ninety percent of human muti-exon genes undergo alternative splicing and it is estimated that greater than 100,000 intermediate to high frequency

splicing events occur in major human cells (Pan, Q. et. al. 2008). Alternative splicing increases the diversity of gene products encoded by the genome and alternatively spliced forms of a single gene can control cell fate (Black, 2003). Although the list of molecules controlling splicing in cells continues to expand, our understanding of how individual splice variants function in controlling cell fate and homeostasis is comparatively limited (Black, 2003).

Alternative splicing of the *Pax6* transcript controls the specific DNA-binding properties of the resulting encoded protein. In the developing lens, two different splice forms of *Pax6* have been detected (Epstein et. al. 1994). These splice variants, known as *Pax6* and *Pax6(5a)* result in two different isoforms. The Pax6(5a) protein retains a portion of the paired domain that is spliced out in the canonical Pax6 isoform. This results in a change in the DNA-binding specificity of the two Pax6 isoforms with the consensus of Pax6(5a) being 5aCON while the consensus of Pax6 being P6CON, (Epstein et. a. 1994), thus expanding the range of target cis-regulatory sequences controlled by this transcription factor in lens tissue.

Both *Pax6* and *Pax6(5a)* are detected in equimolar ratios in the adult human lens epithelia and fiber cells, although both are expressed at higher levels in the lens epithelium. The inference derived from these findings suggests that these two different isoforms of Pax6 function to regulate specific and non-overlapping target genes (Zhang et. al. 2001). These finding are consistent with other studies showing that the over-expression of the splice variant PAX6(5a) could cause congenital cataract (Duncan MK et al 2000; Ducan MK 2004).

Unlike Pax6, which functions as a transcription factor, Calpains are a family of calcium dependent cysteine proteases (Croall and Ersfeld 2007). Calpains can target many different types of proteins including receptors, cytoskeletal proteins, ion channels, and signal transduction proteins (Liu and Schnellmann, 2003, Sato and Kawashima, 2001, Hell et. al. 1996, bi et. al. 1996). Calpain-3, once thought to show muscle specific expression was found to have a specific splice variant, Lp82 found exclusively in the murine lens (Ma et. al. 1998). Lp82 lacks the IS1 and IS2 regions found in the muscle-specific Calpain, p94, and harbors an alternate N-terminus. These alternate regions have to been shown to contribute to the stability and function of Calpains in the lens (Hong et. al. 2000). More recently Calpain-3 has also been shown to be critical for fiber cell differentiation, including the remodeling of the cytoskeleton and membrane (De Maria et. al. 2009). Additionally, Lp82 has been shown to regulate other Calpain species and cascades, which could be significant to cataract formation (Fukiage et. al. 2002).

Additionally, efforts on understanding some of the features shared between lens fiber cells and neuronal cells, such as an elongated cellular morphology, have led some researchers to investigate splicing events and splice variants shared between these diverse cell types (Frederikse et. al. 2012, Bitel, et. al. 2010, Frederikse et al. 2012). Interestingly, what were once considered as "brain specific" splice variants of specific genes have been detected in the lens (Bitel et. al. 2011, Frederikse et. al. 2012, Bitel et. al. 2010). Examples include the neuronal polypyrimideine tract binding (nPTB) protein as well as other neuronal specific splice forms of REST/NRSF,

REST4 found in both neurons and lens tissues. Further studies are needed to understand the significance of these neuronal splice forms in the lens (Bitel et. al. 2010).

1.6.2 miRNA Function in the Lens

MicroRNAs (miRNAs) are small non-coding RNAs, usually around 21 nucleotides long that bind imperfectly to the 3' untranslated regions of target mRNAs (Zamore and Haley 2005, (Filipowicz et. al. 2008). After binding, miRNAs are able to influence gene expression by altering the mRNA's stability or translation into protein (Valencia-Sanchez et. a. 2006, Paillai, et. a. 2007). miRNAs have been found to play key roles in the most basic biological processes including development (Wienholds et. al. 2003) and many miRNAs play critical roles within the pathogenesis of many diseases (Couzin 2008, Meola et. al. 2009).

miRNAs are first transcribed either by specific miRNA genes or as part of introns of protein-coding genes. (Filipowicz et. al. 2008, Bushati and Cohen 2007, Rana 2007, Du and Zamore 2005). Once transcribed, these pri-miRNA then fold into imperfectly paired double-stranded RNA (dsRNA) hairpins. Then the endonuclease Drosha and the DGCR8 proteins further process and cleave these pri-miRNAs to the 7-nucleotide hairpin form known as pre-miRNAs. These pre-miRNAs can be exported out of the nucleus via Exportin5 (Filipowicz et. al. 2008, Bushati and Cohen 2007, Rana 2007, Du and Zamore 2005). Once these pre-miRNAs make it to the cytoplasm, they are then cleaved again by the protein Dicer and TRBP (TAR RNA binding

protein) to produce miRNAs of around 20 nucleotides bound together in a duplex. From this duplex, one strand is selected as the mature miRNA and the other strand is degraded, although in some rare cases both strands could function as mature miRNAs (Filipowicz et. al. 2008, Bushati and Cohen 2007, Rana 2007, Du and Zamore 2005).

Once these miRNAs become mature, they are able to join with ribonucleoprotein complexes called micro-RNPs or miRNA-induced silencing complexes (miRISCs). The association of the miRNAs and these various complexes is a transient process, usually influenced by the pre-miRNA processing functions of Dicer (Filipowicz et. al. 2008, Bushati and Cohen 2007, Rana 2007, Du and Zamore 2005). However, miRNPs primarily contain proteins of the Argonaute (AGO) family. In mammalian systems, Argonaute proteins, partner with mature miRNAs and function in mRNA repression through. Only AGO2 is able to function in RNA interference (RNAi), which actually cleaves mRNA at the center of the miRNA-mRNA duplex and leads to mRNA degradation (Filipowicz et. al. 2008, Peters and Meister 2007, Rana 2007). These small non-coding RNAs have been shown to play a crucial role in many cellular processes as well as helping to regulate tissue specificity (Filipowicz, et. al. 2007, Wienholds et. al. 2003, Zhao et. al. 2007). The lens is no exception and current research is beginning to illuminate the roles of these miRNAs and their composite proteins (Li and Piatigorsky 2009, Frederikse et. al. 2006).

Dicer as well miRNAs were shown to be present within the lens (Frederikse et. al 2006). Dicer is expressed during embryonic and early postnatal stages in elongating fiber cells, differentiation cells, as well as epithelial cells. Dicer staining in rat lenses

seemed to coordinate with nuclear expression. However, in adult lenses, Dicer was only strongly detected in the epithelium of the lens and cells that had not undergone fiber cell differentiation (Frederikse et. a. 2006). Conditional mouse knock-out via the *Pax6* ectoderm enhancer (EE) (Williams, SC. et al. 1998; Dimanling et. al. 2001,) of Dicer in the cornea and lens was shown to cause microphthalmia (Li and Piatigorsky 2009). Furthermore lens degeneration began around E14.5 and by birth, knock-out mice exhibited aphakia. These results signify that Dicer plays a critical role in lens development and homeostasis (Li and Piatigorsky 2009).

Several other miRNAs are associated with lens development and homeostasis (Nakamura et. al. 2010, Tsonis et. al. 2007, Tian et. al. 2010, Peng et. al. 2012, Hoffmann et. al. 2012, Wu et. al. 2012). Although several miRNAs are expressed in the lens, a select few have been studied in detail, which include miR-184 and miR-204. Other miRNAs associated with the lens include: miR-124, mir-125, and the let7 family of miRNAs.

miR-184 represents one of the best characterized miRNA in the lens. It was first detected in the lens epithelium, specifically in the germinative zone, with less consistent expression seen in the anterior region of the epithelium or in fiber cells (Ryan et. al. 2006). miR-184 was shown to target *Bin3,* which is important in the lens as its deletion in mouse mutants (*Bin3*-/-) causes cataracts (Tian et. al. 2010, Ramalingam 2008). It is important to note however, that miR-184 is not exclusively expressed in the lens. Its expression has also been demonstrated in the retina, cornea, and cilliary body/iris tissues (Karali, M. et. al. 2010).

miR-184 has recently been linked with cataracts (Wu, C. 2012, Hoffmann, A. 2012). When comparing transparent and cataract lenses miR-184 was one of the top eight differentially expressed miRNAs (Wu. et. al. 2012). Furthermore, it was shown that changes in the seed sequence (the region of miRNA that binds imperfectly to the 3'UTR of target mRNAs) of miR-184 causes severe familial keratoconus as well as early-onset polar cataracts (Hughes, AE et. al. 2011). Additionally, miR-184 was also unregulated after cataract surgery (Hoffmann, A. et. al. 2012). Further work is necessary to illustrate the full significance of miR-184 in PTC in the lens.

Another miRNA, miR-204, is expressed throughout the anterior epithelial cells, within the germinative zone, as well as weakly in the fiber cells, in adult murine lenses (Ryan et. a. 2006). Studies have also identified a potential role for miR-204 in cataract pathogenesis (Conte et. al. 2010). Interestingly, studies in medaka fish indicate that miR-204 is highly expressed in the lens as well as in other ocular tissue components, is necessary for lens and optic cup development. Furthermore, miR-204 misregulation caused fissure coloboma (Shaham, O et al. 2013). Additionally, miR-204 regulates *Meis2* (Conte et. al. 2010), which itself is implicated in the control of *Pax6* expression in early lens development (Zhang et. al. 2002). Similar to miR-184, differential expression of miR-204 was observed in secondary cataract and it was also found to be downregulated after cataract surgery (Hoffmann et. al. 2012). Thus, future work on miRNAs in the lens will further elucidate their function in PTC in the development and homeostasis of this tissue.

1.6.3 RNA Binding Proteins in the Lens

Similar to microRNA, RNA binding proteins regulate PTC via control of RNA expression and metabolism. Various RNA-protein complexes such as RNA granules function with RNA-binding proteins to implement PTC. Cytoplasmic RNA granules are ribonucleoprotein (RNP) complexes detected in eukaryotic cellular cytoplasm that can function in controlling mRNA via localization, stabilization, and degradation (Lachke and Maas 2011, Anderson and Kedersha 2009, Buchan and Parker 2009, Thomas et. al 2011, Parker and Sheth 2007; Buchan, JR 2014; Ramaswami, M et al. 2013). RNA granules are classified into several different classes as follows: processing bodies (PBs), stress granules (SGs), transport RNP particles, and germ cell-specific granules (GCGs). Transport RNA granules have been previously characterized in many different cell types including neurons and fibroblasts and function in the transport and localization of mRNA within cells (Oleynikov and Singer 2003; Buchan, JR 2014; Ramaswami, M et al. 2013). On the other hand, GCGs are RNA granules that are detected exclusively in the cytoplasm of germ cells and are essential for spermiogenesis (Kotaja and Sassone-Corsi 2007; Voronia et. al 2011; Ramaswami, M et al. 2013). Another class of RNA granules is the Processing bodies (P-bodies) that are constitutively expressed and are associated with mRNA decay. P-body components include decapping enzymes as well as exonucleases (Kedersha and Anderson 2007). Finally, RNA granules that are induced by stress are termed Stress Granules (SGs). SGs mainly contain preinitiation complexes, mRNA, as well as small

ribosomal subunits and their associated initiation factors, and function to mediate translation of heat shock proteins (Kedersha and Anderson 2007; Roucou, X 2009).

The present model for the metabolism of cytoplasmic mRNA, the mRNA cycle, includes activity of both SGs and P-bodies. It is hypothesized that transcripts are concentrated into these mRNPs and then targeted to either stress granules or P-bodies based on the specific cellular condition. From these sites, the mRNAs are fated for either storage or degradation (Olszewska et. al 2012; Roucou, X 2009). Furthermore, both these granules have been shown to interact within the RNA-induced silencing complex and proteins such as Argonaute 2, although the significance of these interactions is not yet understood (Pare et a. 2011; Roucou, X 2009). Interestingly, some of these granules are known to interact with other granules as well as cellular components such as mitochondria, and it has been proposed that there is a symbiotic relationship between the efficiency of RNAi, P-bodies, and mitochondria (Ernoult-Lange et. al 2012; Roucou, X 2009).

RNA and RNA-binding proteins have recently arrived at the forefront in lens research (Duncan 2011). Because of their functional diversity, these regulatory molecules can be hypothesized to function in meeting the various challenges that are presented in differentiation of lens fiber cells. It is possible that the characteristic proteome of lens fiber cells is achievable due to action of RNA granules. For example, in a highly crystallin mRNA-rich transcriptome, fiber cells manage to translate sufficient quantities of proteins from relatively low expressed mRNAs such as transcription factors and signaling molecules, which may involve a role for RNA

granules. Perhaps specific RNA granules may function to extend the life of lens-specific mRNAs by directly binding and shielding them from decay mechanisms, thereby controlling their stability in the lens (Duncan 2011, Lachke et. al 2011). Given that during fiber cell differentiation, nuclei eventually degrade and transcription ceases, such mechanism may operate to temporally and precisely couple transcription and translation of fiber cell transcripts prior to this terminal event. Moreover, it can be further hypothesized that because the fiber cell environment has unusually high amounts of crystallin proteins, it may necessitate a function for transport RNA granules in transport of mRNAs to specific locations within these elongated cells.

In addition to RNA granule components, several types of RNA-binding proteins are identified in the lens and include some that were previously classified as "neuronal specific" proteins. For example, nPTB (neuronal polypyrimidine tract binding protein) is an RNA-binding protein that was previously characterized in association with neuronal differentiation and elongation, and recently has also been detected in differentiating fiber cells (Bitel et. al 2010). Additionally, two proteins of the Fox-1 family of RNA binding proteins, Fox-1 and Fox-2, have also shown to exhibit their neuron-expressed splice variants in the lens.

Several neuronal ELAV family proteins HuB, HuC, and HuD are also present in post-mitotic lens fiber cells, suggesting a potential overlap in some regulatory aspect between lenses and neurons (Bitel et. al 2010). Further investigation into the function of HuB, HuC, and HuD in lens cells could give new insight into splicing, RNA metabolism, and translation (Hinman and Lou 2008; Frederikse et. al 2012).

Other types of proteins have been associated with RNA-binding as well as RNA granules, but have not yet been characterized in the lens. These include the RNA-binding protein Musashi-1 (encoded by *Msi1*) that is present in the equatorial region of the lens, as well as differentiated fiber cells (Raji et. al 2007). Based on its expression it was speculated that *Msi1* functions in lens fiber cell differentiation (Raji et. al 2007). Furthermore *Caprin2,* an RNA granule associated protein also exhibits high expression in lens fiber cells, and is implicated in the FGF signaling (Loren, CE et al. 2009).

TDRD7 represents the first RNA-binding protein encoding gene that is directly linked with cataract in human, mouse and chicken. Tdrd7 is a Tudor domain protein, the founding member of which is the *Drosophila* Tudor. Tdrd7 contains three LOTUS/OST-HTH (Oskar Tudor-Helix Turn Helix) domains near its N-terminus and three Tudor Domains distributed through the remainder of the protein. While the LOTUS/OST-HTH domains are predicted to interact with double-stranded RNA, the Tudor domains are considered to interact with methylated arginine residues within other proteins (Lachke and Maas 2011). Tdrd7 exhibits highly enriched expression in lens fiber cells where it forms Tdrd7-RNA granules that co-localize with other RNA binding proteins like Staufen1 in lens fiber cells (Lachke et. al 2011). *TDRD7* mutations or haploinsufficiency in human patients were linked to congenital or pediatric cataract, respectively. Further, *Tdrd7* nullizygosity in mouse ($Tdrd7^{Grm5}$ mutant mice, identified in an N-ethyl-N-nitrosourea-induced recessive null allele

mutation in *Tdrd7*), or its knock-down in chicken lenses, was shown to cause cataracts, (Lachke et al 2011, Lachke and Maas 2011).

1.7 Tudor Domain Proteins in Cell Differentiation

The Tudor gene was first discovered in a screen for maternal factors that regulate embryonic development or fertility in *Drosophila melanogaster* (Boswell and Mahowald, 1985). The Tudor domain is a highly conserved protein structural motif consisting of around sixty amino acids and is associated with a bent anti-parallel beta-sheet composed of five beta-strands with a barrel-like fold (Sprangers et al. 2003). Tudor domains recognize and bind to methylated lysine or arginine residues within other target proteins and facilitate the assembly of protein complexes (Friber, et al., 2009; Liu et al, 2010a, Liu et al., 2010b). Additionally, Tudor domain proteins are implicated in splicing, small RNA metabolism, histone modifications, and DNA damage (Ponting, 1997; Callebaut and Mornon, 1997). Tudor domain proteins also function as molecular adaptors, assisting to scaffold together molecular complexes (Pek, J.W. et al., 2012). Recent studies have indicated an important function of Tudor proteins in maintaining genomic stability in gametes via regulation of piRNA pathways.

Piwi-interacting RNAs (piRNAs) belong to a class of small non-coding RNAs that are largely described in context of their function in transposon silencing during germline development (Aravin et al. 2007). piRNAs are 24-32 nucleotides in length and abundantly expressed in the testes. Interestingly, piRNA genes exhibit a distinct

clustering pattern within the genome. Although piRNA genes are predominantly grouped in 20-90 kilobase clusters and can be transcribed bidirectionally, majority of them are derived from one strand of DNA (Girard et al., 2006). piRNAs interact with the PIWI subfamily of Argonaute proteins (Somi, M.C., et al. 2011, Ross et al., 2014). Piwi proteins are highly conserved from invertebrates to mammals. Specifically the mouse genome encodes MIWI, MILI, and MIWI2, analogous to the *Drosophila* Piwi, Aubergine and Argonaute3. All of these proteins have the potential to be methylated at specific arginine residues, suggesting the possibility that they are targets of Tudor domain proteins (Chen et al. 2009; Kirino et al., 2009 Liu et al., 2010a, Liu et al., 2010b, Nishida et al., 2009; Vagin et al. 2009).

Some of the factors required for piRNA production found in *Drosophilla* include: *Zucchini* (zuc) and *armitage* (*armi*) in ovarian stroma and *Vasa*, *maelstrom* (*mael*), *krimper*(*krimp*), *armi*, and *spindle-E* (*spn-E*) in testes (Haase et al.,2010; Olivieri et al., 2010; Saito et al., 2010). Primary piRNAs are mostly antisense to transposon mRNAs, and usually show a bias for the uracil at the 5' end; these piRNAs are then in turn loaded onto other proteins Aub and Piwi (Li et al., 2009; Malone et al., 2009). Although thorough understanding of the piRNA biogenesis factors is still elusive today, cytoplasmic granule structures called nuage and Yb bodies are considered to represent the sub-cellular locations for piRNA biogenesis (Findley et al., 2003; Lim and Kai, 2007; Olivieri et al., 2010; Saito et al.,2010; Qi et al., 2011). Contrasting to other known piRNA associated factors, Zuc is

localized to the mitochondria (Olivieri et al., 2010, Saito et al., 2010). The implication of mitochondrial localization of Zuc to the biogenesis of piRNA is presently unknown.

Germline cells of animals contain characteristic cytoplasmic structures called the nuage or germinal granules, which is a ribonucleoprotein complex. In postnatal male mice, the nuage is termed the intermitochondrial cement or chromatid bodies. Several Tdrd-family proteins are components of the nuage. The dynamic localization of these proteins during development suggest that Tdrd proteins are involved in the molecular rearrangement of the nuage.

Tdrd7 is essential for post-meiotic sperm development, and its interaction with Tdrd6 is critical for the biogenesis of chromatoid bodies. Mouse knockout experiments on single and double nullizygous of *Tdrd7* and *Tdrd6* indicate the function of proteins in the remodeling of chromatoid bodies. This includes the initial establishment of the chromatoid bodies, as well as RNP fusion with ubiquitous Processing bodies (P-bodies) or GW bodies. Furthermore, it has been found that Tdrd7 specifically suppresses LINE1 retrotransposons independently of piRNA biogenesis in mice (Tanaka et al. 2011).

Although other Tudor domains have been shown to function in the regulation of splicing, histone modifications, and DNA damage control, the mechanisms that Tdrd family proteins are involved with, outside the germline, have not yet been discerned. Although Tdrd7 forms RNA-granules in lens fiber cells, and are directly associated with cataracts in human, mouse and chicken, details of Tdrd7 function in the lens are not yet identified.

1.8 *iSyTE*: integrated Systems Tool for Eye gene Discovery

Despite significant advances of genomics-level approaches and the advent of new technologies including high-throughput sequencing of nucleic acids, the identification of genes associated with congenital defects including eye defects remains challenging. For example, in human and mice, the identification of genetic mutations that are associated with cataract formation involves numerous steps including genetic mapping, linkage analysis, and sequencing. While other approaches involving mutational analysis on animal models can be performed, these are time consuming as well, mainly because there is no straightforward approach to prioritize high-priority genes from a list of candidate genes identified in these methods.

Recently it was hypothesized that mouse tissue-specific developmental gene expression patterns could inform on the prioritization and identification of congenital structural birth defect genes in humans, especially in non-syndromic cases. A novel bioinformatics tool *iSyTE* (integrated Systems Tool for Eye gene discovery, http://bioinformatics.udel.edu/Research/iSyTE) was developed by Lachke et al. (2012) that applied mouse lens embryonic gene expression patterns based on microarrays to prioritize and identify cataract candidate genes. The first published version of *iSyTE* was based on three stages in lens development (E10.5, E11.5, and E12.5) when the lens transitions from the lens placode stage through the initiation of primary fiber cell differentiation stage.

To specifically identify genes with lens-enriched expression, *iSyTE* depends on a comparative analysis called “in silico subtraction” in which lens microarray datasets

are compared to whole body embryonic tissue (WB) reference dataset. The WB dataset is a representative of averaged gene expression profiles across embryonic tissues. Thus, comparisons to WB result in efficient identification of genes not just expressed in the lens, but rather, which exhibit lens-enriched expression. Based on high lens-enrichment scores, *iSyTE*-mediated gene discovery is based on the hypothesis that significantly high tissue-enriched gene expression may be reflective of potential function for the gene in that tissue. Thus, the list of genes ranked based on their lens-enrichment scores is the central theme of the *iSyTE* database (Lachke and Maas 2012).

The efficacy of *iSyTE* was tested in a retrospective analysis of known human non-syndromic cataract genes. This involved analysis of 24 originally mapped genomic intervals that contain the causative gene among several tens (or hundreds) of potential candidates associated with non-syndromic congenital cataract. Of the 24 intervals tested, *iSyTE* was able to correctly identify the mutant gene among the top two candidates genes within the original mapped interval with ~90% efficacy (21/24). Significantly, the mapped intervals averaged 12.3 Mb and encompassed an average of 80 genes. Furthermore, in addition to highly expressed and enriched Crystallin protein encoding genes, *iSyTE* also readily identifies other important genes (*FOXE3*, *HSF4*, *MAF*, *PAX6*, and *LIM2*) that are not as highly expressed, but are highly enriched in the lens.

In addition to its efficacy in this retrospective analysis, *iSyTE* has proved over the past three years to be successful in prospective analysis in identifying novel genes

associated with cataract. In the first of its prospective analysis, *iSyTE* correctly identified *TDRD7* as the highest priority candidate gene among 108 candidates in a ~10-Mb interval mapped in a case of pediatric cataract. Later, independent human mutations in *TDRD7* were identified in a consanguineous family with recessive inherited congenital cataract. Since these findings, *iSyTE* has greatly expedited gene discovery in the lens, leading to the identification of several new cataract-associated genes (*Pvrl3*, *Sep15*, *MafG*, *MafK*, *Celf1*) and has contributed to the understanding of many other important regulatory pathways in the context of lens biology (*e.g. Sip1*, *CBP*, *p300*, *Caprin2*, *Zbtb8b etc.*) (Lachke *Science*, 2011; Kasaikina,. 2011; Lachke 2012; Wolf , 2013; Manthey, 2014). These findings indicate the significance of *iSyTE* as an effective tool for identifying genes associated with lens biology and cataract.

Gene	Chr	Interval Size (Mb)	No. Genes	*iSyTE* Rank	Reference
BFSP1	20	5.43	22	1	16
BFSP2	3	17.88	106	1	17
CHMP4B	20	3.03	43	34	18
CRYAA1	21	2.79	37	1	19
CRYAB	11	21.08	99	1	20
CRYBA1	17	15.20	129	1	21
CRYBA4	22	0.40	6	1	22
CRYBB1	22	2.54	21	2	23
CRYBB2	22	1.47	5	2	24
CRYBB3	22	3.76	31	1	25
CRYGC	2	32.97	129	1	26
CRYGD	2	32.97	129	2	26
CRYGS	3	2.76	31	1	27
EPHA2	1	5.75	67	1	28
FYCO1	3	12.21	191	21	29
GCNT2	6	5.26	21	7	30
GJA3	13	8.69	50	1	31
GJA8	1	46.04	299	1	32
HSF4	16	11.41	102	2	33
**LIM2*	19	6.71	103	1	34
MAF	16	5.01	18	1	35
MIP	12	24.00	144	1	36
PXDN	2	6.68	18	1	37
TDRD7	9	21.08	108	1	38

Figure 7. *iSyTE* rank for known genes linked to congenital non-syndromic cataract in humans. Majority of the genes (88%) are scored as the number 1 or 2 candidate gene from several within the originally mapped interval (Lachke SA et al., 2012).

1.9 Mutations in Tdrd7 Cause Juvenile Cataracts

Although transcriptional regulation of gene expression in lens development is well defined, the significance of post-transcriptional control of gene expression remains relatively uncharacterized. Furthermore, although RNA granules are critical in post-transcriptional control, their function in mammalian development and organogenesis has not been explored. Tdrd7 is a component of RNA granules in the sperm and lens. Furthermore, *Tdrd7* nullizygosity in mouse causes cataracts and spermiogenesis defects (Lachke et al. 2011).

In humans, *TDRD7* deficiency causes cataracts in two separate pediatric cases. The first case was ascertained through the Developmental Genome Anatomy Project (DGAP, www.bwhpathology.org/dgap), which was of a male patient designated DGAP186 presented with juvenile cataract and hypospadias had a *de novo* balanced paracentric inversion of chromosome 9, 46, XY, inv(9)(q22.33a34.11). This breakpoint disrupted *TDRD7* and caused reduced expression of the gene in patient lymphoblastoid cells, suggestive of *TDRD7* haploinsufficiency (Lachke et al. 2011).

The second independent case of human congenital cataracts involved four siblings that inherited an in-frame triplet deletion mutation in *TDRD7*, which was inherited in an autosomal recessive manner within a consanguineous family. Sequencing confirmed the novel in-frame three base-pair deletion, which is predicted to lead to the deletion of an amino acid V618 that is conserved from fish to human. This variant was not detected in over 300 ethnically matched controls and was

predicted to disrupt TDRD7 protein structure and therefore considered likely to represent a loss of function mutation (Lachke et al. 2011).

Recently, a study examined *TDRD7* polymorphisms in age related cataract in human patients. Five single nucleotide polymorphisms (SNPs) were identified within the *TDRD7* gene and one SNP, rs10981985, was found to be associated with age related cataract in dominant and allele dose genetic models. SNP, rs10981985 was found in the 5' flanking region of Tdrd7 where two transcription factors were predicted to interact with it: HSF2: Heat shock factor protein 2, and LYF-1: lymphocyte-specific DNA-binding protein. The rs10981985 A allele, was found to be lower in patients with cortical age related cataract compared to control subjects. This led the authors to hypothesize that the rs10981985 G to A polymorphism could have a protective effect within the Han Chinese population (Zheng, C. et al. 2013).

Considering these data, I hypothesized that Tdrd7 has an essential function in post-transcriptional control of gene expression in the mammalian lens. The specific aims of my Master's thesis tested this hypothesis by performing detailed phenotypic and molecular characterization of the lens tissue in the *Tdrd7-/-* germline targeted knockout mouse mutant. The *Tdrd7* deletion mutant mice used in this thesis were generated by Dr. Shinichiro Chuma's group (Kyoto University, Japan) and represent an independently derived *Tdrd7* null mouse mutant model in addition to the ENU mutagenesis line originally reported in Lachke et al. (2011). Thus, this thesis focused on characterization of ocular defects in this *Tdrd7-/-* germline targeted knockout mouse mutants.

This thesis describes a multi-disciplinary experimental approach to gain novel insights into the molecular and cellular basis of the lens pathology exhibited in *Tdrd7*-/- mutants. This research has led to the identification of a novel Tdrd7 function in the regulation of fiber cell structure through direct interactions of regulators with the actin cytoskeleton.

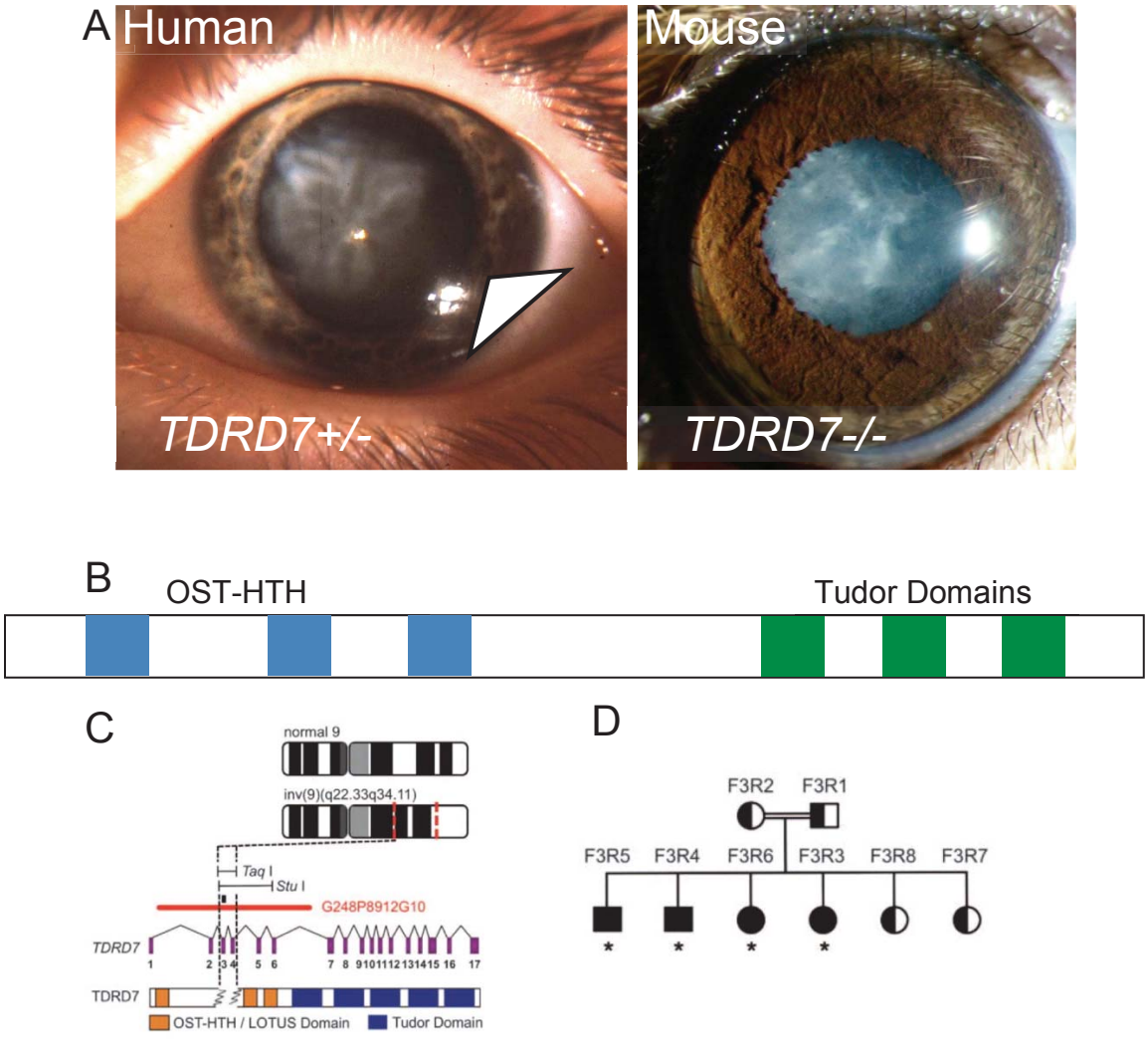

Figure 8. Tdrd7 deficiency causes cataract in human and mouse. (A) The image on left represents the eye of a pediatric patient with severe cataract at age two years. The image on right represents the eye of a Tdrd7 null mouse mutant, also exhibiting severe cataract at age 3 month. Tdrd7 contains three OST-HTH domains as well as three Tudor domains that bind to RNA and methylated arginines residues within other proteins, respectively (B). Image C represents the paracentric inversion of chromosome 9 in pediatric patient; inversion breakpoints are shown by red lines and the dotted black line marks breakpoint that disrupts TDRD7 within the 2.6-kb region shown and in TDRD7 protein. Image D indicates the autosomal recessive congenital cataract within a family with TDRD7 mutation (Lachke et al. 2011).

METHODS AND MATERIALS

1.10 Animals

All animals were treated in accordance with the protocols established by the Association for Research in Vision and Ophthalmology (ARVO). The Animal Care and Use Committee of The University of Delaware approved all experimental protocols involving mutant mice and their controls. The target germline knockout strain studied has been designated *Tdrd7*$^{tm1.1Chum}$; and strain of origin is (C57BL/6J x 129S6/SvEvTac) for F1. One loxP site was inserted upstream of exon 8 and an FRT flanked PGK-neomycin selection cassette together with a second loxP site was inserted downstream of exon 12. Exons 8-12 were subsequently removed by cre excision (Tanaka, T et al. 2011). Wild type ICR outbred mice were obtained from Harlan Laboratories (Frederick, MD) and used for *in situ* hybridization, immunofluorescence, and RNA expression analyses. Mice were housed in a 14 h light to 10 h dark cycle, and mutant and littermate control mice were housed together to control for cage-dependent differences.

1.11 DNA Isolation for Mouse Genotyping

PCR amplification was performed on the BioRad® T100 Thermal Cycler (Hercules, CA). Mouse tail tissue for DNA isolation was obtained according to IACUC regulations; approximately 1 cm of tail tissue was used. The Puregene® Genomic

DNA Purification Kit (Gentra Systems, Minneapolis, Minnesota) was used for genomic DNA isolation. Freshly excised mouse tail samples were placed in microcentrofuge tubes on ice and stored at -80°C for long term storage. For cell lysis, 300 µl Cell Lysis Solution and 1.5 µl of 10mg/mL Proteinase K Solution (Invitrogen, Grand Island, New York) were added and the samples were mixed by inverting 25 times. Samples were incubated overnight at 55°C. For protein precipitation, samples were cooled to room temperature, and 100 µl of Protein Precipitation Solution was added to the cell lysate. Samples were then mixed by inverting 10 times, and centrifuged at 13,000 x g for 3 minutes to form a precipitated protein pellet. If a pellet did not form, the samples were inverted again followed by incubation on ice for 5 to 15 minutes and centrifuged again. After centrifugation, the supernatant was transferred to a new clean 1.5 mL centrifuge tube containing 300 µl of 100% isopropanol. Samples were then mixed by inverting gently approximately 30 times, and centrifuged at 13,000 x g for 5 minutes. The supernatant was then carefully removed via pipette. 300 µl of 70% ethanol was then added to the sample and inverted several times to wash the DNA pellet. The sample was centrifuged at 13,000 x g for 5 minutes, and the ethanol was carefully removed via pipette. The samples were drained on a clean absorbent paper and allowed to air dry for 30 minutes. Finally, to rehydrate the DNA, 30 – 100 µl of DNA Hydration Solution was added to the samples, and allowed to rehydrated at 65 °C for 1 hour. Samples were then gently mixed overnight on a shaker at 100rpm for DNA to enter into solution. Once the DNA was isolated,

the samples were quantitated with the NanoDrop® ND 1000 Spectrophotometer (NanoDrop, Wilmington, Delaware) and stored at 20 – 25 °C (RT) until needed.

1.12 Mouse Genotyping

Samples were prepared for PCR (polymerase chain reaction) by adding 2.5 µl of CoralLoad PCR Buffer (Qiagen, Valencia, California), 1.25 µl Dimethyl Sulfoxide, Fisher BioReagents™ (Thermo Fisher Scientific, Waltham, Massachusetts Waltham, MA), 18.125 µl Nuclease Free water, 0.5 µl each of the forward and reverse primers and 1 µl of genomic DNA to a 0.2 mL PCR micro-centrifuge tube (VWR, Radnor, PA). Samples were evenly mixed by inverting and spun down. The samples were then placed into the BioRad® T100 Thermal Cycler PCR machine, and the appropriate cycling program was used. The thermo cycler settings are as follows: 5 minutes at 95^{o}C, 30 seconds at 95^{o}C, 1 minute at 56 ^{o}C 30 seconds at 42^{o}C, repeated 35X and stored at 4^{o}C until needed. Once the PCR program was completed, 24 µl of sample was loaded onto a 1% agarose gel with a final concentration of 0.01% ethidium bromide (EtBr)(Thermo Fisher Scientific, Waltham, Massachusetts). PCR products were then size separated by electrophoresis, using approximately 100 volts for 30 – 45 minutes. A 100 bp DNA Ladder (Thermo Fisher Scientific, Waltham, Massachusetts) was used as a marker for DNA band sizes. Agarose gels were imaged on the GelDoc-IT® ^{2} 310 Imager (UVP Upland, CA).

Primer	Forward	Reverse	Band Size
Tdrd7-WT-g	5' GAG TAA CTC TGG GCG CAG TC 3'	GCC ATA GCA ATC AGT GAG CA 3'	250 bp
Tdrd7-KO-g	5' GTC TAA CCC ATT CAG GGA TGA AGA 3'	5' GAA TCC TCA CCA GTT AGC CTC ACC 3'	500 bp

1.13 Isolation of Embryos

Mice were euthanized according to IACUC standards. For embryonic samples, mouse crosses were set up the evening and were tested for a vaginal plug early morning the next day. If a plug was detected, the developing embryo was considered to be at day 0.5 post coitum (dpc). For specific embryonic stages, pregnant females were euthanized on the appropriate day after a vaginal plug was observed. Using forceps, the skin anterior to the urethra was drawn up to tighten the skin for cutting. Scissors were then used to cut from the urethra, cutting along the ventral midline until at the rib cage, opening the body cavity. Secondary incisions were then made perpendicular to the primary incision on either side of the lower abdomen to open the body cavity.

The uterus with embryos was then removed from the body cavity, and the embryos were removed from their embryonic sacs and placed in 1X PBS for further dissection. If embryonic tissue was required for use in immunostaining experiments, the head tissue was incubated with 4% PFA for 30 minutes shaking on ice, washed

with 1X PBS for 10 minutes and then transferred to 30% sucrose over night. After the embryonic head tissue was saturated in 30% sucrose overnight, it was transferred to a 1:1 mix of 30% sucrose and Tissue-Tek® O.C.T. Compound (optimum cutting temperature)(Sakura® Finetek, Torrance, California) for approximately 1-2 minutes. The samples were then transferred to 100 percent O.C.T. for approximately 1-2 minutes. The embryonic head was then embedded in a Tissue-Tek® Cryomold® (Sakura® Finetek, Torrence, California) filled with O.C.T. Compound and immediately placed on dry ice, to freeze the samples and stored at -80°C.

1.14 Light Microscopy

Eyes were dissected from mutant and control mice and carefully cleaned in 1x phosphate buffered saline (PBS) solution under a Nikon SMZ1500 (Melville, NY) dissecting microscope. Eyes were photographed under light field and dark field optics. Lens was extracted, cleaned, and imaged in 1X PBS using a Zeiss Axiophot light microscope (Carl Zeiss Microscopy, Thornwood, NY).

1.15 Histology

For histologic analysis, whole eyes were fixed in 4% paraformaldehyde (PFA) for 18h, washed with 1X PBS for 10 minutes, and then transferred to 70% ethanol, and stored at 4°C until paraffin embedding. Paraffin-embedding was performed at the Comparative Pathology lab at the College of Agriculture and Natural Resources, University of Delaware. Sections (6 μm) were prepared, stained with H&E, and

photographed on an upright microscope a Zeiss Axiophot light microscope (Car Zeiss Microscopy, Thornwood, NY) by standard methods.

1.16 Scanning Electron Microscopy (SEM)

For scanning electron microscopy whole eyes were fixed in a solution of 0.08 M Sodium Cacodylate buffer pH 7.5 (Electron Microscopy Sciences, Hatfield, PA, USA), 1.25 gluteraldehye (Electron Microscopy Sciences) and 1% paraformaldehyde (Electron Microscopy Sciences) for 5 hours at room temperature. The lenses were then dissected from the eye and transferred to fresh fixative for an additional 48 hours at room temperature. After this incubation, the lenses were washed in 1X PBS for 10 minutes. With two lenses per animal, one was peeled to expose cortical fiber cells, while the second was peeled to expose nuclear fiber cells. Peeled lenses were then processed through an ethanol dehydration series (25%, 50%, 70% 100%) with exposure to each dilution for 10 minutes. The lenses were then subjected to a 2.5-hour 100% ethanol incubation. The lenses were critical point dried using an incubation series of hexamethyldisilazane (Electron Microscopy Sciences) (33%, 66%, 100%, diluted in ethanol). Dried lenses were mounted on aluminum stubs and coated with gold/palladium for 3 minutes. Samples were viewed with a field emission scanning electron microscope Hitachi S-4700 (Tokyo, Japan). SEM analyses were performed on three biological replicates for control and mutants.

1.17 Immunofluorescence Staining

All immunofluorescence experiments were performed as previously described (Lachke et al.; 2011). Briefly, lenses were isolated fixed in 4% PFA for 30 minutes

and transferred to 30% sucrose overnight. Then lenses were transferred to a succession of 1:1 of 30% sucrose and OCT and then 1:3 of sucrose to OCT and then and 100% OCT (OCT, Tissue Tek, Torrance California). Once in OCT eyes were immediately embedded in Optimum Cutting Temperature media and frozen using dry ice (OCT, Tissue Tek, Torrance California). Fourteen μm thick sections were cut with a cryostat and mounted on ColorFrost plus slides (Fisher Scientific, Hampton, New Hampshire). For staining with most antibodies, sections were fixed previously in 4% Paraformaldehyde (PFA) for 30 minutes at 4°C. Sections were blocked in 5.0% chicken serum for 1 h at room temperature, followed by an incubation with the appropriate dilution of primary antibody overnight at 4°C. Sections were then washed three times for 10-minutes each and detected with the appropriate AlexaFluor 594 labeled secondary antibody (Molecular Probes, Eugene Oregon) prepared in 1% chicken serum and then mounted with VECTASHIELD® containing DAPI (Vector Biolabs, Burlingame, CA). Slides were then visualized using a Zeiss LSM 780 confocal microscope (Carl Zeiss Inc, Göttingen, Germany). Identical conditions were used to do the imaging of each antibody at different ages to ensure the validity of comparisons.

1.9 Lens Dissections

Lenses were collected from *Tdrd7*+/- heterozygous and *Tdrd7*-/- germline knockout mice at P4 for RNA isolation (if not stated otherwise, at least 10 lenses per biological replicate; three independent biological replicates analyzed for each genotype). Lenses

were dissecting in RNase, DNase free 1X PBS, in RNase DNase free petri dishes, using micro-dissection, during which the retina, blood vessels, and cornea were carefully removed with forceps that were also sprayed with RNAse away as well as 70% ethanol. Lenses were then flash frozen on dry ice and then stored at -80°C until RNA isolation was performed.

1.10 RNA Isolation Total RNA Isolation

Lenses were collected from *Tdrd7+/-* heterozygous and *Tdrd7-/-* germline knockout mice at stage P4 as described. From each genotype (control or null mutant), lenses were collected as $n = 15$ per biological replicate and for three independent biological replicates. Lenses flash frozen and stored at -80°C were thawed on ice. RNA isolation was performed using the mirVana™ (Ambion®) miRNA isolation kit, (Life Technologies, Grand Island, NY) following the supplier recommended protocol for total RNA isolation.

1.11 Small and Large RNA Isolation

RNA isolation was performed using the mirVana™ (Ambion®) miRNA isolation kit, (Life Technologies, Grand Island, NY) following the supplier recommended protocol for large and then small RNA separately from the same sample.

1.12 cDNA Synthesis

Total RNA (2 µg) was used to synthesize cDNA using Bio-Rad iScript™ cDNA Synthesis Kit (Bio-Rad Laboratories, Hercules, CA). For cDNA synthesis reactions, the RT Cocktail was prepared using the RT buffer, primer mix and enzyme mix provided in the kit, the specifications are as follows: RNA was diluted to 0.5 µg/ul, and used to prepare cDNA by adding RNase/DNase free water, iScript Pre-mix (5x), and iScript Enzyme (reverse transcriptase) in a PCR tube. Total volume 20 µl. The reaction parameters are as follows: Incubate complete reaction mix: 5 minutes at 25ºC, 30 minutes at 42ºC, 5 minutes at 85ºC, Hold at 4ºC (optional).

1.13 Quantitative Reverse Transcription-PCR (qRT-PCR)

Quantitative Reverse-Transcription PCR (qRT-PCR) was performed using RealMasterMix Fast Probe Kit (5 PRIME, Gaithersburg, MD) on the ABI 7500 Fast Real-Time PCR System and Software v2.0.3 (Applied Biosystems: Carlsbad, CA). All samples were prepared in a 96-well reaction plate with three biological replicates and technical triplicates. The master-mix was prepared as follows: 8.5 µl molecular grade water, 10 µl 5PRIME RealMasterMix Fast SYBR Low ROX, 0.5 µl of forward and reverse primers each, and 0.5 µl of cDNA per sample. The following cycling conditions were used for all experiments: 40 cycles of 30 seconds at 95^{o}C, 15 seconds at 58^{o}C and 15 seconds at 68^{o}C. A select list of differentially regulated genes, identified by microarray analysis, was used for validation and is provided in supplemental Table 1. Mean fold change (F.C.) was calculated using log (base 10)

transformed data in a nested ANOVA by determining the mean and standard deviations. These values were then back transformed to obtain the final F.C. values.

1.14 RNA Sequencing

The University of Delaware Sequencing and Genotyping Center performed all RNA-Sequencing and the following preparations. Messenger RNA was purified from the total RNA samples using Oligo dT conjugated magnetic beads, and converted to adaptor-tagged, paired-end fragments which were then used for cluster generation onto a TruSeq v3 flow cell according to the Illumina® TruSeq™ RNA Sample Preparation Kit v2. Sequencing was carried out using the SBS Sequencing Kit on an Illumina HiSeq 2000 Sequencer (University of Delaware Genotyping and Sequencing Center). The images were analyzed using the Illumina Pipeline software (version RTA 1.13.48/CASAVA 1.8.2), and bases were called and translated to generate FASTQ sequence files. The preparation and sequencing procedures did not deviate from standard protocols and the procedure for large RNA-Seq was performed as per the manufacturer's recommendations. The library preparation was Illumina TruSeq Directional RNA, sequencing was performed on a 2x75 paired end run using the Illumina HiSeq 2500.

1.15 Bioinformatics Analysis of RNA-Seq Data

Bioinformatics processing was performed in collaboration with Dr. Shawn Polson at the University of Delaware Center for Bioinformatics and Computational

Biology Core facility. Support from the University of Delaware Center for Bioinformatics and Computational Biology Core Facility was made possible through funding from the NIH National Institute of General Medical Sciences (8 P20 GM103446-12), and National Science Foundation EPSCoR (EPS-081425).

Quality of Illumina reads was assessed using CLC Genomics Workbench Quality Assessment tool (v. 6.5). Reads were end-trimmed to remove adapter sequence, obtain a minimum average sequence quality ($Q \geq 0.01$), and to allow a maximum of one ambiguous base per read using the Trim Sequences Tool in CLC Genomics Server (v. 5.5). After trimming, reads below 50 bp were discarded. Remaining intact pairs were mapped to the Mouse reference genome (version GRCm38.73 as downloaded from ENSEMBL) using the CLC Genomics RNAseq mapping tool (80% identity over 80% of query). For C1 and C2 and T2 and T3, 92-96% of the reads mapped to the reference; however for C3 and T1, only about 60-65% of reads map to reference; these reads were then not used in further analysis. Mapping pairs were compared to the reference annotation to obtain raw counts (unique and total exon reads) for both genes and transcripts (isoform). All targets (genes/transcripts) with a minimum of 1 count per million in two samples were considered for differential expression analysis. Count data was subjected to differential expression analysis in R/Bioconductor (v. 3.0.1) using the EdgeR package (v. 3.2.4). *P*-values were adjusted for multiple comparisons using the method of FDR method of Benjamini & Hochberg (1995). Further annotations were linked from ENSEMBL Biomart using the biomaRt R package (v. 2.16.0).

1.16 Phalloidin Whole Mount Staining of Lens

Lenses were dissected from the eye, fixed for 2 h in 4% paraformaldehyde (PFA, washed three times for 15 min each in PBS with 0.1% Triton X-100, and stained in PBS with 0.25% Triton X-100, a 1:2,000 dilution of DAPI, FluoroPure™ grade (Invitrogen, Grand Island, NY), and 1:200 Alexa Fluor 561–labeled phalloidin (Molecular Probes, Eugene, Oregon) overnight at 4°C. Lenses were subjected to three 15-min room temperature washes in 0.1% Triton X-100 in PBS before storage in PBS at 4°C. Whole stained lenses were placed epithelial side down in an uncoated 35-mm #1 glass-bottom culture dish (MatTek Corp., Ashland, MA) filled with 1 percent agarose gel cover the bottom and 1X PBS as a buffer for imaging and imaged in the XY plane with a LSM 780 VIS confocal microscope fitted with a 20X dipping objective lens, a 30-mW argon krypton laser, and a 5-mW helium-neon laser (Carl Zeiss)

1.17 Wheat Germ Agglutinin Staining of the Lens

For wheat germ agglutinin (WGA), P4 and P22 sections were fixed previously fixed in 4% Paraformaldehyde (PFA) for 45 minutes at 4°C. Sections were blocked in 2.5% BSA (Fisher BioReagents™ Thermo Fisher Scientific, Waltham, Massachusetts Waltham, MA) for 1 h at room temperature, followed by an incubation with 1:200 dilution of primary antibody Wheat Germ Agglutinin, Alexa Fluor® 488 Conjugate (Molecular Probes, Eugene, Oregon) and DRAQ5™ (BioStatus Limited, Leicestershire, United Kingdom) for 1 hour at room temperature. Sections were then

washed three times for 10-minutes each and then mounted with 1 drop of *p*-phenylenediamine antifade media. Slides were then visualized using a Zeiss Elyra PS1 super resolution microscope (Carl Zeiss Inc, Göttingen, Germany). Identical conditions were used to do the imaging of each antibody at different ages to ensure the validity of comparisons.

1.18 Protein-Protein Interaction Mapping Combined with *iSyTE* Expression

Protein-protein interaction information on human TDRD7 was obtained from the NCBI database. Protein-protein interaction data was also obtained via the Human Protein Reference Database or BioGrid[3.2]. These interactions were documented with references shown in the PubMed database and only interactions that met one of the following criteria were considered valid: Two-hybrid, Affinity Capture-MS, Two-hybrid, Affinity Capture-Western. In particular, co-localization of protiens was not considered validation of protein-protein interactions. Once proteins that interact with Tdrd7 were identified, these were then also investigated for their own interacting proteins, hereby termed "nearest neighbors" of Tdrd7. Proteins that directly interacted with Tdrd7 as well as its nearest neighbors were searched within the *iSyTE* database for their highest ranking, representative of lens-enrichment. Each protein that Tdrd7 was found to interact with as well as its nearest neighbors arising from that interacting protein, were all grouped together for analysis. Once the Tdrd7-protein intereactome was completed and combined with *iSyTE* data, heatmap colors were assigned to proteins according to their *iSyTE* values. Any *iSyTE* ranking under 300 (highest lens

enrichment) were assigned the color ED1C24, a bright and deep red. *iSyTE* rankings from 301- 500 (high lens enrichment) were assigned the color E34128, a lighter red. *iSyTE* rankings from 501- 1000 (medium lens enrichment) were assigned the color F37E72, a salmon pink color. *iSyTE* rankings from 1001- 2000 (lens enrichment) were assigned the color FDE3E0 a light pink. *iSyTE* rankings over 2000 (non-lens enriched) were assigned the color E6E7E8, a light gray. Thus, the color-coding of the protein interactions gave indications of their enrichment specifically for the lens, in turn prioritizing clusters and potential high-priority targets of Tdrd7 within its network of protein interactions. Finally, the Tdrd7-protein-protein interaction network was interrogated for candidates that were also differentially expressed in *Tdrd7-/-* mutant lens according to RNA-Seq analysis.

1.19 RNA Immunoprecipitation

Postnatal day 15 (P15) wild-type ICR lenses (15-20) were dissected and used with the 17-700 | Magna RIP™ RNA-Binding Protein Immunoprecipitation Kit according to the manufacturer's protocol. This method differed from the machufacture's protocol in that lenses were freshly dissected and transferred into lysis buffer instead of PBS. The protocol is as follows:

Freshly dissected lenses were washed freshly three times with ice-cold PBS and then teased apart in lysis buffer. On average, $1–5\times10^6$ cells were needed to generate a sufficient amount of mRNP lysate for a typical immunoprecipitation reaction and therefore the goal was to obtain an extremely concentrated mRNP lysate

with approximately 20–50 mg/ml total protein in a volume. The cells were then pelleted by centrifugation and the cell pellet was lysed in ice-cold lysis buffer supplemented with RNase and protease inhibitors.

Magnetic beads were re-suspended by rotation, both control (Mouse IgG) and test samples (Tdrd7 antibody) were first incubated with 50 µL of magnetic beads and wash buffer vortexed and placed on a magnetic separator; this process was repeated twice and then only 100 µL of wash buffer was added with ~5 µg of the antibody of interest to the tube. The tubes were then incubated with rotation for 30 minutes at room temperature. The tubes were then centrifuged briefly and placed on the magnetic separator to remove the supernatant. Another 500 µL of wash buffer was added and the tubes were vortexed again briefly, again the tubes were placed on the magnetic separator and this process was repeated three times. The tubes were then placed on ice.

Once the beads and antibody was prepared, the RIP immunopreciptiation buffer was made containing 900 µL of buffer with 35 µL of 0.5 M EDTA and 5 µL of TNA inhibitor per reaction. The magnetic beads with antibody were placed on the magnetic separator one more time and the supernatant was removed and the 900 µL of wash buffer was added along with 100 µL of the thawed lysate. A control 10 µL of the supernatant of RIP lysate was also taken and placed into a new tube for "input". The tubes were then incubated with rotation overnight at 4°C. The next day, the tubes were centrifuged and placed on the magnetic separator to discard the supernatant. 500 µL of RIP Wash Buffer was added to each tube and vortexed briefly; the tubes were then

placed on the magnetic separator to discard supernatant. This was repeated five times to wash the beads a total six times with 500 µL of cold RIP Wash Buffer.

Each immunoprecipitate required 150 µL of proteinase K buffer containing 117 µL of RIP Wash Buffer, 15 µL of 10% SDS, 18 µL of 10 mg/mL proteinase K. Each immunoprecipitate was re-suspend in 150 µL of proteinase K buffer and then incubated at 55°C for 30 minutes with shaking to digest the protein. After the incubation, the tubes were centrifuged briefly and placed on the magnetic separator. The supernatant was transfered into a new tube and 250µL of RIP Wash Buffer was added to each tube contacting the supernatant. 400 µL of phenol:chloroform:isoamyl alcohol was then added to each tubes followed by vortexing for 15 seconds and then centrifuged at 14000 rpm for 10 minutes at room temperature to separate the phases. 350 µL of the aqueous phase was carefully removed and placed in a new tube. This was followed by the addition of 400 µL of chloroform. The tubes were then vortexed for 15 seconds and centrifuged at 14000 rpm for 10 minutes at room temperature to separate the phases. 300µL of the aqueous phase was carefully removed and placed in a new tube. In each tube 50 µL of Salt Solution I, 15 µL of Salt Solution II, 5 µL of Precipitate Enhancer was then added followed by then 850 µL of absolute ethanol. The solution was then mixed and kept at -80°C overnight to precipitate the RNA.

The next day the tubes were centrifuged at 14,000 rpm for 30 minutes at 4°C and the supernatant were discarded carefully. The pellet was then washed once with 80% ethanol, centrifuged again at 14,000 rpm for 15 minutes at 4°C. The supernatant was again discarded and the tubes were then carefully opened to air dry the pellets.

Once the pellets were dry they were then re-suspended in 10 to 20 μL of RNase-free water, and stored at -80°C for downstream analysis including RT-PCR after quality assessment and quantification.

1.20 Two-Dimensional Gel Electrophoresis and Mass Spectrometry

1.20.1 2-D Gel Electrophoresis (2-DE)

These experiments were performed in collaboration with Dr. Robert Mason's laboratory at Alfred I DuPont Hospital for Children. The 2D-DIGE experiments were performed in collaboration with the Cell Science Core Laboratory at the Nemours Alfred I duPont Hospital for Children. P4 and P15 lenses were lysed in DIGE lysis buffer containing 7M urea, 2M thiourea, 4% CHAPS, 30mM tris at pH 8.5. Resulting supernatants were precipitated using a TCA protein precipitation procedure with an acetone wash (2-D Clean Up Kit, GE Lifesciences). Samples were resuspended in DIGE lysis buffer, pH was adjusted to 8.5, and 40 μg of each sample was DIGE labeled using 200 pmole of CyDye per 40 μg of protein (DIGE Minimal Labeling Fluor, GE Lifesciences). A pooled internal standard was generated using 10 μg of each sample and DIGE labeling with a separated CyDye fluor.

1.20.2 Protein and Peptide Identifications

This project was made possible by the Nemours Center for Pediatric Research that is supported by a grant from the NIH National Institute of General Medical

Sciences - NIGMS (P20GM103464). This project was done in collaboration with the laboratory of Dr. Robert Mason. First dimension, isoelectric focusing, was performed using 24 cm immobilized pH gradient (IPG) strips with a non-linear pH gradient of pH3 to 10 (ReadySrips IPG Strips, Bio-Rad Labs) for a total of 40.5 kVh over 9 hours on a IPGphor II (Amersham Biosciences). IPG strips were rehydrated in buffer containing 10 µg experiment protein sample, 10 µg control protein sample, 8 µg pooled internal sample, 7M urea, 2M thiourea, 4% CHAPS, 20 mM DTT, and 2% 3-10 pharmalyte. IPGs were equilibrated for 15 minutes twice in a SDS buffer containing 6 M urea, 30% glycerol, 2% SDS, 75 mM Tris-HCl pH 8.8 and either 65 mM DTT (first equilibration) or 135 mM iodoacetamide (second equilibration). Second dimension separation was performed on 24 x 20 cm of 10% acrylamide SDE-PAGE gels. Gels were imaged using a Typhoon Trio (GE Life Sciences) and analyzed using DeCyder 2-D Differential Analysis Software (GE Life Sciences). Additional pick gels were run by rehydrating IPGs in similar buffer with additional 500 µg or 800 µg of unlabeled P15 lens protein using the same procedure for first or second dimension regardless of total protein loaded. Pick gels were stained with Imperial Protein Stain (Thermo Fisher) and spots were matched to previous gels. This analysis demonstrated that spot 951 was significantly reduced in the P15 experimental group compared to control (P=0.039, average ratio -1.64). Spot 951 and a nearby lower MW spot were excised. The lower MW was not significant, but it was picked to see if spot 951 was a post-translational modification of the same protein. Excised spots were sent

for identification at the Proteomics and Mass Spectrometry Core Facility at Delaware Biotechnology Institute for identification.

We acknowledge Leila Choe at the UD Proteomics and Mass Spectrometry Facility, supported in part by the Delaware INBRE, NIH grant number 8 P20 GM103446-13, for portions of this work. Gel spots of interest were excised for analysis. The enzymatic digestion procedure was performed with trypsin (Promega) at 37C as previously described (Finehouse EJ and Lee KH, 2002) and included reduction/alkylation with dithiothreitol (BioRad) and iodoacetamide (Sigma), respectively. Subsequently, samples were desalted and concentrated using Ziptips (Millipore) and applied to a target plate with alpha-Cyano-4-hydroxycinnamic acid matrix (Sigma). Data were collected on a 4800 MALDI TOFTOF Analyzer (ABSciex) in positive ion, reflector mode over a mass range of 850-4000 m/z. Select peaks were further analyzed by tandem mass spectrometry (MS/MS) at 1kV with default calibration. The combined MS and MS/MS data were submitted to Mascot v2.4 (Matrix Science) and searched against NCBI (*Mus musculus* taxonomy), with trypsin specificity, 300ppm mass tolerance, 0.3Da MSMS tolerance, and the following variable modifications: carbamidomethylation (C) and oxidation (M). Protein identifications were made based on database matches of 99% confidence or greater, including three MSMS matches >99% confidence.

PHENOTYPIC CHARACTERIZATION OF LENS DEFECTS IN *TDRD7* KNOCK OUT MOUSE MUTANTS

Previously, Lachke et al. described that *Tdrd7* deficiency causes cataract in human, mouse and chicken (Lachke et al., 2011). Two different *Tdrd7* null mouse mutant models have been developed. Dr. Simon John's group at The Jackson Laboratory used an ENU mutagenesis screen to identify a mouse mutant carrying a C to T transition that generates a nonsense mutation in *Tdrd7* exon 13, which generates a null allele as demonstrated by western blot and immunostaining analyses (c.2187C>T (Q723X)) (Lachke et al. 2011). Dr. Shinichiro Chuma's laboratory has separately developed a *Tdrd7* targeted germline knockout mouse mutant that carries a deletion of exons 8-12 (Tanaka et al. 2011). The eye defects in *Tdrd7* ENU mutants have been characterized by Lachke et al. (2011), although not in profound detail. On the other hand, although the *Tdrd7* targeted germline knockout mouse mutants are reported to exhibit ocular defects including cataracts (Tanaka et al. 2011), these have not been characterized to any detail. Both *Tdrd7* mouse mutant models exhibit fully penetrant cataracts (Figure 9) that closely phenocopy the phenotype observed in human, and therefore the study of these models have the potential to provide unique insights into the pathophysiology of this disease.

Although the exact onset of the cataract phenotype may differ between the two *Tdrd7* null mutants, possibly reflecting their different strain background (targeted mutant is on C57Bl6 while ENU mutant is on C3H background), by postnatal day 30 (P30), both models exhibit a flattened iris and severe cataracts with an unmistakable posterior post-capsule rupture. The difference in the nature of the null mutant alleles could also account for the phenotypic variation within the age of onset. In my thesis, I focused on the characterization of the eye and lens defects in the less studied *Tdrd7* targeted germline knockout mouse henceforth referred to as *Tdrd7-/-* mouse mutants.

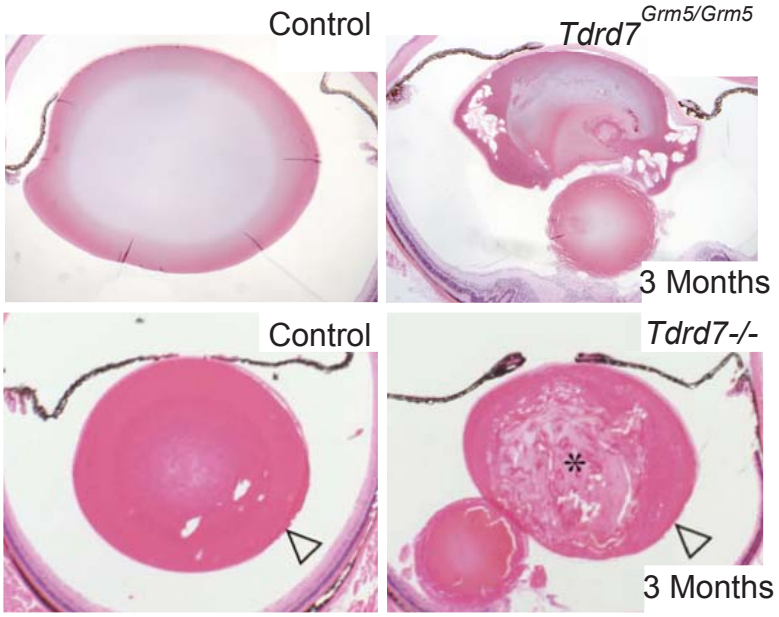

Figure 9. *Tdrd7-/-* Mutant Mouse Models. The top panel shows 3-month lens of the previously characterized (Lachke et al. (2011) Science) mouse mutant, which contains a nonsense mutation, c.2187C>T(Q723X). The *Tdrd7*^{Grm5} mouse mutant model was identified in an ENU mutagenesis screen in collaboration with Dr. Simon John (The Jackson Laboratory, Bar Harbor, Maine). The bottom panel of this figure displays the 3-month lens of the *Tdrd7* targeted knockout mouse mutant model developed by Dr. Schinichiro Chuma (Kyoto University, Kyoto, Japan) (Tanaka et al. (2011) PNAS) that has not been characterized. Left panels show the control animal lens, while the right panels show the lens from the two different *Tdrd7-/-*. Both mouse mutants show a severe lens defect that results in a posterior post capsule rupture.

1.21 Light Microscopic Analysis of Eye Phenotype in *Tdrd7* Mutants

I first validated that the *Tdrd7-/-* germline knockout mouse mutants exhibited lens defects and iris flattening at 3 months of age (Figure 10) as previously reported (Tanaka et al. 2011). To identify the earliest age when the ocular phenotypes are first evident, I analyzed *Tdrd7-/-* mutants at different stages to identify the exact onset of the cataract phenotype. I analyzed mutant lenses at stages P30, P28, P24, P22, and P18 by light and dark microscopy and grid imaging and found both eye defects to be fully penetrant as a result of *Tdrd7* nullizygosity in these stages except P18 (Figure 11). To identify the postnatal day stage between P18 and P22 when an ocular phenotype can be discerned, I carefully analyzed *Tdrd7-/-* eye and lenses at P19, P20, and P21 and observed no difference between mutant and controls at these stages. I conducted a thorough analysis of seven litters totaling 98 eyes and lenses at P18 and P22 stages and determined that P22 was the first stage that eye defects are detected in *Tdrd7-/-* mutants.

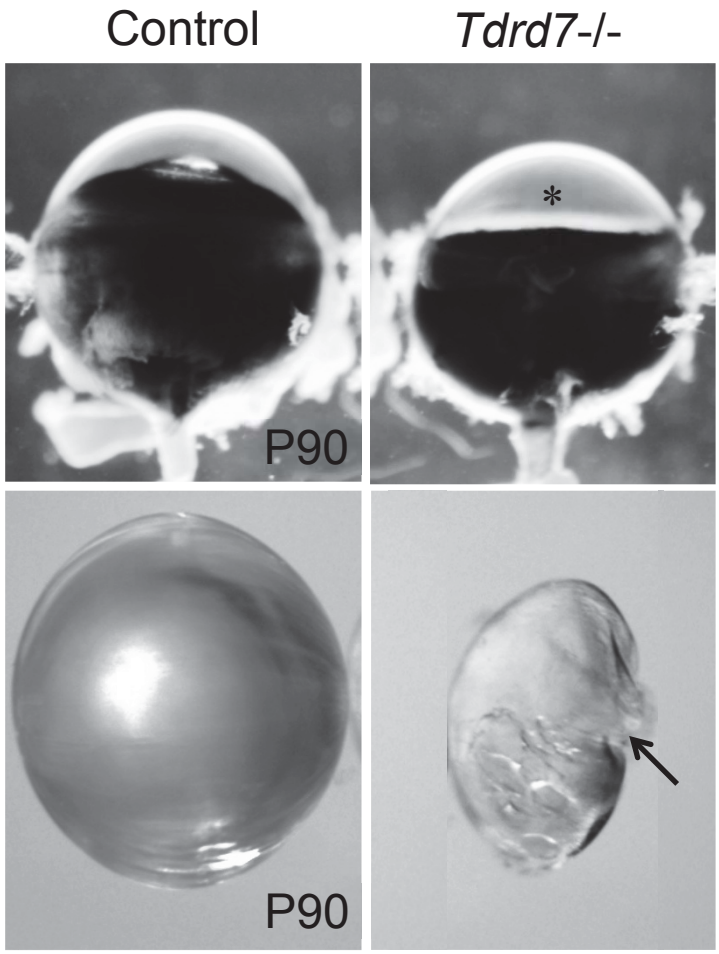

Figure 10. Presentation of ocular defects in 3-month (P90) old *Tdrd7-/-* mouse mutants as examined by light microscopy. The *Tdrd7-/-* eye shows a flattened iris and a smaller size lens with posterior rupture and cataract (Right panels). Conversely, the control (*Tdrd7+/-*) eye exhibits a normal iris and a clear lens (Left panels). The flattened iris is indicated by an asterisk. Arrow points to posterior capsule rupture in lens.

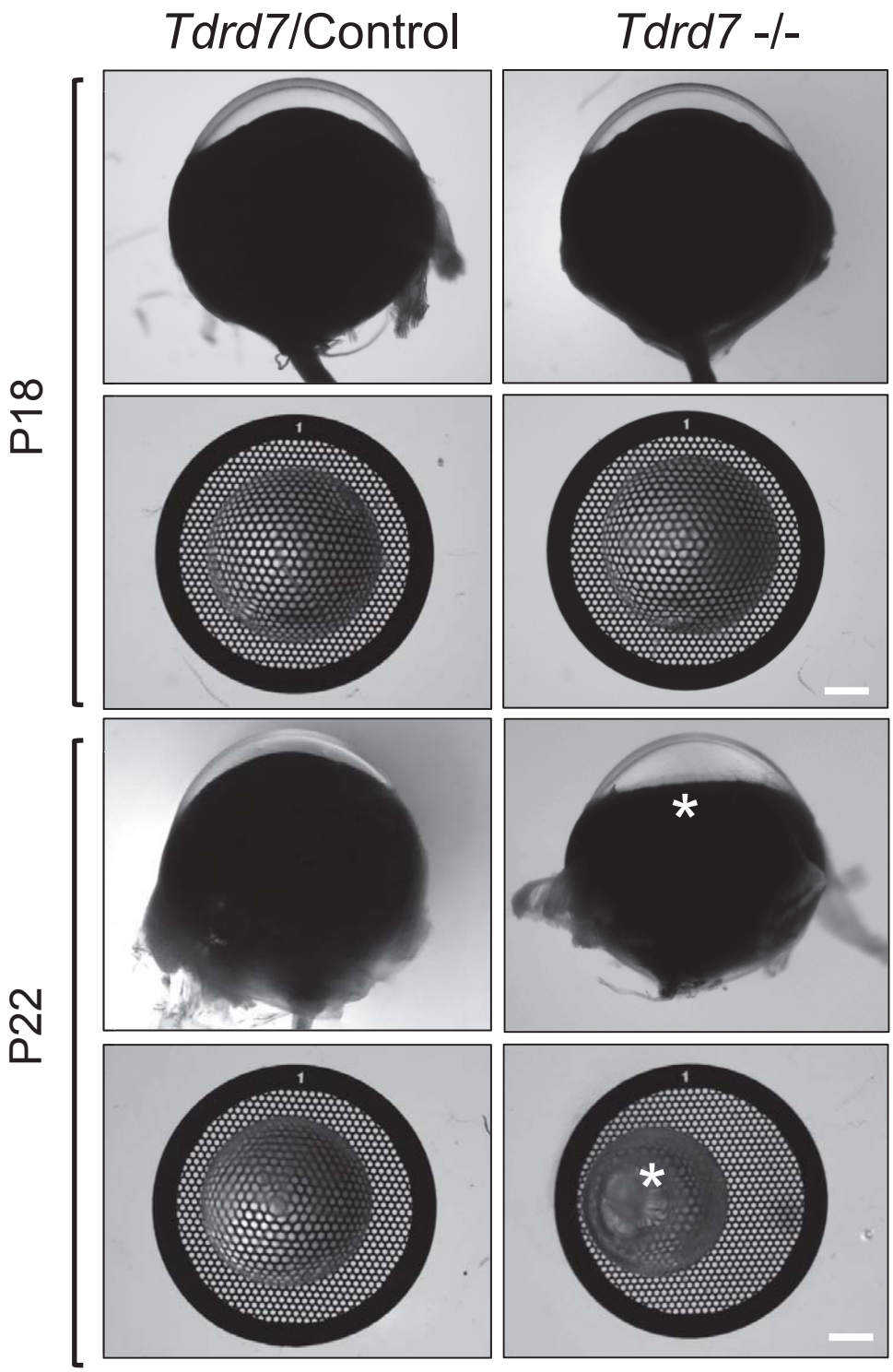

Figure 11. *Tdrd7-/-* germ-line knockout mouse mutants develop visible eye defects by at postnatal day 22. Light microscopy of control (*Tdrd7+/-*) (left) and *Tdrd7-/-* eye and lens (right) indicates no visible difference at postnatal day 18 (P18). However, at P22 (bottom panels), *Tdrd7-/-* mutants exhibit a flattened iris (asterisk, left image) and cataract (asterisk, right image) compared to control.

1.22 Histological Characterization of the Lens Phenotype in Tdrd7 Mutants

Since there was no observable phenotype in *Tdrd7-/-* eyes at P18 based on light microscopy, I next tested if histological analysis could distinguish lens abnormalities. *Tdrd7-/-* mutant and control (*Tdrd7*+/-) eye were characterized at the histological level for a wide range of developmental stages including early postnatal and embryonic stages. Although severe lens defects were observed at P30, when the *Tdrd7-/-* mutant lens exhibits disrupted structural morphology and posterior capsule rupture (Figure 12), no difference was observed between control and null lenses at P18 or earlier stages. The P22 *Tdrd7-/-* mutant lens shows mild defects in lens architecture as well as the beginning of a posterior rupture (Figure 12). From these data, I concluded that while histology could reveal interesting features of the defects in *Tdrd7-/-* lens at later stages (P30), this analysis was could not identify a robust phenotype at P22, which is better detected by light microscopy. This data indicates that light microscopy imaging is a more sensitive approach to detect lens cataracts than histological analysis.

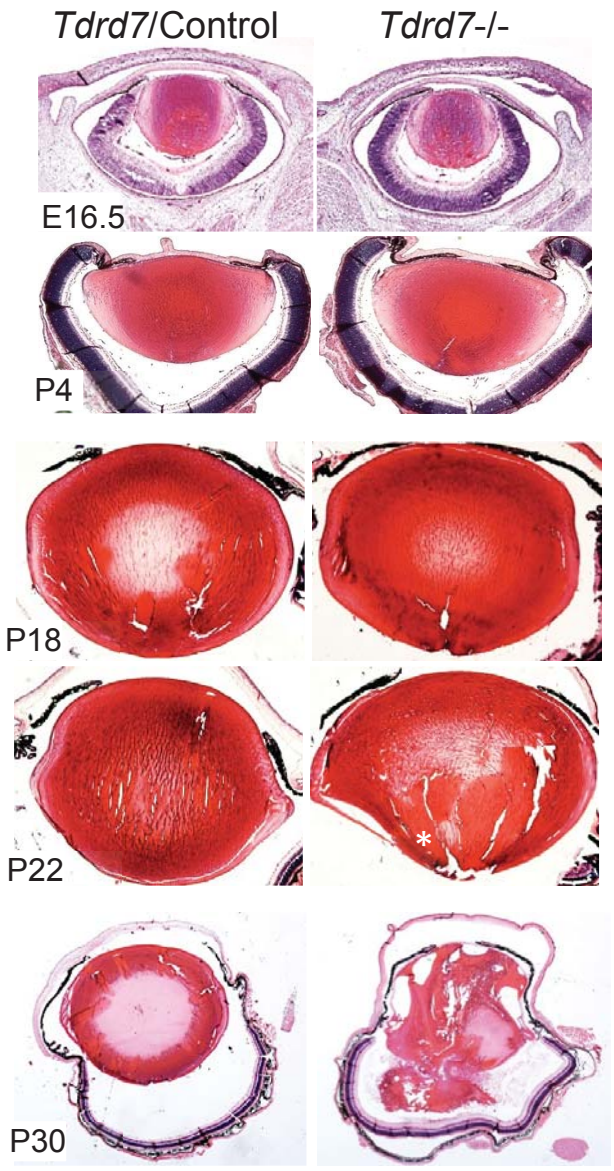

Figure 12. Histological characterization of *Tdrd7-/-* and control lenses. The left panel shows control (*Tdrd7+/-*) lens, while the right panel shows the *Tdrd7-/-* lenses at stages E16.5, P4, P18, P22, and P30. At P30 *Tdrd7-/-* lenses exhibit profound lens defects (asterisk) at 100% penetrance while subtle changes (asterisk) are detected at P22. No defect is discernable between mutant and control lenses at other stages.

1.23 Analysis of the *Tdrd7-/-* Lens Defects by Scanning Electron Microscopy

Histology-based analysis was not able to detect lens defects in stages earlier than the application of light microscopy, so I investigated the application of alternate high-resolution methods to characterize the *Tdrd7-/-* lens. Therefore, I performed scanning electron microscopy (SEM) on *Tdrd7-/-* and control lenses. Lens fiber cells assemble together in distinct fiber cell architecture. I hypothesized that SEM could potentially recognize the subtle defects in mutant fiber cells that are not distinguishable by other lower resolution methods.

The lens is a difficult tissue to examine using SEM because it lacks blood supply and therefore cannot be fixed by traditional methods. , Therefore, immersion fixation is the only method that can be utilized to effect its chemical presentations for adequate structural analysis (Kusak et al. 2004). Fiber cells have a granular cytoplasm composed of soluble proteins as well as crystallins, polysomes, and cytoskeletal elements including actin, intermediate filaments, and microtubules (Alcala and Maisel, 1985; Fitzgerald and Casselman, 1990; Ireland and Maisel, 1984).

There are two basic types of lateral membrane interdigitations between fiber cells that vary minimally in shape, size and periodic arrangement between species. The first type is a cellular outpocketing, termed the “ball”, and an invagination called as “socket”. Numerous such “ball” structures, regularly arrayed along the length of fiber cells, fit into complementary-shaped “sockets” formed between neighboring fiber cells of adjacent growth shells (Kusak et al 2004). The second type is a cellular

outpocketing, membrane protrusion, that originates from the angle formed by a board and narrow face of fiber cells. This is important since it fits into complementary-shaped imprint or groove formed on the narrow face of a neighboring fiber cell. These membrane interdigations are frequently characterized by patches of square array membranes (Kusak et al 2004).

Structural features of the apical, lateral, as well as the basal plasma membrane of fiber cells suggest cellular polarization. The apical membranes of fibers overlap in a precise manner with the other apical membrane fibers of the same growth shell to form anterior sutures. These intricacies that connect individual fiber cells within the lens resemble the interlocking parts of a zipper. The same phenomenon occurs with the basal membranes of fiber cells. The morphology of the apicolateral border of lens fibers is comparable to the apicolateral border of lens epithelial cells. These cells contain numerous micropinocytotic and endocytotic events, square array membranes with small amounts of gap junctions, and a lack of tight junctions (Kusak et al 2004). Fibers are moved progressively farther away from their source of nutrition as a function of lens development and growth and this cell-cell motif helps accommodate this cell specific obstacle (Kusak et al 2004).

For initial SEM analysis, *Tdrd7-/-* lenses were examined at stages after the onset of the cataract, allowing me to confirm that application of SEM could enable the visualization of a phenotypic defect. *Tdrd7-/-* lenses at P28 were examined first since these show presence of cataracts without overt lens capsule rupture. *Tdrd7-/-* lenses at P28 exhibit profound defects in cortical fiber cells (Figure 13).

Once it was established that phenotypic differences between *Tdrd7-/-* mutant and control (*Tdrd7+/-*) lens could be reproducibly detected by SEM analysis at stage P28, I proceeded to test earlier stages. Similar to P28, *Tdrd7-/-* lenses at P18 exhibited a membrane protrusion defect in cortical fiber cells. These data demonstrated that the onset of the lens defects in *Tdrd7-/-* mutants begins earlier than what could be discerned using histology and light microscopy. The changes in fiber cell morphology and packing as revealed by SEM analysis offer clue into the factors such as fiber cell morphology defects that may contribute to the development of cataract in *Tdrd7-/-* mouse mutants. These data lead to the conclusion that although cataracts are not observed until P22, already by P18, differences in fiber cell organization between the *Tdrd7-/-* mutant and control lenses is discernable by SEM.

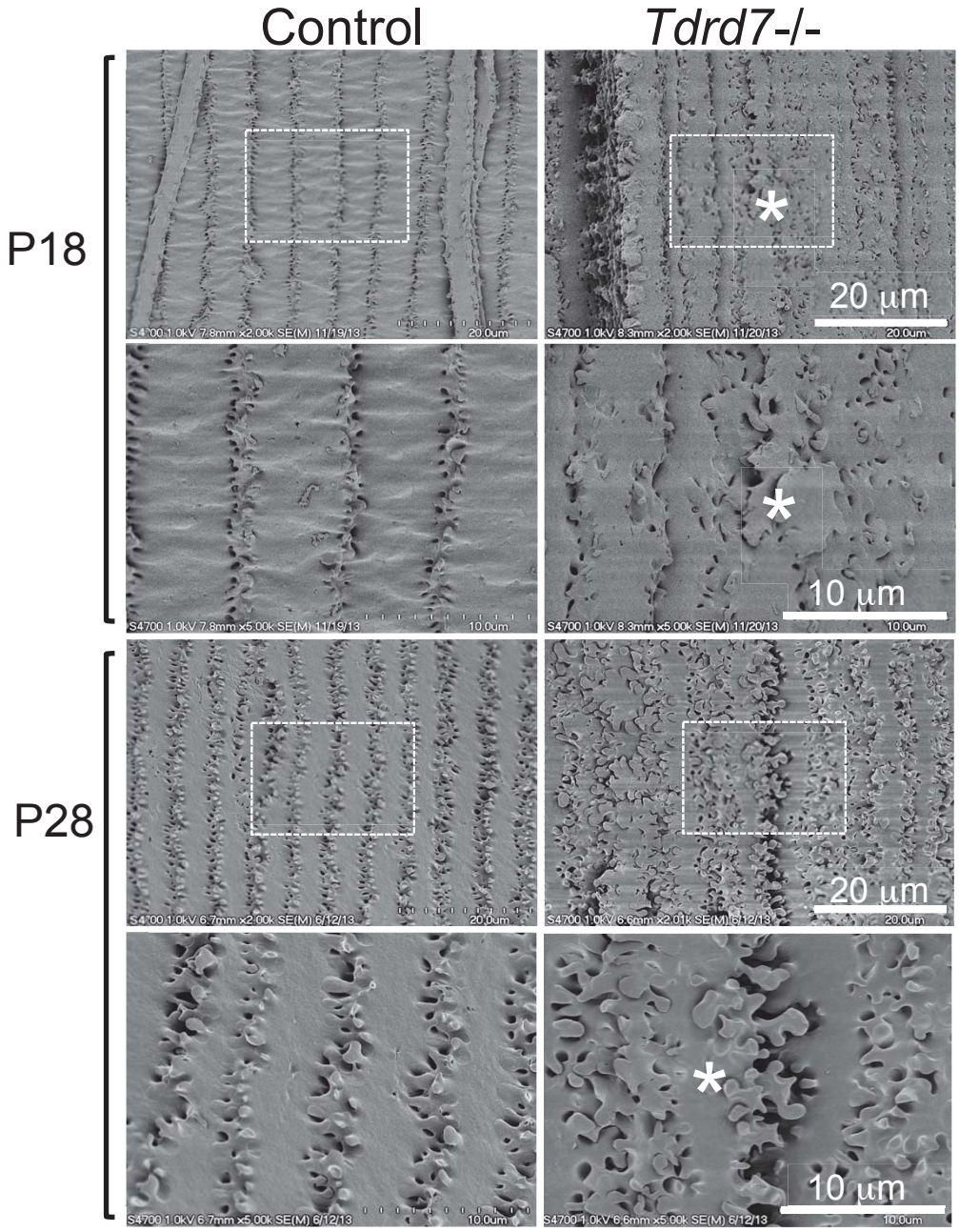

Figure 13. Scanning Electron Microscopy-based analysis of *Tdrd7*-/- Mouse Mutants Lens. The top panel shows no difference between control and null lenses. The bottom panel shows only a slight difference between the control and the null lenses. The *Tdrd7*-/- lens shows slight misshapen architecture as well as the beginning of a posterior rupture (noted by the asterisk).

1.24 Discussion

It has previously been shown that deficiency in *Tdrd7* causes eye defects including cataracts in human, mouse and chicken, however the onset of the lens phenotype was not elucidated for the mouse mutant models. Using a previously uncharacterized *Tdrd7*-/- mouse model for the lens, I determined the onset of the lens phenotype by applying light microscopy, histology, and SEM analysis.

Tdrd7-/- eyes and lenses show a distinct phenotype including both penetrant cataracts as well as a flattened iris. The flattened iris as well as the cataracts is clearly visible with light microscopy by postnatal day 22 (P22). Although the cataract is penetrant and visible with light microscopy at P22, the cataract is not always clearly visible with histological analysis. Only eight days later when the lens has fully ruptured is the phenotype truly recognizable with histological analysis alone.

Although *Tdrd7*-/- mouse mutant lenses do not exhibit a phenotype observable by light microscopy or histology at P18, they exhibit a dramatic cataract phenotype at P22. However, examination of P18 *Tdrd7*-/- lenses, which appear transparent and devoid of defects, using high resolution SEM imaging reveal fiber cell membrane protrusion defects and disruption of fiber cell organization and structure.

These findings suggest that both histology and light microscopy may miss the true onset of lens defects and cataracts in mouse mutants, especially if such defects result from the accumulation of fiber cell morphology and packing. This is one example of how important it is to utilize high-resolution microscopy for comprehensive phenotypic analysis. Future efforts can be directed toward establishing

a protocol for analysis of *Tdrd7-/-* lenses at earlier stages in order to firmly establish the earliest onset of phenotype in the *Tdrd7-/-* lenses using a high resolution method such as SEM.

Early postnatal lenses cannot be viewed using SEM, so this should not be the only high-resolution analysis utilized to evaluate the exact phenotypic onset. TEM analysis could also be used as another high resolution imaging technology that could be used in future work to further characterize *Tdrd7-/-* lenses.

Tdrd7 is known as an adaptor molecule, and functions in bringing other proteins other proteins to perform different cellular mechanisms (Takashi, H. et al. 2011). The architectural changes occurring within the lens of this mouse model suggest that Tdrd7 could be interacting with other proteins that affect lens cellular structure. With the absence of Tdrd7, changes could be occurring slowly within earlier lenses but not accumulated yet to be observed with current technology. The drastic change within the lens phenotype between P18 and P22 *Tdrd7-/-* lenses suggests that of the absence of Tdrd7 causes either: (1) an accumulation of molecules, (2) or a build of faulty protein interactions that climaxes with the disruption of lens homeostasis and transparency.

MOLECULAR CHARACTERIZATION OF *TDRD7* KNOCKOUT MOUSE MUTANT LENS

1.25 Investigation of Differentially Regulated RNAs in *Tdrd7-/-* Mouse Mutant Lenses

To determine the molecular changes that underlie the lens fiber cell defects and cataracts in *Tdrd7-/-* mutant lens, I sought to take an unbiased whole genome transcriptional profiling approach by performing deep RNA-sequencing analysis (RNA-Seq) on mutant and control (*Tdrd7+/-*) lenses. While designing high-throughput expression profiling approaches at whole genome-levels, it is critical to select the affected tissue samples at a stage that is prior to the full manifestation of the phenotype. This is because as the defect is manifested, it is expected that the downstream molecular changes also progress to secondary and tertiary alterations. Detailed phenotypic characterization of *Tdrd7-/-* lens (please see Chapter 3) indicates that lens fiber cell defects can be detected using SEM in mutants at stage P18, when there are no defects visible by light microscopy. Therefore, I selected postnatal day 4 (P4), 14 days prior to the SEM based detection of the phenotype, to perform RNA-Seq on mutant lenses. I hypothesized that gene expression alternations that are detected at this stage will potentially represent the primary molecular changes that result in the lens due to Tdrd7 deficiency.

RNA-Seq was performed in biological triplicates (15 lenses per replicate) on *Tdrd7-/-* mutant and control (*Tdrd7+/-*) lenses at stage P4 and the differentially regulated genes were identified and sorted based on fold change and *p*-values. As other Tudor domain proteins, *e.g.* SMN and SPF30 (Pellizzoni, et al. 1999; Little, JT and Jurica, MS, 2008), are described to function in pre-mRNA splicing (Pek et al. 2012), I chose to perform paired-end 75-nucleotide sequencing of RNA fragments so the data could be analyzed in future for potential splice form variants.

After sequencing and data analysis as described in Methods, differentially regulated genes (DRGs) in *Tdrd7-/-* lens were identified and classified according to their functional categories. DRGs were sorted on their fold change, separated into up-regulated and down-regulated candidates and analyzed independently at different fold change-cut offs (*e.g.* 1.5-fold, 2.0-fold, *etc.*), significant FDR values (0.05 or below), as well as different counts per million-cut offs (2 or higher counts per million, 10 or higher counts per million) using the web-based software DAVID (Database for Annotation, Visualization and Integrated Discovery, http://david.abcc.ncifcrf.gov/) to identify enriched biological themes that they represent. At the 1.5-fold and 10 counts per million cut offs (high stringency), the DRGs were enriched for the following categories: Translation, Ribosome, ATP binding, Cytoskeleton, Cell Cycle, Cell Morphogenesis, Proteolysis, Cation Binding, Transcription, Integral to Membrane, and Alternative Splicing.

To validate the sequencing data, select candidate genes from the RNA-Seq identified DRGs were confirmed by qRT-PCR (Figures 17-21 and Tables 1-3). To gain

further insights into the *Tdrd7-/-* DRG list, I performed a comparative analysis with *iSyTE* data (published and unpublished) on lens embryonic and postnatal lens (Lachke et al. 2012). This analysis indicates that 44% (*n*=25 of 57) of DRGs are significantly lens-enriched (*iSyTE* ranked under 500). At the 1.5-fold and 2 counts per million cut offs (medium stringency), 193 DRGs were identified (Table in Appendix).

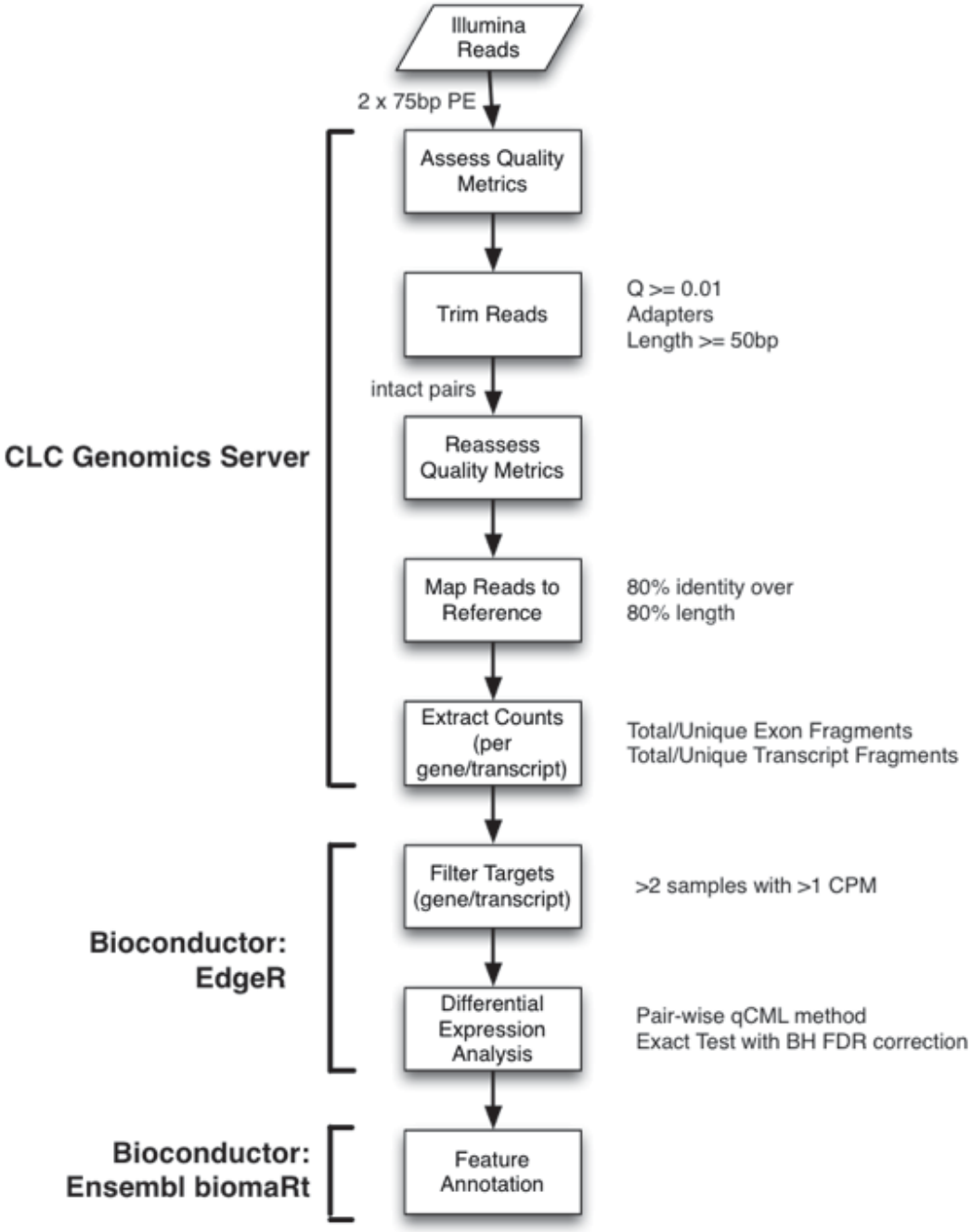

Figure 14. Bioinformatics approach for analyzing *Tdrd7-/-* RNA-Sequencing data. First, read quality was assessed, adaptors were removed, followed by a second quality evaluation. Once sequence integrity was assured, sequences were mapped back to the reference genome, counts per transcript were obtained, and differential analysis was performed.

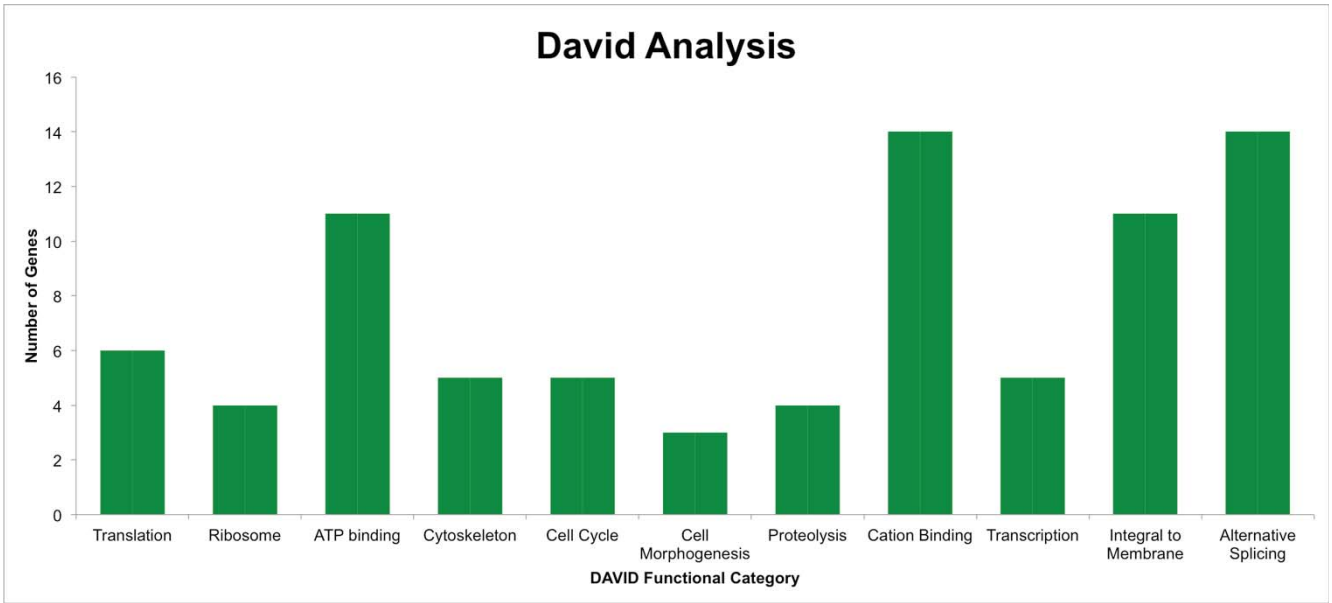

Figure 15. DAVID (Database for Annotation, Visualization and Integrated Discovery) analysis of *Tdrd7-/-* DRGs, which groups genes by gene ontology terms. These terms correspond to the categories shown in the table below. Although some groups only contain three genes, since only 57 total genes were used for analysis, 3 genes accounts for 5 percent of the total genes about 1.4 fold.

Table 1. Gene ontology from DAVID analysis of *Tdrd7-/-* DRGs. The 57 total genes above 1.5 fold change and expressed within the lens were group according to DAVID gene ontologies. This table corresponds to Figure 15.

Term	Number of Genes
Translation (GO:00064120)	6
Ribosome (GO:00058400)	4
ATP binding (GO:0032559)	11
Cytoskeleton (GO:0005856)	5
Cell Cycle (GO:0007049)	5
Cell Morphogenesis (GO:0000902)	3
Proteolysis (GO:0006508)	4
Cation Binding (GO:0043169)	14
Transcription (GO:0006350)	5
Integral to Membrane (GO:0016021)	11
Alternative Splicing	14

Table 2. Up-regulated genes above 1.5 fold in *Tdrd7-/-* lenses. Sequencing results of all genes with a positive fold change above 1.5 (control compared to *Tdrd7-/-* lenses) and as well as expression (over 10 counts per million) in the lens. This table also shows the *iSyTE* rank of these genes. Sequencing resulted from mouse lenses sequenced using the Illumina HiSeq 2500.

Gene	Fold-change	FDR-corrected Pvalue	Min Rank iSyTE
Tmprss11e	2.4	1.5E-26	43
mt-Atp8	2.4	3.5E-23	NA
Eif2s3y	1.9	3.1E-04	5592
Trak2	1.8	9.3E-25	1913
Uox	1.8	1.5E-08	126
Poln	1.8	2.9E-08	211
Bicd1	1.8	2.6E-12	1155
Idi1	1.7	3.2E-22	NA
Gcg	1.7	1.9E-07	33
Ddx3y	1.7	4.0E-03	4679
E330034G19Rik	1.7	2.1E-16	33
Arntl2	1.7	1.0E-04	63
Lars2	1.6	1.4E-02	2348
Plekhs1	1.6	1.3E-09	NA
Rpl39	1.6	3.2E-12	173
Med21	1.6	8.4E-14	534
Rnf113a1	1.6	5.6E-12	24
Scfd2	1.6	5.5E-03	2586
Tceb1	1.6	1.8E-11	851
Clgn	1.6	8.8E-05	331
mt-Nd6	1.5	2.4E-12	NA
Hspb11	1.5	2.1E-06	385
Ammecr1	1.5	2.0E-07	2689
Sh3bgrl	1.5	3.2E-06	2366
Cetn3	1.5	3.8E-13	786
mt-Nd3	1.5	2.4E-10	NA
Zfp40	1.5	1.4E-06	676
Stxbp6	1.5	2.5E-11	121
Uchl3	1.5	1.2E-05	3056
Casp7	1.5	6.1E-10	78

Table 3. Down-regulated genes above 1.4 fold in *Tdrd7-/-* lenses. Sequencing results of all genes with a positive fold change above 1.4 (control compared to *Tdrd7-/-* lenses) and as well as expression (over 10 counts per million) in the lens. This table also shows the *iSyTE* rank of these genes. Sequencing resulted from mouse lenses sequenced using the Illumina HiSeq 2500.

Gene	Fold-change (FC)	FDR-corrected Pvalue	Min Rank iSyTE
Abcc6	2.2	2.1E-09	3512
Bgn	1.9	3.9E-07	1399
Brsk2	1.9	1.1E-09	1203
Chrna4	1.9	5.8E-15	291
Hspb1	1.9	1.1E-07	28
Rpl17	1.8	6.3E-05	213
Rpl13	1.7	4.4E-03	2869
Hspb6	1.7	6.1E-08	61
Adcy5	1.7	6.4E-10	828
Wnk2	1.6	4.4E-11	2764
Cckbr	1.6	8.1E-06	61
Ppm1e	1.6	6.7E-09	352
Dcakd	1.6	3.2E-07	392
Gpsm2	1.6	2.9E-17	960
Snx22	1.6	5.8E-15	86
Mylk	1.6	8.7E-12	519
Gltp	1.5	6.7E-10	191
Lpin1	1.5	5.1E-09	115
Dgcr6	1.5	3.9E-07	750
Cdk18	1.5	9.0E-06	NA
Pkdcc	1.5	9.9E-08	1937
Actn2	1.5	4.2E-05	189
Pabpn1	1.5	1.9E-05	2646
Nfasc	1.5	2.9E-05	905
Rpl38	1.5	5.7E-05	208
Nr2f6	1.5	3.9E-07	106
Mapk7	1.5	5.5E-06	1668

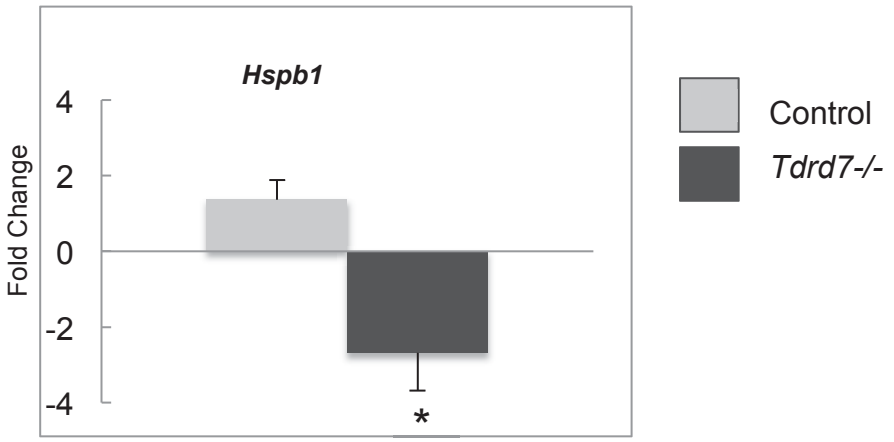

Figure 16. qRT-PCR graph of *Hspb1*. Results are means with standard deviation mRNA normalized to beta actin (internal control) mRNA. *Tdrd7-/-* and control P4 lenses were tested, and control lenses set equal to 1. Bars are standard deviation (S.D.). Fold change calculated in Microsoft Excel, P-values calculated using nested Anova, sample size of three for control and null lenses. One star indicates *p*-value less than 0.05.

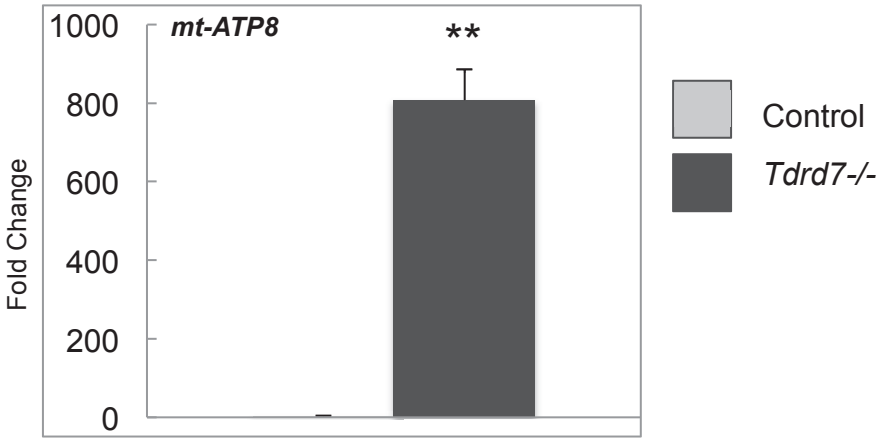

Figure 17. qRT-PCR graph of *mt-ATP8*. Results are means with standard deviation mRNA normalized to beta actin (internal control) mRNA. *Tdrd7-/-* and control P4 lenses were tested, and control lenses set equal to 1. Bars indicate standard deviation (S.D.). Fold change calculated in Microsoft Excel, P-values calculated using nested Anova, sample size of three for control and null lenses. Two stars indicate *p*-value less than 0.01.

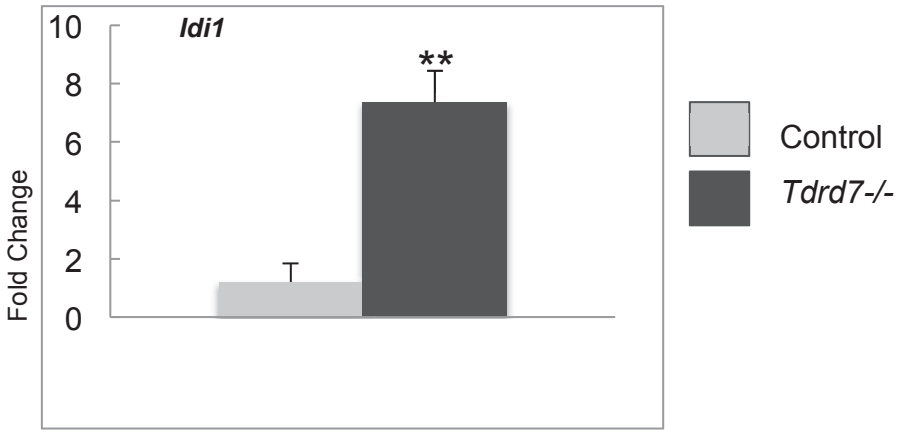

Figure 18. qRT-PCR graph of *Idi1*. Results are means with standard deviation mRNA normalized to beta actin (internal control) mRNA. *Tdrd7-/-* and control P4 lenses were tested, and control lenses set equal to 1. Bars indicate standard deviation (S.D.). Fold change calculated in Microsoft Excel, P-values calculated using nested Anova, sample size of three for control and null lenses. Two stars indicate *p*-value less than 0.01.

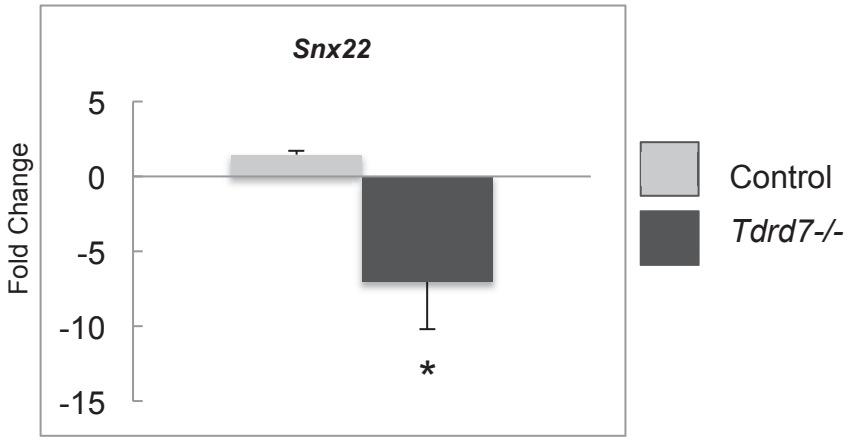

Figure 19. qPCR graph of *Snx22*. *Tdrd7-/-* and control P4 lenses were tested and normalized to beta actin. Results are means with standard deviation mRNA normalized to beta actin (internal control) mRNA. *Tdrd7-/-* and control P4 lenses were tested, and control lenses set equal to 1. Bars indicate standard deviation (S.D.). Fold change calculated in Microsoft Excel, P-values calculated using nested Anova, sample size of three for control and null lenses. One star indicates *p*-value less than 0.05

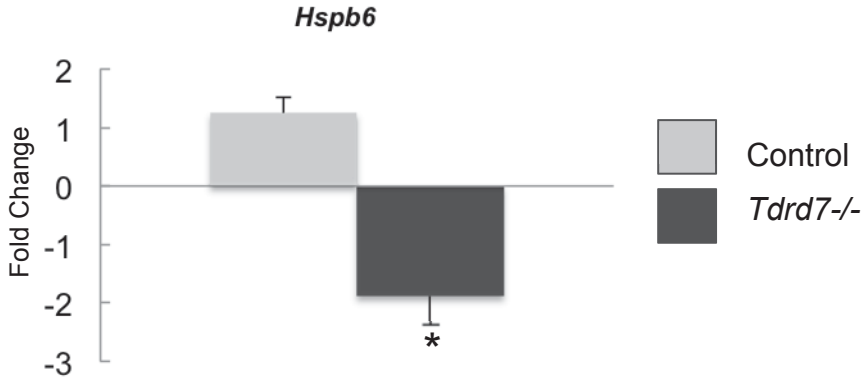

Figure 20. qPCR graph of *Hspb6*. *Tdrd7-/-* and control P4 lenses were tested and normalized to beta actin. Results are means with standard deviation mRNA normalized to beta actin (internal control) mRNA. Control and null P4 lenses tested, control lenses set equal to 1. Bars indicate standard deviation (S.D.). Fold change calculated in Microsoft Excel, P-values calculated using nested Anova, sample size of three for control and null lenses. One star indicates *p*-value less than 0.05

The data was initially analyzed using DAVID and the differentially regulated genes were than curated into functional groups, based on ontology (Figure 15 and Table 1).

1.26 Tdrd7 2D DIGE

To gain further understanding of Tdrd7 function in the lens, a global proteomics-based approach was taken. Specifically, I sought to examine if the changes observed on the transcript level in *Tdrd7-/-* lens translated to protein changes, or to identify other translational changes that resulted in altered proteome without affecting transcripts in the mutant. Therefore, I performed 2D DIGE on *Tdrd7-/-* and control

lens so that overall changes in protein expression (the lens proteome) could be analyzed. However, from previous experiences of other lens researchers, I expected the analysis of the lens proteome to be challenging due to presence of extremely high quantities of crystallin proteins. Nevertheless, I reasoned that any change(s) in proteins that could be detected in spite of the high crystallin protein load in the lens is likely indicative of its high significance in the manifestation of the cataract phenotype in these mutants.

Since the RNA-Seq analysis was performed well before visible phenotypic changes were observed in the mutant lens, this stage was selected for the 2D DIGE analysis as well, so as to allow comparisons between these datasets. However, because it takes time for mRNA changes to translate to protein changes and because the P4 stage is at two weeks prior to observation of SEM-detected phenotypic changes (P18), a second stage at P15 was selected just prior to P18 in order to capture any significant protein changes that was closer to the age of onset and possibly could relate to the phenotype.

While proteins were differentially expressed between P4 and P15 in control lens, indicative of normal alterations in the lens proteome, only one target spot was detected to be differentially expressed and reduced in *Tdrd7-/-* lens at fold change higher than 1.5 with a significant *p*-value. The differentially expressed spot was relatively low molecular weight and close to the molecular weight of crystallins. This spot was isolated and subjected to LC/MS analysis. This data identifies the protein to be Hspb1, which serves to validate our RNA-Seq findings (Figure 22).

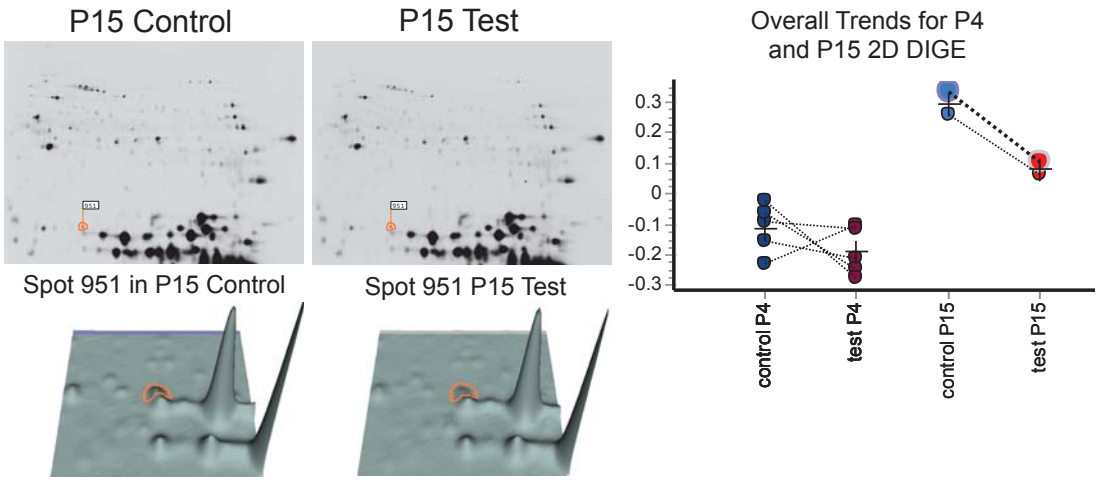

Spot	T-Test	Average Ratio	Overall Appearance	P15 Appearance
951	0.039	-1.64	14 out of 21 total project samples	4 out of 6 group samples

Figure 21. 2D DIGE results that show a protein (Spot 951) is down regulated in both P4 and P15 *Tdrd7-/-* lenses however only in P15 lenses show a significant *p*-value. The protein was identified as Hspb1 by LC-MS/MS analysis. Note that Hspb1 increases in abundance with age and is down regulated in the 1.64 fold with a p-value of 0.039.

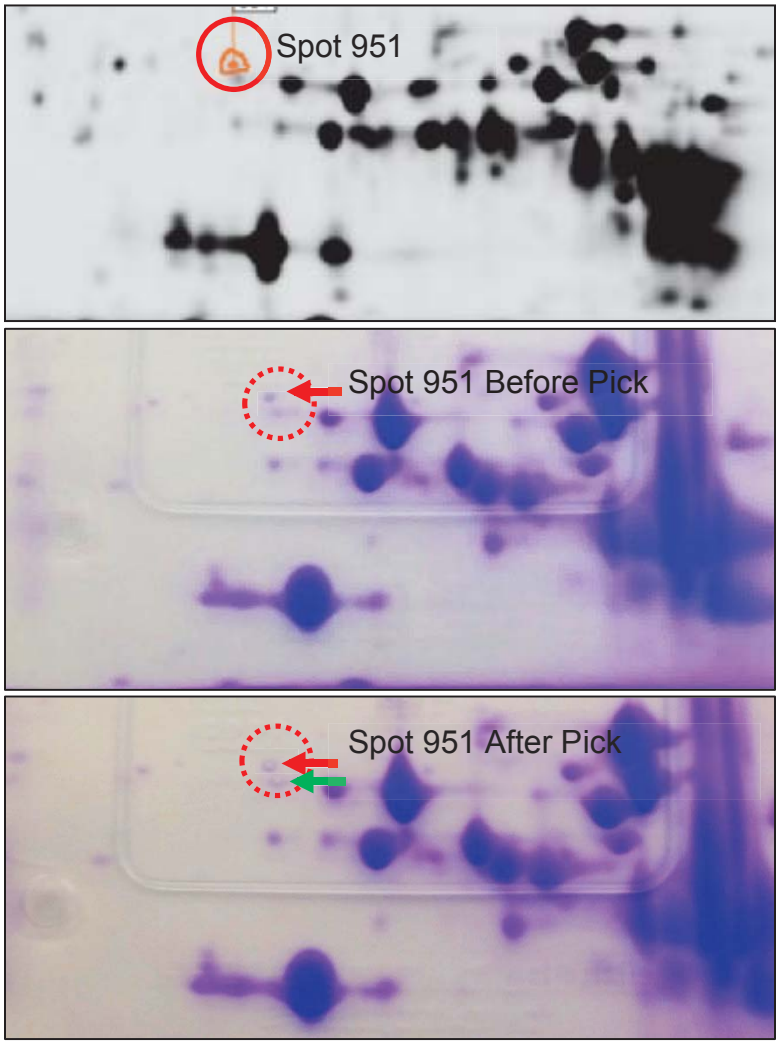

Figure 22. Spot 951, later identified as Hspb1 is first circled in red and then designated by the red arrow, however compared to crystallins it has relatively low abundance. In order to ensure that it is not contaminated, the nearby spot, visualized by a green arrow, was also picked to help distinguish peptides. The confidence of Hspb1 from LC-MS/MS was confirmed with a 100% Protein CI as well as a 100% Best Ion CI.

1.27 Discussion

RNA-Seq identified several DRGs in *Tdrd7-/-* lens. These DRGs were investigated for their relevance/contribution to the lens defect phenotype by performing analyses using DAVID, *iSyTE*, and literature based approaches. I discuss a few interesting findings that are likely to be relevant to the phenotype. *Tmprss11e* was up-regulated in *Tdrd7-/-* lens and encodes the protein transmembrane protease serine that forms serpin inhibitory complexes. Serpins are known to be inhibitors of serine proteases and most serpins have a structure that would present a loop to interact with the protease active site cleft (Hobson JP et al. 2004). Interestingly, another serpin protein, pigment epithelium-derived factor (PEDF) is critical in the lens. It has been shown that down-regulation of PEDF results in decreased protein expression of vimentin and increased expression of αB-crystallin. Studies have shown that *PEDF* may regulate or protect the lens epithelial cells by paracrine or autocine processes (Yang, J et al. 2010). Vimentin is a critical protein for cellular shape, and is known to function in the formation of cytoskeleton (Mendez, MG et al. 2010), while mutations in the gene encoding αB-crystallin cause cataract (Berry, V et al. 2001). Consequently, these proteins have the potential for further investigations in *Tdrd7-/-* mouse mutants.

An actin depositing protein encoding gene *Actn2* is down-regulated in *Tdrd7-/-* mutant lens. Down-regulation of *Actn2* may be contributive to the lens defects observed in *Tdrd7-/-* mutants. Lens transparency depends on numerous cellular

properties and the organization of fiber cell cytoskeleton is especially critical as these cells are highly elongated and are aligned in a specific manner (Rao, P.V. and Maldala, R. 2006). Cytoskeletal proteins are important for the organization of cytosolic and membrane-bound proteins in the lens. Namely actin-based microfilaments, microtubules, and intermediate are critical to the maintenance of lens transparency (Kuszak JO 2004; Zelenka PS; Lee A. et al. 2000; Tardieu, A 1988). Thus, this finding is of significance to the lens and will be discussed in more detail in the next chapter.

The actin cytoskeleton participates in and regulates a variety of biological functions including morphogeneiesis, cell migration, polarity, adhesion, trafficking, transcription, and cell survival (Bloemendal H et al 1984; Ireland M et al. 1983; Kibbelaar MA et al 1998). Actin provides a structural framework that provides cellular shape and polarity; actin dynamics interact with cell adhesion proteins and the plasma membrane to provide the mechanical force driving cellular movement and division. Studies have focused on the organization of actin filaments into polygonal arrays within the lens epithelium. The contractile activity of actomyosin and the tensile strength offered by this structure are properties believed to be critical in the lens for the maintenance of structure and function (Rafferty, NS 1985). Furthermore, actin is a major cytoskeletal protein in lens fiber cells and its function in this context has been characterized in several species (Lo, WK et al. 1997; Lee, A. et al. 2000; Weber, GF and Menko AS. 2006). Lens fiber cell elongation and differentiation are associated with profound changes in cell morphology. Fiber cell elongation is accompanied by

extensive membrane cytoskeleton remodeling (Weber, GF and Menko AS. 2006). As differentiation proceeds, lens fiber cells assemble actin into cortical filaments. Actin filaments play a critical role in lens cellular function; previous research has found that elongated actin bundles are always parallel to the cell membranes. A number of actin bundles were found to form a chain with periodic short intervals these actin bundles were frequently associated with adherens junctions and other regions of fiber cell membranes (Lo, WK et al. 1997). The interactions of F-actin with other regulatory proteins directly affect the cellular shape and organization of fiber cells which in turn regulate lens homeostasis. These findings provide new evidence that Tdrd7 functions in the regulation of the actin cytoskeleton during differentiation and/or growth of the lens. Without the potential regulatory role of Tdrd7, the organization of actin and therefore fiber cell architecture becomes disturbed.

One of the benefits of RNA-Sequencing is the massive amount of data generated, however one of the challenges of this type of investigation is the significant analysis needed for accurate interpretation. This thesis used tools such as DAVID analysis, qRT-PCR, and outside resources such as *iSyTE* in order to fully understand and interpret the Tdrd7 RNA-Sequencing data. Altogether, RNA-Seq has identified several promising candidates genes whose mis-regulation in *Tdrd7-/-* lenses may contribute to the cataract phenotype. However even twenty genes is a considerable task for validation as well as a deeper understanding of mechanism within the lens that translates to cataract. Different avenues of data analysis must be utilized in order to

identify the most critical targets that truly influence lens homeostasis and or pathogenesis in Tdrd7 null mutant lenses.

Although P4 sequencing has given several candidate genes that could be used for further analysis, it was previously not known how many of these candidates translated to the protein level. By performing 2D-DIGE analyses on both P4 and P15 samples, only expression changes that translated to protein changes would be observed and potentially some of the mRNA expression could be validated. As expected, the trends for both the P4 and P15 lenses were similar, however the magnitude of the changes were larger in the P15 samples. These findings indicate that by the time phenotypic changes were observed potentially more protein changes could be found that were not yet statistically significant at the P15 time point.

Protein changes are one indication of the cellular pathways within the cells of the lens, however other factors can also affect the function and homeostasis of cells. For instance, some mRNA changes may not translate to protein expression; however other mechanisms when disrupted could cause molecular changes that contribute to phenotypes. Our finding that Hspb1 is reduced in the *Tdrd7-/-* lens is of significance. Interestingly, Hspb1 protein was identified by Lachke et al. to be down-regulated in the $Tdrd7^{Grm5}$ null mouse mutant lens. Further, Lachke et al. had demonstrated that $Tdrd7^{Grm5}$ null lens at P4 and P30 as well *Tdrd7*-knockdown lens epithelial cell lines exhibited Hspb1 down-regulation on the transcript level. Finally, my RNA-Seq analysis also identifies Hspb1 transcripts to be down-regulated in *Tdrd7-/-* lens. Thus, although entirely new candidates were not detected, the 2DE analysis served to

independently validate our RNA-Seq findings (Figure 22) data on the protein level. Importantly, because Hspb1 was now identified in an unbiased proteomic screen, this served to indicate its importance in manifestation of the cataract phenotype in *Tdrd7-/-* mutants.

CELLULAR CHARACTERIZATION OF FIBER CELL DEFECTS OF *TDRD7* NULL MOUSE MUTANTS

The absence of Tdrd7 in the lens causes a definitive cataract phenotype that is one hundred percent penetrant by P22. However the severe changes seen in the lens phenotype between a short interval of four days - between P18 and P22 - indicate severe changes in the cellular morphology or physiology that are present prior to the onset of the cataract phenotype. My RNA-Seq data have indicated several potential candidate genes for further molecular analysis. However, prioritization of a select few biologically significant candidates from 57 (at 10 counts per million cut-off) or from 193 (at the 2 counts per million cut off) presents a daunting challenge.

I took an integrated approach toward prioritization of candidates from the DRGs identified in the RNA-Seq experiments and gain insight into their relevance in manifestation of the cataract phenotype. This approach involved, 1) identifying Tdrd7 binding proteins and their nearest neighbors, 2) overlaying lens gene expression information from *iSyTE*, and 3) overlaying lens-gene enrichment expression from *iSyTE*. I then performed molecular experiments to further investigate the high-priority candidates that were identified by this approach. To gain insight into the fiber cell defects at the cell biological level, I examined the pattern of F-actin by staining for phalloidin on whole-mount P22 lenses as well as sectioned lenses at P4 and P22

stages. Furthermore, to understand the effect of potential changes in F-actin on cellular shape, I performed wheat germ agglutinin (WGA) staining on lens sections from mutant and control. Based on the data obtained in these experiments I present a model to outline the function on Tdrd7 in mediating post-transcriptional control of gene expression for specific proteins that in turn function to maintain the cellular characteristic architecture of lens fiber cells. Finally, the model also serves to explain the timeline of events in *Tdrd7-/-* mouse lens that contribute to the generation of lens defects due to deficiency of this important regulatory protein.

1.28 Tdrd7 Protein-Protein Interaction Mapping

To prioritize promising candidates for further analysis, an integrated analysis on Tdrd7 protein-protein interaction (PPI) network data as well as lens expression data according to *iSyTE* was utilized. According to NCBI databases and the Tdrd7-PPI network, TDRD7 has experimentally demonstrated to directly interact with seven proteins. These proteins include ATXN2, TACC1, CABLES1, CDK17, NRF1, GABPB1, and FRAT1. When this PPI data was overlaid with *iSyTE* lens expression and enrichment data, the most highly lens enriched protein identified was ATXN2 (Figure 22).

ATXN2 expression is highly enriched in the lens based on its *iSyTE* rank, which is 352 and within the top 1.5% of lens enriched genes. According to protein-protein analysis, ATXN2 directly binds to 42 other proteins of which nine are recognized by *iSyTE* to be among the top 5% of lens-enriched genes (*iSyTE* ranking

less than top 1000). These proteins include ACTN2, NEDD8, PABPC2, BAG6, CUL3, TSG101, SH3GL2, WWOX, and SH3KBP1 (Figure 23). I hypothesized that ATXN2 and its lens-enriched interacting partners may be potentially applied to prioritize the DRGs identified by RNA-Seq in Tdrd7 mutant lens.

From all of the interacting partners of Tdrd7, only one was in the 1.5% *iSyTE* enriched genes, Atxn2. Furthermore, out of the 42 interacting partners of Atxn2 only 9 were in the top 5% of *iSyTE*-enriched genes. Out of these seven candidates, only one of these was also found to be downregulated from our RNA-Sequencing data. Remarkably, the most lens enriched binding partner of Atxn2 was Actn2. These interactions presented additional evidence in support of *Actn2* as a potential target of Tdrd7 in the lens. I next investigated the developmental expression of *Atxn2* and *Actn2* in the lens by analyzing *iSyTE* data.

iSyTE expression showed that *Atxn2* and *Actn2* were both significantly expressed in the embryonic and postnatal lens. Interestingly, *Actn2* expression in wild type lenses is sharply up-regulated in early postnatal stages between P4 and P12 prior to being down-regulated at P20 and later stages. On the other hand, *Atxn2* expression was relatively high in all postnatal stages analyzed. The dynamic up-regulation of *Actn2* expression in early postnatal stages between P4 and P12 may be of significance in lens differentiation in normal lens.

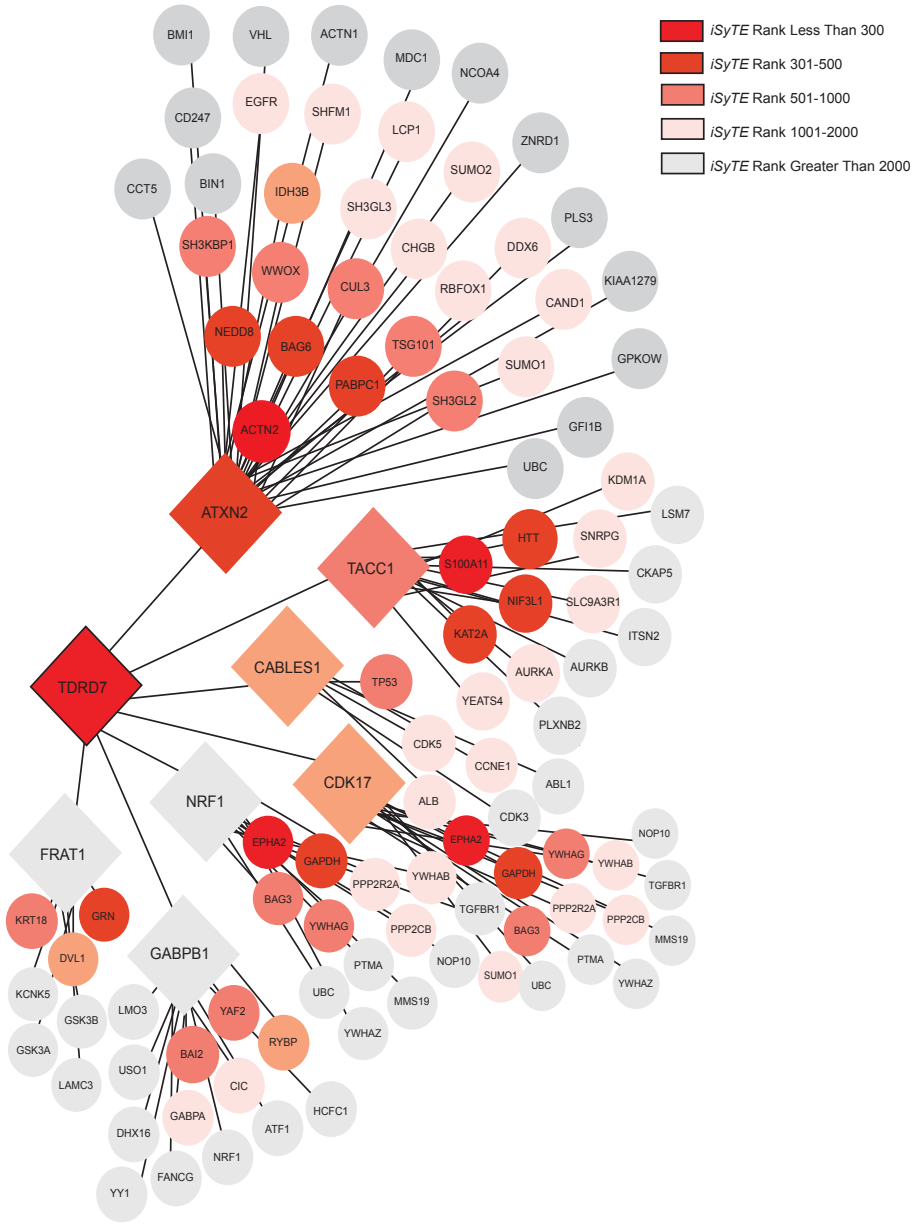

Figure 23. Protein-protein interaction mapping of Tdrd7 integrated with *iSyTE* data. *iSyTE* ranks below 300 (highly lens-enriched, top ~1%) were assigned the color ED1C24, a bright and deep red. *iSyTE* ranks between 301- 500 were assigned the color E34128, a lighter red. *iSyTE* ranks between 501-1000 were assigned the color F37E72, a salmon pink color. *iSyTE* ranks between 1001- 2000 were assigned the color FDE3E0 a light pink. *iSyTE* ranks above 2000 were assigned the color E6E7E8, a light gray.

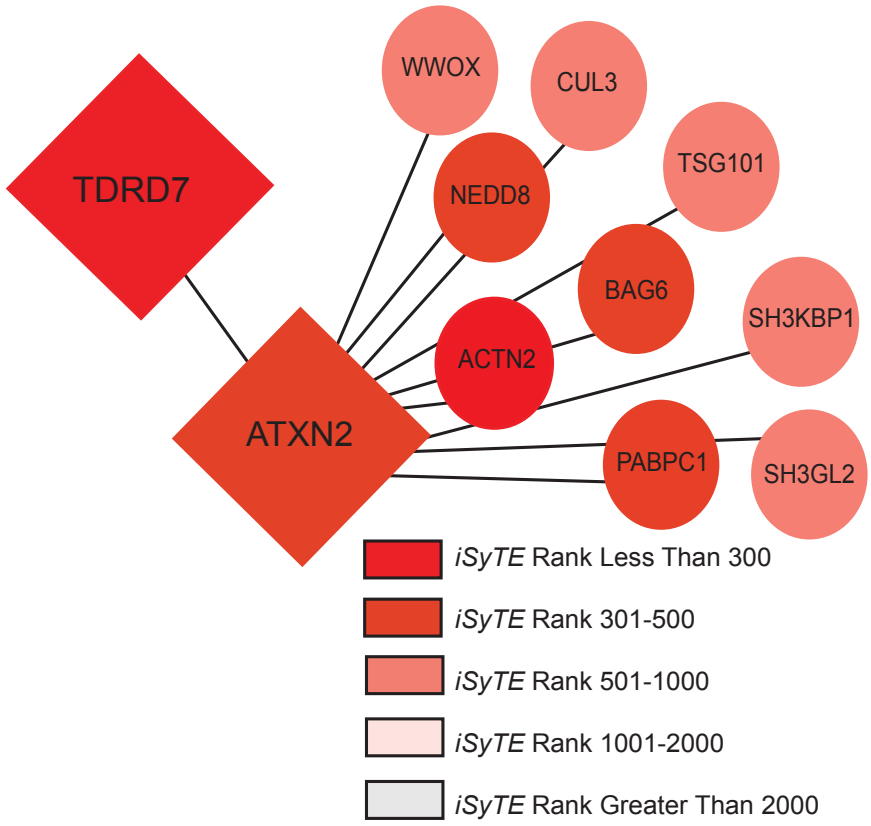

Figure 24. *Atxn2* gene expression is highly enriched in the murine lens. Atxn2 is the most highly enriched gene that has been identified to direct binding protein partner of Tdrd7. The most highly lens-enriched candidate that interacts with Atxn2 is Actn2. This indicates that Tdrd7 may potentially be within a protein complex with Actn2 protein. Further, it supports candidacy of Actn2 for further investigation in the lens.

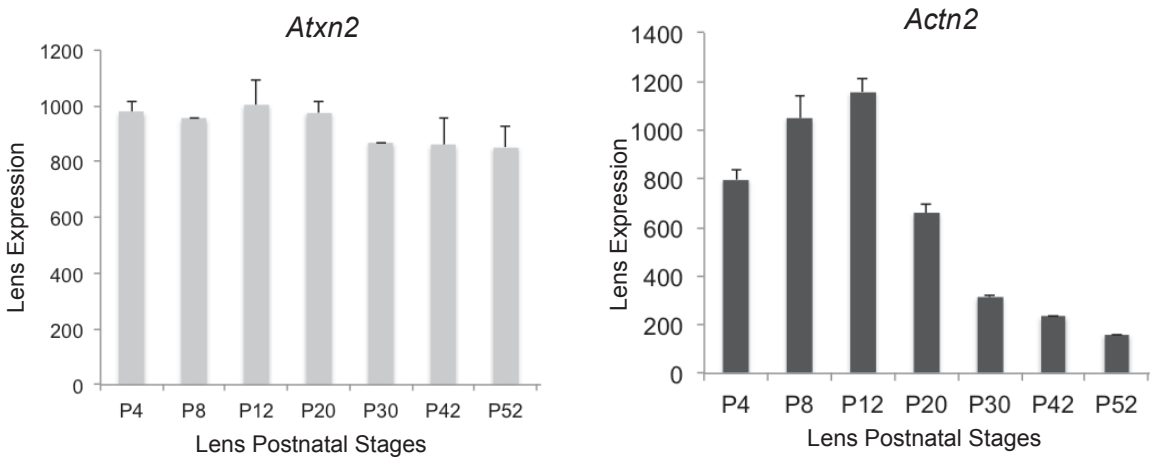

Figure 25. *iSyTE* expression of genes *Atxn2* and *Actn2* in the embryonic and postnatal lens. Analysis of lens expression data in *iSyTE* microarray database (both published, and new, unpublished) identified both *Atxn2* and *Actn2* to be significantly expressed at these stages. While *Atxn2* expression remains high through all lens developmental stages tested, *Actn2* expression is sharply up-regulated between P4 and P12 stages, prior to being down-regulated at P20 and later stages. Up-regulation of *Actn2* expression in early postnatal stages between P4 and P12 may be of significance in normal lens development.

1.29 RNA Immunoprecipitation (RIP)

Because Tdrd7 is predicted to bind RNA, I sought to investigate if Tdrd7 protein was associated with RNA in the lens. I undertook an RNA Immunoprecipitation (RIP) assay followed by qRT-PCR analysis of candidate target transcripts. I used a Tdrd7-specific antibody to perform RIP on lens tissue lysate from stage P15 ICR wild type lens and then tested the level of *Actn2* transcripts in Tdrd7-RIP pulldown complex (Figure 25).

I selected P15 stage for RIP assays to increase the likelihood that interactions between Tdrd7-targets represented molecular changes pertinent to the phenotype. This stage is both close to when *Actn2* expression is highest. Moreover, this stage is just three days prior to the lens fiber cell defect detected by SEM analysis. Further, I

validated that the RIP assays were working well by testing (and confirming) candidates *Hspb1* and *Crybb3* that were previously identified by Lachke et al. in Tdrd7 RIP assays (Figure 26).

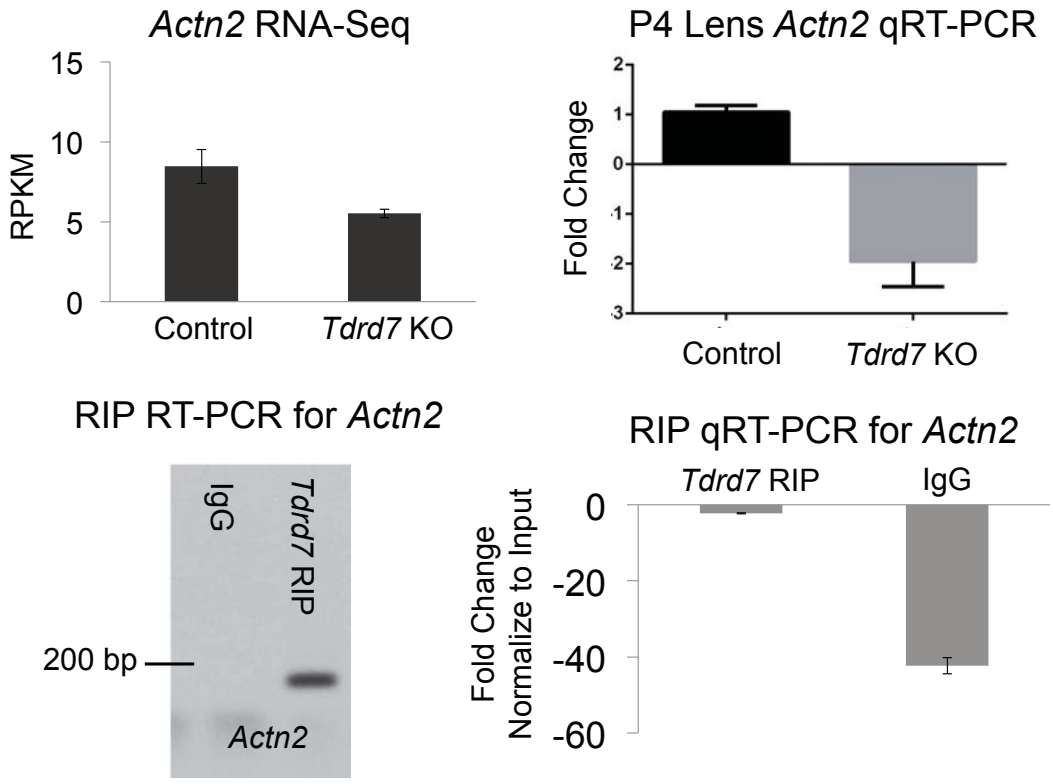

Figure 26. *Actn2* is downregulated in *Tdrd7-/-* mutant lenses and Tdrd7 directly binds to *Actn2* mRNA. Both RNA-Seq as well as qRT-PCR indicate that *Actn2* is down regulated in P4 *Tdrd7-/-* mutant lenses. RIP analysis has been validated in WT ICR P15 lenses using both RT PCR as well as qRT PCR. Both methods demonstrate that Tdrd7 can bind to *Actn2* mRNA in the lens.

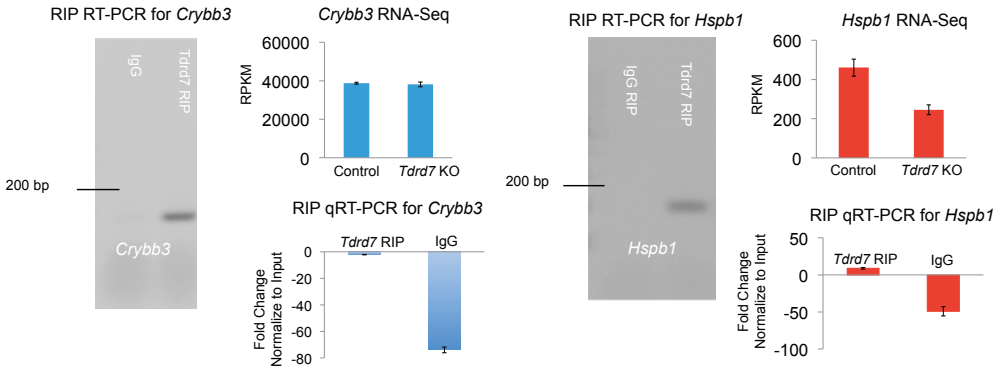

Figure 27. Validation of previously identified Tdrd7-RIP target RNAs in mouse P15 WT lens. *Tdrd7-/-* mutant lenses show down-regulation of *Hspb1*. Although *Crybb3* is not down-regulated in P4 *Tdrd7-/-* mutant lenses (but is down-regulated in *Tdrd7*^{Grm5} homozygous null mutant at P30), Tdrd7 has been shown to directly bind to *Hspb1* and *Crybb3* mRNA in mouse P15 WT ICR lens.

1.30 Phallodin Staining of F-Actin

Actn2 is among four actin-binding proteins belonging to a family called α-actinins. These proteins are related to dystrophin and the spectrins. Within non-muscle cells, Actn2 functions in binding F-actin to the cell membrane (Jalan-Sakrikar, N et al. 2012). Actn2 is generally located near microfilament bundles and adherens-type junctions. Furthermore, Actn2 and Actn3 have also been shown to function in the localization of actin-containing filaments (Mills, MA et al 2001). Moreover, α-actinin binds to the cytoplasmic domain of β1-integrin. This suggests that α-actinins may be directly linked to the cytoskeleton (Otey, CA et al. 1993).

Since actinins have been shown to affect the special localization of actin, and specifically because Tdrd7 directly associates with *Actn2* (Actinin 2) mRNA in wild type lenses, we hypothesized that fiber cell cytoskeletal defects partially originate from an irregular network of filamentous actin networks. These disrupted networks contribute to the cataract phenotype observed in *Tdrd7-/-* mutant lenses. To test this

hypothesis, I performed whole mount phalloidin staining on *Tdrd7-/-* and control P22 lenses to visualize the pattern of F-actin in the lens. This assay revealed a difference in the spatial localization of F-actin differed from the controls. While F-actin appeared uniformly distributed in control lens, it was unequally distributed along the length of fiber cells in the *Tdrd7-/-* lenses. In mutant lens, although the overall cytoskeleton structure was not entirely altered, F-actin appeared in aggregates were detected along the fiber cell cytoskeleton throughout the lens tissue (Figure 27).

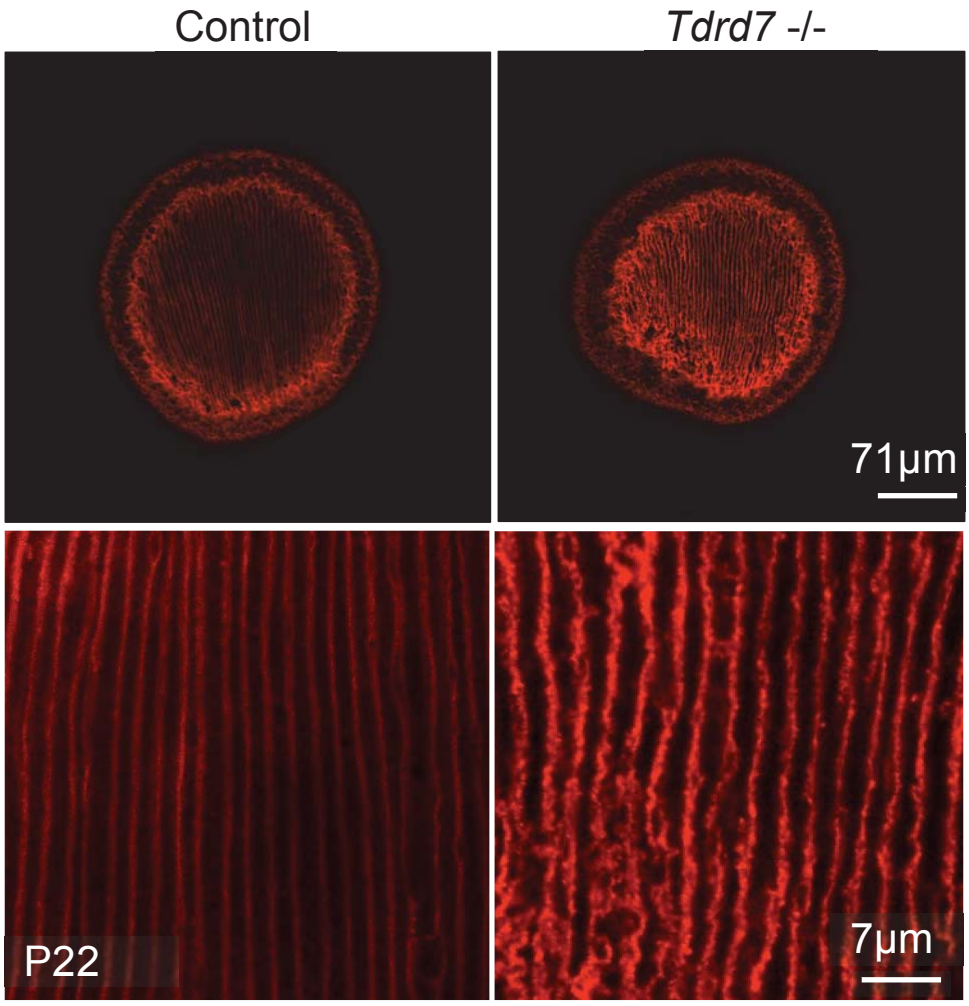

Figure 28. Phalloidin staining of F-actin in P22 *Tdrd7-/-* and control lenses. Control lenses show linear fiber cell architecture and organization, however *Tdrd7-/-* lenses seem to develop disordered cellular appearance as well as disjointed fiber cell packing. Actin appears to accumulate or clump on the edges of fiber cells.

Phalloidin staining on P4 sections were also used to visualize the examine actin distribution in the development of *Tdrd7-/-* mouse mutant lenses. At P22, while levels of actin appeared similar in both control and *Tdrd7-/-* mutant lens, the F-actin

distribution was altered in mutant lens. As with whole mount staining, F-actin aggregates were detected in the *Tdrd7-/-* mutant lens (Figure 28).

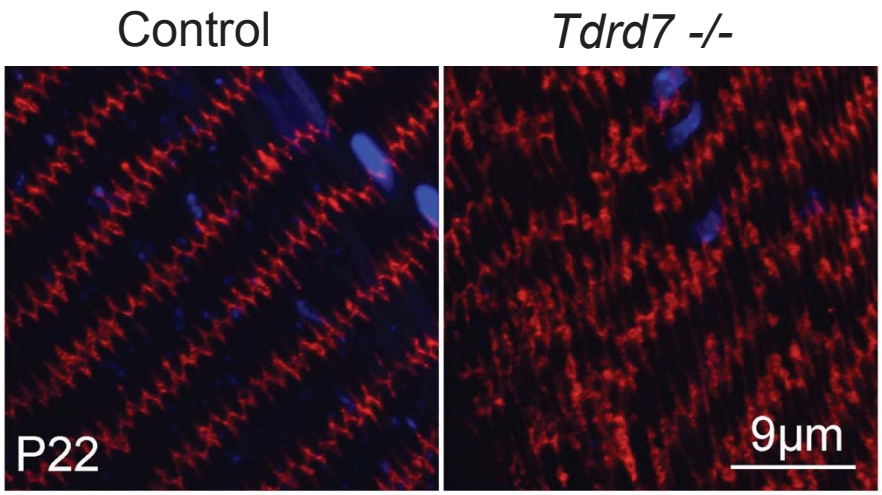

Figure 29. Phallodin staining of lens sections from P22 *Tdrd7-/-* mutant and control. *Tdrd7-/-* shows "clumping" of actin on the cytoskeleton. Actin cytoskeleton morphology was also disrupted.

1.31 Wheat Germ Agglutinin Staining

To investigate the effect F-actin misregulation on fiber cell shape, I next performed wheat germ agglutinin (WGA) staining on P4 and P22 control and mutant lens sections. WGA is a lectin protein that binds to *N*-acetylglucosamine and *N*-acetylneuraminic acid, *N*-acetylgalactosamine and is applied in staining of cell membranes. As expected, WGA staining for both P22 and P4 controls lenses exhibited a largely hexagonal pattern of fiber cells in saggital sections. In *Tdrd7* null lenses however, the hexagonal pattern was disrupted for P4 and almost nonexistent for P22 samples (Figure 28).

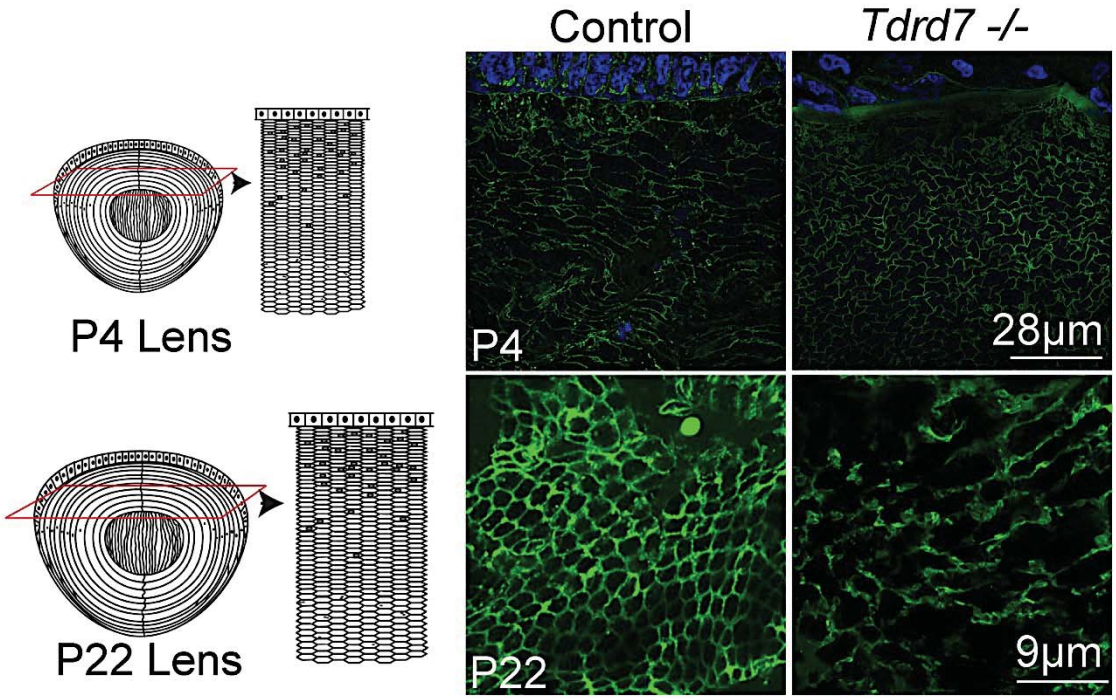

Figure 30. WGA staining of *Tdrd7-/-* mutant and control lens at P4 and P22 stage. Sagittal lens sections from control and mutants were stained with WGA to identify cellular structure of lens fibers. Normal lens fibers exhibit expected the distinct hexagonal structure that is observed in controls. However, *Tdrd7-/-* lens exhibits deformed structure at P4. By P22, the fiber cell shape is severely abnormal in *Tdrd7-/-* lens.

To investigate WGA and actin staining pattern in the *Tdrd7-/-* mutant lens, sections were co-stained with phallodin and WGA at P4 and P22. While P22 control lenses showed normal WGA and actin interactions as well as hexagonal structures, the *Tdrd7-/-* mutant lenses exhibited disruption of both markers (Figure 32).

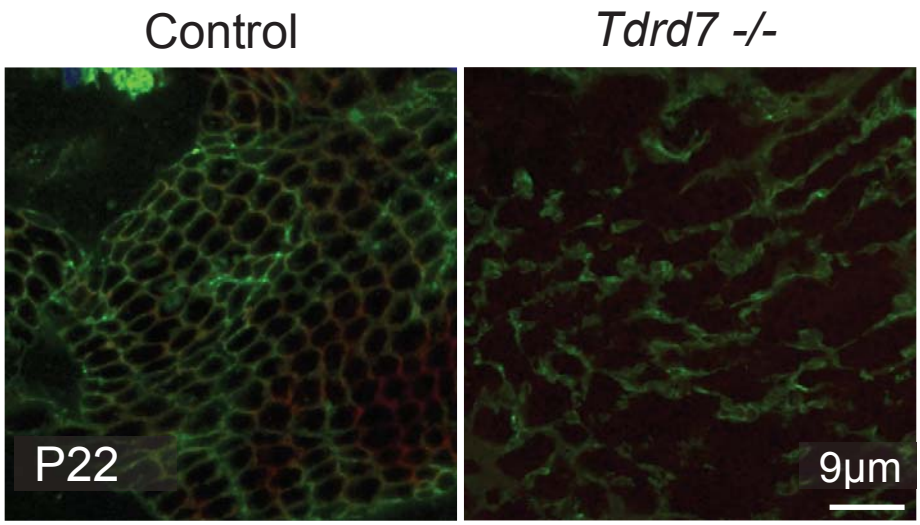

Figure 31. Co-staining of phalloidin and WGA (Green) in sagittal P22 *Tdrd7-/-* mutant and control lenses. Actin (Red) localizes to edges of the hexagonal shapes of the fiber cells in the control lenses but not in the *Tdrd7* null lenses. The shapes of hexagons are abnormal in the *Tdrd7-/-* lenses compared to the controls.

1.32 Discussion

By stage P22, *Tdrd7-/-* mutant lenses exhibit a 100% penetrant cataract phenotype. Despite this fully penetrant phenotype in these mutants, drastic changes that lead to cataract formation transpire within a short period of only four days between P18 and P22, prior to which the lens are completely transparent. The abnormal fiber cell morphology detected by SEM analysis in P18 *Tdrd7-/-* mutants indicate that intense cellular changes occur before the onset of the cataract phenotype, in turn reflecting even earlier alterations in molecular mechanistic events in these animals. However, resolving these causative molecular changes is challenging.

I have investigated the molecular mechanism of cataract in *Tdrd7-/-* lens by applying an integrated approach. Namely I analyzed RNA-Seq data with protein-protein interaction data and *iSyTE* enrichment analysis has provided new insights into the function of Tdrd7 in the lens. This integrated approach has allowed me to identify a new regulatory function for previously characterized proteins in lens homeostasis and development. Namely, these experiments indicated that Tdrd7 regulates lens fiber cell cytoskeleton by regulating F-actin deposition. It does so by potential direct binding to *Actn2* RNA, which encodes a α-actinin protein that is involved in F-actin distribution. It could be hypothesized that in normal wild type lens, Tdrd7 interaction with *Actn2* transcripts leads to their increased stability in turn ensuring the build-up of a critical amount of Actn2 protein necessary for appropriate F-actin deposition in lens fiber cells. Disruption of Tdrd7 function results in reduced *Actn2* transcripts and consequently in abnormal deposition of F-actin, which contributes to membrane protrusion defects in fiber cells that culminate in the formation of cataract.

However, the possibility can be entertained that other mechanisms, besides *Actn2* down-regulation, also contribute to the abnormal fiber cell morphology in *Tdrd7-/-* lens. In this alternate model, the F-actin aggregates observed in mutant are a secondary effect of disorganized fiber cells that are established early in *Tdrd7-/-* lens. However, the early changes in Actn2, long before the onset of the phenotype, supports the action of this gene in favor of causative than reflective.

Actin is one of the principal components of the cytoskeleton and is necessary for lens transparency as well as homeostasis. Cytoskeletal remodeling is essential in fiber

cell differentiation, and without proper actin distribution, this process is disrupted. In non-muscle cells, actin plays a critical role in regard to the attachment of the actin cytoskeleton to cell-substrate and cell-to-cell contacts (Cooper., 2000). Thus, based on these findings that elucidate Tdrd7 function in regulation of F-actin distribution, it is likely that abnormal cytoskeletal organization could play a large role in the disrupted architecture seen in *Tdrd7-/-* mouse mutant lenses.

CONCLUSIONS AND FUTURE DIRECTIONS

This thesis seeks to characterize Tdrd7 function in the lens through the careful analysis of *Tdrd7-/-* mouse mutants on the phenotypic, cellular and molecular levels. While phenotypic characterization using SEM, light microscopy and histological analysis reveal defects in the mutant lens at different levels of resolution; RNA-Seq analysis identifies 57 genes that are differentially expressed at ±1.5 fold cut-off. An integrated analysis of these DRGs, based on Tdrd7 protein-protein interaction (PPI) network data as well as lens expression according to *iSyTE*, leads to prioritization of promising candidates for further analysis. In particular, the Tdrd7 PPI network analysis identifies Atxn2, a cytoplasmic RNA granule protein, as a direct interacting protein of Tdrd7. These networks also identify Actn2, an F-actin crosslinking protein, as a binding partner of Atxn2, whose transcripts are downregulated in *Tdrd7-/-* mutant lens.

The protein Actn2 has been described to function in deposition F-actin; additionally, *Actn2*-KD zebrafish has lens/cataract phenotype (Gupta et al. 2012). Thus cell biological analysis of F-actin reveals abnormal fiber cell architecture in *Tdrd7-/-* mutant lens. Tdrd7-pulldown complexes in RIP assays exhibit high enrichment of *Actn2* transcripts in normal lens tissue. These experiments serve to demonstrate that Tdrd7 functions by directly interacting with *Actn2* transcripts in the

lens, and therefore has the potential to affect F-actin within the lens (Figure 33 and 34).

Actin is one of the most highly abundant proteins found within eukaryotic cells and is also vital for the accurate formation of the cytoskeleton and its exchanges with the extracellular matrix (Tojkander S. Gateva, G and Lappalainen, P. 2012). Within the lens changes in actin dynamics have been shown to correlate with lens differentiation. Specifically there is an increase in the ratio of F-actin to G actin while fiber cell differentiation occurs (Nowak, RB and Fowler, VM 2012). These changes in actin filaments alter cytoskeletal organization and therefore cellular shape. When the architecture of the actin cytoskeleton is disturbed, fiber cell differentiation is stunted; specifically the epithelial elongation does not occur and therefore lens defects arise (Cheng, C et al. 2013). These findings support how critical the actin cytoskeleton is for the cell in general and specifically for the differentiation and networks of lens fiber cells (Nowak, RB and Fowler, VM 2012; Mousa, GY and Trevithick, JR, 1977; Iwig, M et al. 1981).

Many cytoskeletal-associated proteins other than alpha-actinin including vinculin, talin and integrins have previously been shown to play an important role in the actin cytoskeleton membrane dynamics (Nowak, RB and Fowler, VM 2012). Other molecules including specrin, actin and tropomyosin have previously been reported to assemble within the plasma membrane of both undifferentiated and differentiated fiber cells (Woo, M. K et al.; 2000). Furthermore other experiments have demonstrated that alpha actinin can also potentially bind to beta1 integrin,

another protein associated with lens homeostasis (Otey, CA et al 1990). Recent work has illustrated how critical beta 1-integrin is within the lens and also how it can affect F-actin (Scheilblen, DA et al. 2014). These previous experiments are a solid foundation for the hypothesis that Tdrd7 functions in the regulation and distribution of F-actin within the lens (Nowak, RB and Fowler, VM 2012).

Both Hspb1 (Hsp25/27/HSPB1) and actin are induced by cellular stress and Hspb1 provides resistance against both heat shock and oxidative stress. Hspb1 also interferes with various cell signaling pathways and can function as a chaperone within the cell (Garrido et al., 2006; Parcellier et al. 2005). Additionally, Hspb1 has been shown previously to interrupt apoptotic pathways by blocking the release of cytochrome c (Bruey, JM et al. 2000). Previous research has shown that in other tissues Hspb1 helps to regulate actin dynamics by influencing the contraction of actin filaments (Moreno-Dominguez, A. et al. 2014). During differentiation, fiber cells undergo high levels of stress while undergoing drastic changes in cellular shape; all of these processes require cellular mechanisms to control and regulate these severe molecular changes.

Interestingly, Hspb1 is known to interact with actin *in vitro* (Graceffa, P. 2011). Previous research has shown that Hspb1 is involved in the capping of actin filaments, *in vivo* evidence demonstrates that phosphorylated Hspb1 is required for providing actin stability after a cell experiences heat stress. Furthermore, phosphorylation of Hspb1 has been hypothesized to play an important role in the regulation of F-actin dynamics in response to growth factors and stress. The

microfilament network is one of the earliest targets of oxidative stress and phosphorylation of Hspb1 is strongly induced by reactive oxygen metabolites. Thus, Hspb1 phosphorylation may be involved in regulation of actin dynamics in response to oxidative stress (Lavoie, JN et al 1993). The accumulation of unregulated oxidative stress in the lens has been shown to causes cataracts previously (Berthoud, VM 2009). Research presented in this thesis elucidates the interactions of Tdrd7, Hspb1, and F-actin in maintaining lens homeostasis and transparency.

Other proteins involved in actin regulation include actin cross-linking proteins such as filamin and actinin that provide structural support and organize actin filaments into bundles. Conversely, other actin regulating proteins include actin-severing proteins; these proteins function in increasing the number of actin filaments. This thesis reiterates the importance of Tdrd7 and its affect on actin distribution in the lens. Co-staining of proteins like Hspb1 and Actin in the lens, as well as staining for Actn2 should be performed as future work. These experiments will help elucidate the cytoskeletal regulatory components of this pathway regulated by Tdrd7.

In future, proteomics based approaches to identify the protein-binding partners of Tdrd7 leading to defining the "Tdrd7-interactome" in the lens will further advance the function of this protein. Such an approach involving immunoperciptation (IP) of Tdrd7 and its associated proteins from the lens tissue followed by mass spectrometry will identify protein interactions of Tdrd7 in a non-biased screen. Depending on the results of the IP further staining could be performed, specifically co-staining of proteins like Hspb1 and Actin in the lens as well as staining for Actn2. It would be

interesting to test if any recognized arginine-methylated proteins are identified in such a screen, as it would lead to investigation of a new area of arginine-methylated regulation in the lens. It would also be interesting to learn if other RNA granule component proteins in addition to Atxn2 are identified as Tdrd7 targets.

One potential concern that can be addressed in future research is related to some of the early post-natal stages used in these studies. Because P4 is two weeks prior to the observation of the lens fiber cell defects, it may potentially be so early that important candidate genes were missed. Future studies could focus on the identifying new targets at later lens stages, which are temporally closer to the onset of the phenotype.

This could be useful very useful for the sequencing data since the control used in this study was a heterozygous lenses instead of a complete wild type lenses. This was used in order to discern the most profound differences occurring within that lens that cause such an intense phenotype. Nonetheless since one of the control and null lenses were removed from sequencing analysis, the data does loose some of its power. This may account for the fact that within the dataset there were less candidate genes come pared to other sequencing datasets. Another alternative explanation for the relatively small candidate gene list is that all of the lenses used for sequencing were pooled together. Although this does give better quality RNA, it also may hide variation between samples so larger changes become diluted and therefore are missed by sequencing cut-offs. These questions could be further addressed in future research, where more sequencing could be performed.

Tdrd7 is implicated in post-transcriptional regulation in lens as well as non-lens tissue (Lachke et al. 2011, Tanaka et al. 2011). Therefore, in addition to its protein-binding partners, it would be beneficial to understand the binding sites of Tdrd7 within lens-expressed RNAs. Additionally, the sequencing results suggest that there is more to be discovered regarding Tdrd7's interactions with the mitochondria. Several mitochondrial mRNAs were found to be upregulated in the *Tdrd7-/-* lenses. This thesis was not able to fully investigate the molecular mechanism of these changes however this could be a new field of study for future investigation. These findings in the future may elucidate how Tdrd7 interacts with RNA and proteins and how these different molecular functions contribute to lens homeostasis.

Finally, research in this thesis serves to demonstrate that an integrated approach using cell biology, high resolution phenotypic characterization, and state-of-the-art molecular analysis including RNA-sequencing, combined with bioinformatics analysis can identify novel connections and provide new insights into regulatory mechanisms in tissue development. This thesis contributes to the understanding of the molecular mechanism of a novel RNA binding protein and RNA granule component in the lens, and therefore provides unique insights into the pathophysiology of a prevalent eye disease cataract.

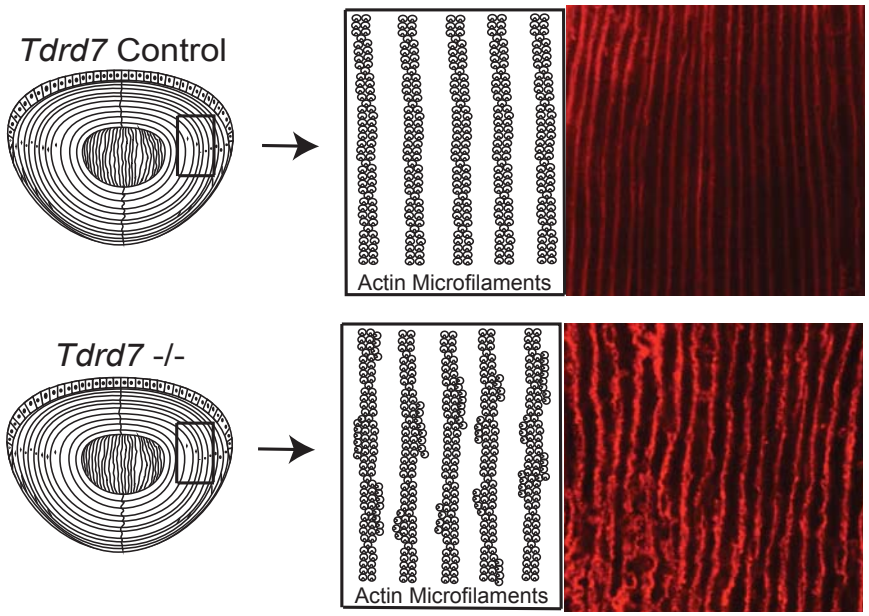

Figure 32. Tdrd7 affects F-actin distribution in the lens. In this thesis, I provide evidence that Tdrd7 is involved in the spatiotemporal positioning of F-actin within the mouse lens. It can be hypothesized that alteration of the structure of actin, results in alteration of microfilaments, in turn affecting the overall architecture of lens fiber cells.

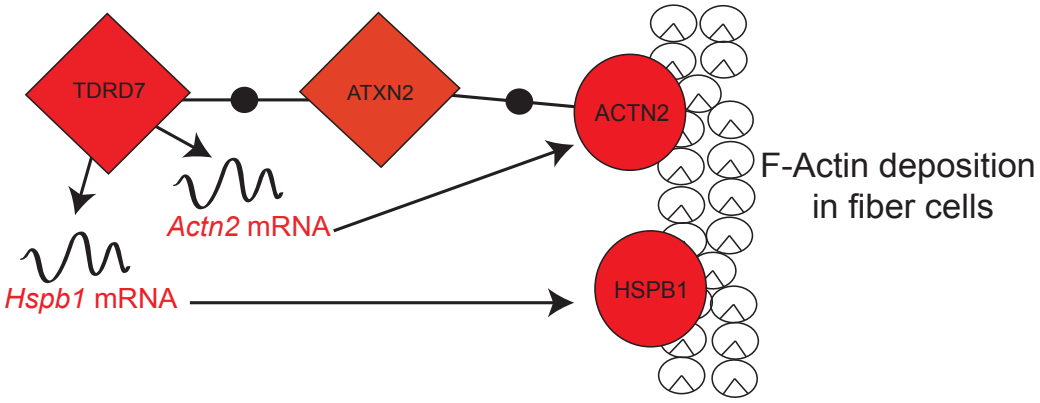

Figure 33. Proposed partial mechanism of Tdrd7 within the lens. Tdrd7 not only regulates critical lens mRNAs for Hspb1 and Actn2, but also interacts with other important proteins like Atxn2, to regulate the distribution and architecture of the actin cytoskeleton.

REFERENCES

AAO, A. A. o. O. A. S. P. (2001) 'Cataract in the Adult Eye', 1-62.

Akamatsu, W., Okano, H. J., Osumi, N., Inoue, T., Nakamura, S., Sakakibara, S. I., Miura, M., Matsuo, N., Darnell, R. B. and Okano, H. (1999) 'Mammalian ELAV-like neuronal RNA-binding proteins HuB and HuC promote neuronal development in both the central and the peripheral nervous systems', *Proceedings of the National Academy of Sciences of the United States of America*, 96(17), 9885-9890.

Alizadeh, A., Clark, J., Seeberger, T., Hess, J., Blankenship, T. and Fitzgerald, P. G. (2004) 'Characterization of a mutation in the lens-specific CP49 in the 129 strain of mouse', *Investigative Ophthalmology & Visual Science*, 45(3), 884-891.

Anderson, S., Bankier, A. T., Barrell, B. G., Debruijn, M. H. L., Coulson, A. R., Drouin, J., Eperon, I. C., Nierlich, D. P., Roe, B. A., Sanger, F., Schreier, P. H., Smith, A. J. H., Staden, R. and Young, I. G. (1981) 'SEQUENCE AND ORGANIZATION OF THE HUMAN MITOCHONDRIAL GENOME', *Nature*, 290(5806), 457-465.

Andley, U. P. (2008) 'The lens epithelium: Focus on the expression and function of the alpha-crystallin chaperones', *International Journal of Biochemistry & Cell Biology*, 40(3), 317-323.

Aravin, A. A., Hannon, G. J. and Brennecke, J. (2007) 'The Piwi-piRNA pathway provides an adaptive defense in the transposon arms race', *Science*, 318(5851), 761-764.

Arora, A., McKay, G. J. and Simpson, D. A. C. (2007) 'Prediction and verification of miRNA expression in human and rat retinas', *Investigative Ophthalmology & Visual Science*, 48(9), 3962-3967.

Artman, L., Dormoy-Raclet, V., von Roretz, C. and Gallouzi, I. E. (2014) 'Planning your every move: The role of beta-actin and its post-transcriptional regulation in cell motility', *Seminars in Cell & Developmental Biology*, 34, 33-43.

Ashery-Padan, R., Marquardt, T., Zhou, X. L. and Gruss, P. (2000) 'Pax6 activity in the lens primordium is required for lens formation and for correct placement of a single retina in the eye', *Genes & Development*, 14(21), 2701-2711.

Babizhayev, M. A. (2011) 'Mitochondria induce oxidative stress, generation of reactive oxygen species and redox state unbalance of the eye lens leading to human cataract formation: disruption of redox lens organization by phospholipid hydroperoxides as a common basis for cataract disease', *Cell Biochemistry and Function*, 29(3), 183-206.

Baltz, A. G., Munschauer, M., Schwanhausser, B., Vasile, A., Murakawa, Y., Schueler, M., Youngs, N., Penfold-Brown, D., Drew, K., Milek, M., Wyler, E., Bonneau, R., Selbach, M., Dieterich, C. and Landthaler, M. (2012) 'The mRNA-Bound Proteome and Its Global Occupancy Profile on Protein-Coding Transcripts', *Molecular Cell*, 46(5), 674-690.

Bantseev, V. and Youn, H. Y. (2006) 'Mitochondrial "movement" and lens optics following oxidative stress from UV-B irradiation - Cultured bovine lenses and human retinal pigment epithelial cells (ARPE-19) as examples', *Signal Transduction Pathways, Pt B: Stress Signaling and Transcriptional Control*, 1091, 17-33.

Barbee, S. A., Estes, P. S., Cziko, A. M., Hillebrand, J., Luedeman, R. A., Coller, J. M., Johnson, N., Howlett, I. C., Geng, C. Y., Ueda, R., Brand, A. H., Newbury, S. F., Wilhelm, J. E., Levine, R. B., Nakamura, A., Parker, R. and Ramaswamil, M. (2006) 'Staufen- and FMRP-containing neuronal RNPs are structurally and functionally related to somatic P bodies', *Neuron*, 52(6), 997-1009.

Bassett, E. A., Williams, T., Zacharias, A. L., Gage, P. J., Fuhrmann, S. and West-Mays, J. A. (2010) 'AP-2 alpha knockout mice exhibit optic cup patterning defects and failure of optic stalk morphogenesis', *Human Molecular Genetics*, 19(9), 1791-1804.

Bassnett, S. and Mataic, D. (1997) 'Chromatin degradation in differentiating fiber cells of the eye lens', *Journal of Cell Biology*, 137(1), 37-49.

Bassnett, S., Shi, Y. R. and Vrensen, G. (2011) 'Biological glass: structural determinants of eye lens transparency', *Philosophical Transactions of the Royal Society B-Biological Sciences*, 366(1568), 1250-1264.

Belecky-Adams, T. L., Adler, R. and Beebe, D. C. (2002) 'Bone morphogenetic protein signaling and the initiation of lens fiber cell differentiation', *Development*, 129(16), 3795-3802.

Benndorf, R., Hayess, K., Ryazantsev, S., Wieske, M., Behlke, J. and Lutsch, G. (1994) 'PHOSPHORYLATION AND SUPRAMOLECULAR ORGANIZATION OF MURINE SMALL HEAT-SHOCK PROTEIN HSP25 ABOLISH ITS ACTIN POLYMERIZATION-INHIBITING ACTIVITY', *Journal of Biological Chemistry*, 269(32), 20780-20784.

Bennett, T. M., Mackay, D. S., Siegfried, C. J. and Shiels, A. (2014) 'Mutation of the Melastatin-Related Cation Channel, TRPM3, Underlies Inherited Cataract and Glaucoma', *Plos One*, 9(8), 13.

Berry, V., Francis, P., Reddy, M. A., Collyer, D., Vithana, E., MacKay, I., Dawson, G., Carey, A. H., Moore, A., Bhattacharya, S. S. and Quinlan, R. A. (2001) 'Alpha-b crystallin gene (CRYAB) mutation causes dominant congenital posterior polar cataract in humans', *American Journal of Human Genetics*, 69(5), 1141-1145.

Berthoud, V. M. and Beyer, E. C. (2009) 'Oxidative Stress, Lens Gap Junctions, and Cataracts', *Antioxidants & Redox Signaling*, 11(2), 339-353.

Berthoud, V. M., Minogue, P. J., Yu, H., Schroeder, R., Snabb, J. I. and Beyer, E. C. (2013) 'Connexin50D47A Decreases Levels of Fiber Cell Connexins and Impairs Lens Fiber Cell Differentiation', *Investigative Ophthalmology & Visual Science*, 54(12), 7614-7622.

Bhat, S. P. (2001) 'The ocular lens epithelium', *Bioscience Reports*, 21(4), 537-563.

Bi, X., Chang, V., Molnar, E., McIlhinney, R. A. J. and Baudry, M. (1996) 'The C-terminal domain of glutamate receptor subunit 1 is a target for calpain-mediated proteolysis', *Neuroscience*, 73(4), 903-906.

Bitel, C. L., Nathan, R., Wong, P., Kuppasani, S., Matsushita, M., Kanazawa, H. and Frederikse, P. H. (2011) 'Evidence That 'Brain-Specific' Fox-1, Fox-2, and nPTB Alternatively Spliced Isoforms Are Produced in the Lens', *Current Eye Research*, 36(4), 321-327.

Bitel, C. L., Perrone-Bizzozero, N. I. and Frederikse, P. H. (2010) 'HuB/C/D, nPTB, REST4, and miR-124 regulators of neuronal cell identity are also utilized in the lens', *Molecular Vision*, 16(244-47), 2301-2316.

Black, D. L. (2003) 'Mechanisms of alternative pre-messenger RNA splicing', *Annual Review of Biochemistry*, 72, 291-336.

Bloemendal, H., Berbers, G. A. M., Dejong, W. W., Ramaekers, F. C. S., Vermorken, A. J. M., Dunia, I. and Benedetti, E. L. (1984) 'INTERACTION OF CRYSTALLINS WITH THE CYTOSKELETAL PLASMA-MEMBRANE COMPLEX OF THE BOVINE LENS', *Ciba Foundation Symposia*, 106, 177-&.

Boswell, R. E. and Mahowald, A. P. (1985) 'TUDOR, A GENE REQUIRED FOR ASSEMBLY OF THE GERM PLASM IN DROSOPHILA-MELANOGASTER', *Cell*, 43(1), 97-104.

Boutz, P. L., Stoilov, P., Li, Q., Lin, C. H., Chawla, G., Ostrow, K., Shiue, L., Ares, M. and Black, D. L. (2007) 'A post-transcriptional regulatory switch in polypyrimidine tract-binding proteins reprograms alternative splicing in developing neurons', *Genes & Development*, 21(13), 1636-1652.

Brameier, M., Herwig, A., Reinhardt, R., Walter, L. and Gruber, J. (2011) 'Human box C/D snoRNAs with miRNA like functions: expanding the range of regulatory RNAs', *Nucleic Acids Research*, 39(2), 675-686.

Bratkovic, T. and Rogelj, B. (2014) 'The many faces of small nucleolar RNAs', *Biochimica Et Biophysica Acta-Gene Regulatory Mechanisms*, 1839(6), 438-443.

Breshears, L. M., Wessels, D., Soll, D. R. and Titus, M. A. (2010) 'An unconventional myosin required for cell polarization and chemotaxis', *Proceedings of the National Academy of Sciences of the United States of America*, 107(15), 6918-6923.

Bresnick, A. R. (1999) 'Molecular mechanisms of nonmuscle myosin-II regulation', *Current Opinion in Cell Biology*, 11(1), 26-33.

Bruey, J. M., Ducasse, C., Bonniaud, P., Ravagnan, L., Susin, S. A., Diaz-Latoud, C., Gurbuxani, S., Arrigo, A. P., Kroemer, G., Solary, E. and Garrido, C. (2000) 'Hsp27 negatively regulates cell death by interacting with cytochrome c', *Nature Cell Biology*, 2(9), 645-652.

Bryantsev, A. L., Kurchashova, S. Y., Golyshev, S. A., Polyakov, V. Y., Wunderink, H. F., Kanon, B., Budagova, K. R., Kabakov, A. E. and Kampinga, H. H. (2007) 'Regulation of stress-induced intracellular sorting and chaperone function of Hsp27 (HspB1) in mammalian cells', *Biochemical Journal*, 407, 407-417.

Bu, L., Jin, Y. P., Shi, Y. F., Chu, R. Y., Ban, A. R., Eiberg, H., Andres, L., Jiang, H. S., Zheng, G. Y., Qian, M. Q., Cui, B., Xia, Y., Liu, J., Hu, L. D., Zhao, G. P., Hayden, M. R. and Kong, X. Y. (2002) 'Mutant DNA-binding domain of HSF4 is associated with autosomal dominant lamellar and Marner cataract', *Nature Genetics*, 31(3), 276-278.

Buchan, J. R. (2014) 'mRNP granules Assembly, function, and connections with disease', *Rna Biology*, 11(8), 1019-1030.

Callebaut, I. and Mornon, J. P. (1997) 'The human EBNA-2 coactivator p100: Multidomain organization and relationship to the staphylococcal nuclease fold and to the tudor protein involved in Drosophila melanogaster development', *Biochemical Journal*, 321, 125-132.

Callebaut, I. and Mornon, J. P. (2010) 'LOTUS, a new domain associated with small RNA pathways in the germline', *Bioinformatics*, 26(9), 1140-1144.

Castello, A., Fischer, B., Eichelbaum, K., Horos, R., Beckmann, B. M., Strein, C., Davey, N. E., Humphreys, D. T., Preiss, T., Steinmetz, L. M., Krijgsveld, J. and Hentze, M. W. (2012) 'Insights into RNA Biology from an Atlas of Mammalian mRNA-Binding Proteins', *Cell*, 149(6), 1393-1406.

Chee, K. S. N., Kistler, J. and Donaldson, P. J. (2006) 'Roles for KCC transporters in the maintenance of lens transparency', *Investigative Ophthalmology & Visual Science*, 47(2), 673-682.

Chen, C., Jin, J., James, D. A., Adams-Cioaba, M. A., Park, J. G., Guo, Y. H., Tenaglia, E., Xu, C., Gish, G., Min, J. R. and Pawson, T. (2009) 'Mouse Piwi interactome identifies binding mechanism of Tdrkh Tudor domain to arginine methylated Miwi', *Proceedings of the National Academy of Sciences of the United States of America*, 106(48), 20336-20341.

Chen, C., Nott, T. J., Jin, J. and Pawson, T. (2011) 'Deciphering arginine methylation: Tudor tells the tale', *Nature Reviews Molecular Cell Biology*, 12(10), 629-642.

Cheng, C., Ansari, M. M., Cooper, J. A. and Gong, X. H. (2013) 'EphA2 and Src regulate equatorial cell morphogenesis during lens development', *Development*, 140(20), 4237-4245.

Chong, J. H. A., Tapiaramirez, J., Kim, S., Toledoaral, J. J., Zheng, Y. C., Boutros, M. C., Altshuller, Y. M., Frohman, M. A., Kraner, S. D. and Mandel, G. (1995) 'REST - A MAMMALIAN SILENCER PROTEIN THAT RESTRICTS SODIUM-CHANNEL GENE-EXPRESSION TO NEURONS', *Cell*, 80(6), 949-957.

Chow, R. L., Altmann, C. R., Lang, R. A. and Hemmati-Brivanlou, A. (1999) 'Pax6 induces ectopic eyes in a vertebrate', *Development*, 126(19), 4213-4222.

Chow, R. L. and Lang, R. A. (2001) 'Early eye development in vertebrates', *Annual Review of Cell and Developmental Biology*, 17, 255-296.

Cirillo, D., Livi, C. M., Agostini, F. and Tartaglia, G. G. (2014) 'Discovery of protein-RNA networks', *Molecular Biosystems*, 10(7), 1632-1642.

Cirulli, E. T. and Goldstein, D. B. (2010) 'Uncovering the roles of rare variants in common disease through whole-genome sequencing', *Nature Reviews Genetics*, 11(6), 415-425.

Clark, J. I., Matsushima, H., David, L. L. and Clark, J. M. (1999) 'Lens cytoskeleton and transparency: a model', *Eye*, 13, 417-424.

Cole, R. A. and Fowler, J. E. (2006) 'Polarized growth: maintaining focus on the tip', *Current Opinion in Plant Biology*, 9(6), 579-588.

Conaco, C., Otto, S., Han, J. J. and Mandel, G. (2006) 'Reciprocal actions of REST and a microRNA promote neuronal identity', *Proceedings of the National Academy of Sciences of the United States of America*, 103(7), 2422-2427.

Conte, I., Carrella, S., Avellino, R., Karali, M., Marco-Ferreres, R., Bovolenta, P. and Banfi, S. (2010) 'miR-204 is required for lens and retinal development via Meis2 targeting', *Proceedings of the National Academy of Sciences of the United States of America*, 107(35), 15491-15496.

Couzin, J. (2008) 'MicroRNAs make big impression in disease after disease', *Science*, 319(5871), 1782-1784.

Creighton, C. J., Nagaraja, A. K., Hanash, S. M., Matzuk, M. M. and Gunaratne, P. H. (2008) 'A bioinformatics tool for linking gene expression profiling results with public databases of microRNA target predictions', *Rna-a Publication of the Rna Society*, 14(11), 2290-2296.

Croall, D. E. and Ersfeld, K. (2007) 'The calpains: modular designs and functional diversity', *Genome Biology*, 8(6), 11.

Cvekl, A. and Ashery-Padan, R. (2014) 'The cellular and molecular mechanisms of vertebrate lens development', *Development*, 141(23), 4432-4447.

Cvekl, A. and Duncan, M. K. (2007) 'Genetic and epigenetic mechanisms of gene regulation during lens development', *Progress in Retinal and Eye Research*, 26(6), 555-597.

Cvekl, A. and Mitton, K. P. (2010) 'Epigenetic regulatory mechanisms in vertebrate eye development and disease', *Heredity*, 105(1), 135-151.

Cvekl, A. and Tamm, E. R. (2004) 'Anterior eye development and ocular mesenchyme: new insights from mouse models and human diseases', *Bioessays*, 26(4), 374-386.

Cvekl, A. and Wang, W. L. (2009) 'Retinoic acid signaling in mammalian eye development', *Experimental Eye Research*, 89(3), 280-291.

Cvekl, A., Yang, Y., Chauhan, B. K. and Cveklova, K. (2004) 'Regulation of gene expression by Pax6 in ocular cells: a case of tissue-preferred expression of crystallins in lens',

International Journal of Developmental Biology, 48(8-9), 829-844.

Dassi, E. and Quattrone, A. (2012) 'Tuning the engine An introduction to resources on post-transcriptional regulation of gene expression', *Rna Biology*, 9(10), 1224-1232.

David, L. L., Azuma, M. and Shearer, T. R. (1994) 'CATARACT AND THE ACCELERATION OF CALPAIN-INDUCED BETA-CRYSTALLIN INSOLUBILIZATION OCCURRING DURING NORMAL MATURATION OF RAT LENS', *Investigative Ophthalmology & Visual Science*, 35(3), 785-793.

De Maria, A., Shi, Y. R., Kumar, N. M. and Bassnett, S. (2009) 'Calpain Expression and Activity during Lens Fiber Cell Differentiation', *Journal of Biological Chemistry*, 284(20), 13542-13550.

de Thonel, A., Le Mouel, A. and Mezger, V. (2012) 'Transcriptional regulation of small HSP-HSF1 and beyond', *International Journal of Biochemistry & Cell Biology*, 44(10), 1593-1612.

Dejong, W. W., Leunissen, J. A. M. and Voorter, C. E. M. (1993) 'EVOLUTION OF THE ALPHA-CRYSTALLIN SMALL HEAT-SHOCK PROTEIN FAMILY', *Molecular Biology and Evolution*, 10(1), 103-126.

Delpire, E. and Mount, D. B. (2002) 'Human and murine phenotypes associated with defects in cation-chloride cotransport', *Annual Review of Physiology*, 64, 803-843.

Development of the Ocular Lens (2004), The Edinburgh Building, Cambridge CB2 2RU, UK: Cambridge University Press.

Dickson, D. H. and Crock, G. W. (1972) 'INTERLOCKING PATTERNS ON PRIMATE LENS FIBERS', *Investigative Ophthalmology*, 11(10), 809-&.

Dieci, G., Preti, M. and Montanini, B. (2009) 'Eukaryotic snoRNAs: A paradigm for gene expression flexibility', *Genomics*, 94(2), 83-88.

Dimanlig, P. V., Faber, S. C., Auerbach, W., Makarenkova, H. P. and Lang, R. A. (2001) 'The upstream ectoderm enhancer in Pax6 has an important role in lens induction', *Development*, 128(22), 4415-4424.

Donner, A. L., Lachke, S. A. and Maas, R. L. (2006) 'Lens induction in vertebrates: Variations on a conserved theme of signaling events', *Seminars in Cell & Developmental Biology*, 17(6), 676-685.

Doshi, B. M., Hightower, L. E. and Lee, J. (2009a) 'The role of Hsp27 and actin in the

regulation of movement in human cancer cells responding to heat shock', *Cell Stress & Chaperones*, 14(5), 445-457.

Doshi, B. M., Hightower, L. E. and Lee, J. (2009b) 'The role of Hsp27 and actin in the regulation of movement in human cancer cells responding to heat shock', *Cell Stress & Chaperones*, 14(5), 445-457.

Doshi, B. M., Hightower, L. E. and Lee, J. (2010a) 'HSPB1, actin filament dynamics, and aging cells', *Aging, Cancer, and Age-Related Diseases: Common Mechanism?*, 1197, 76-84.

Doshi, B. M., Hightower, L. E. and Lee, J. (2010b) 'HSPB1, actin filament dynamics, and aging cells', *Aging, Cancer, and Age-Related Diseases: Common Mechanism?*, 1197, 76-84.

Dotti, C. G., Sullivan, C. A. and Banker, G. A. (1988) 'THE ESTABLISHMENT OF POLARITY BY HIPPOCAMPAL-NEURONS IN CULTURE', *Journal of Neuroscience*, 8(4), 1454-1468.

Du, T. T. and Zamore, P. D. (2005) 'microPrimer: The biogenesis and function of microRNA', *Development*, 132(21), 4645-4652.

Duncan, M. K. (2011) 'A New Focus on RNA in the Lens', *Science*, 331(6024), 1523-1524.

Duncan, M. K., Xie, L. K., David, L. L., Robinson, M. L., Taube, J. R., Cui, W. W. and Reneker, L. W. (2004) 'Ectopic Pax6 expression disturbs lens fiber cell differentiation', *Investigative Ophthalmology & Visual Science*, 45(10), 3589-3598.

Durinck, S., Moreau, Y., Kasprzyk, A., Davis, S., De Moor, B., Brazma, A. and Huber, W. (2005) 'BioMart and Bioconductor: a powerful link between biological databases and microarray data analysis', *Bioinformatics*, 21(16), 3439-3440.

Durinck, S., Spellman, P. T., Birney, E. and Huber, W. (2009) 'Mapping identifiers for the integration of genomic datasets with the R/Bioconductor package biomaRt', *Nature Protocols*, 4(8), 1184-1191.

Edbauer, D., Neilson, J. R., Foster, K. A., Wang, C. F., Seeburg, D. P., Batterton, M. N., Tada, T., Dolan, B. M., Sharp, P. A. and Sheng, M. (2010) 'Regulation of Synaptic Structure and Function by FMRP-Associated MicroRNAs miR-125b and miR-132', *Neuron*, 65(3), 373-384.

Egelman, E. H. (2003) 'Actin's prokaryotic homologs', *Current Opinion in Structural Biology*, 13(2), 244-248.

Ender, C., Krek, A., Friedlander, M. R., Beitzinger, M., Weinmann, L., Chen, W., Pfeffer, S., Rajewsky, N. and Meister, G. (2008) 'A Human snoRNA with MicroRNA-Like Functions', *Molecular Cell*, 32(4), 519-528.

Enright, A. J., John, B., Gaul, U., Tuschl, T., Sander, C. and Marks, D. S. (2004) 'MicroRNA targets in Drosophila', *Genome Biology*, 5(1), 14.

Epstein, J. A., Glaser, T., Cai, J. X., Jepeal, L., Walton, D. S. and Maas, R. L. (1994) '2 INDEPENDENT AND INTERACTIVE DNA-BINDING SUBDOMAINS OF THE PAX6 PAIRED DOMAIN ARE REGULATED BY ALTERNATIVE SPLICING', *Genes & Development*, 8(17), 2022-2034.

Ernoult-Lange, M., Benard, M., Kress, M. and Weil, D. (2012) 'P-bodies and mitochondria: Which place in RNA interference?', *Biochimie*, 94(7), 1572-1577.

Eulalio, A., Behm-Ansmant, I. and Izaurralde, E. (2007) 'P bodies: at the crossroads of post-transcriptional pathways', *Nature Reviews Molecular Cell Biology*, 8(1), 9-22.

Faber, S. C., Robinson, M. L., Makarenkova, H. P. and Lang, R. A. (2002) 'Bmp signaling is required for development of primary lens fiber cells', *Development*, 129(15), 3727-3737.

Fan, J. G., Dong, L. J., Mishra, S., Chen, Y. W., FitzGerald, P. and Wistow, G. (2012) 'A role for gamma S-crystallin in the organization of actin and fiber cell maturation in the mouse lens', *Febs Journal*, 279(16), 2892-2904.

Farnswor.Pn, Fu, S. C. J., Burke, P. A. and Bahia, I. (1974) 'ULTRASTRUCTURE OF RAT EYE LENS FIBERS', *Investigative Ophthalmology*, 13(4), 274-279.

Faulkner-Jones, B., Zandy, A. J. and Bassnett, S. (2003) 'RNA stability in terminally differentiating fibre cells of the ocular lens', *Experimental Eye Research*, 77(4), 463-476.

Filipowicz, W., Bhattacharyya, S. N. and Sonenberg, N. (2008) 'Mechanisms of post-transcriptional regulation by microRNAs: are the answers in sight?', *Nature Reviews Genetics*, 9(2), 102-114.

Findley, S. D., Tamanaha, M., Clegg, N. J. and Ruohola-Baker, H. (2003) 'Maelstrom, a Drosophila spindle-class gene, encodes a protein that colocalizes with Vasa and RDE1/AGO1 homolog, Aubergine, in nuage', *Development*, 130(5), 859-871.

Finehout, E. J. and Lee, K. H. (2003) 'Comparison of automated in-gel digest methods for

femtomole level samples', *Electrophoresis*, 24(19-20), 3508-3516.

Firtina, Z. and Duncan, M. K. (2011) 'Unfolded Protein Response (UPR) is activated during normal lens development', *Gene Expression Patterns*, 11(1-2), 135-143.

Fischer, R. S., Lee, A. and Fowler, V. M. (2000) 'Tropomodulin and tropomyosin mediate lens cell actin cytoskeleton reorganization in vitro', *Investigative Ophthalmology & Visual Science*, 41(1), 166-174.

Fischer, R. S., Quinlan, R. A. and Fowler, V. M. (2003) 'Tropomodulin binds to filensin intermediate filaments', *Febs Letters*, 547(1-3), 228-232.

FitzGerald, P. G. (2009) 'Lens intermediate filaments', *Experimental Eye Research*, 88(2), 165-172.

Fitzgerald, P. G. and Casselman, J. (1990) 'DISCRIMINATION BETWEEN THE LENS FIBER CELL 115 KD CYTOSKELETAL PROTEIN AND ALPHA-ACTININ', *Current Eye Research*, 9(9), 873-882.

Foster-Barber, A. and Bishop, J. M. (1998) 'Src interacts with dynamin and synapsin in neuronal cells', *Proceedings of the National Academy of Sciences of the United States of America*, 95(8), 4673-4677.

Frederikse, P. H., Donnelly, R. and Partyka, L. M. (2006) 'miRNA and Dicer in the mammalian lens: expression of brain-specific miRNAs in the lens', *Histochemistry and Cell Biology*, 126(1), 1-8.

Frederikse, P. H., Kasinathan, C. and Kleiman, N. J. (2012) 'Parallels between neuron and lens fiber cell structure and molecular regulatory networks', *Developmental Biology*, 368(2), 255-260.

Friberg, A., Corsini, L., Mourao, A. and Sattler, M. (2009) 'Structure and Ligand Binding of the Extended Tudor Domain of D. melanogaster Tudor-SN', *Journal of Molecular Biology*, 387(4), 921-934.

Fukiage, C., Nakajima, E., Ma, H., Azuma, M. and Shearer, T. R. (2002) 'Characterization and regulation of lens-specific calpain Lp82', *Journal of Biological Chemistry*, 277(23), 20678-20685.

Gamba, G. (2005) 'Molecular physiology and pathophysiology of electroneutral cation-chloride cotransporters', *Physiological Reviews*, 85(2), 423-493.

Ganatra, D. A., Kaid, J. S. R., Parmar, T. J., Patel, A. R., Rajkumar, S., Arora, A. I., Kayastha,

F. B., Pal, A. K., Gajjar, D. U. and Vasavada, A. R. (2013) 'Estrogen mediated protection of cytoskeleton against oxidative stress', *Indian Journal of Medical Research*, 137, 117-124.

Ganot, P., CaizerguesFerrer, M. and Kiss, T. (1997) 'The family of box ACA small nucleolar RNAs is defined by an evolutionarily conserved secondary structure and ubiquitous sequence elements essential for RNA accumulation', *Genes & Development*, 11(7), 941-956.

Geatrell, J. C., Gan, P. M., Mansergh, F. C., Kisiswa, L., Jarrin, M., Williams, L. A., Evans, M. J., Boulton, M. E. and Wride, M. A. (2009) 'Apoptosis gene profiling reveals spatio-temporal regulated expression of the p53/Mdm2 pathway during lens development', *Experimental Eye Research*, 88(6), 1137-1151.

Girard, A., Sachidanandam, R., Hannon, G. J. and Carmell, M. A. (2006) 'A germline-specific class of small RNAs binds mammalian Piwi proteins', *Nature*, 442(7099), 199-202.

Glaser, T., Jepeal, L., Edwards, J. G., Young, S. R., Favor, J. and Maas, R. L. (1994) 'PAX6 GENE DOSAGE EFFECT IN A FAMILY WITH CONGENITAL CATARACTS, ANIRIDIA, ANOPHTHALMIA AND CENTRAL-NERVOUS-SYSTEM DEFECTS', *Nature Genetics*, 7(4), 463-471.

Glisovic, T., Bachorik, J. L., Yong, J. and Dreyfuss, G. (2008) 'RNA-binding proteins and post-transcriptional gene regulation', *Febs Letters*, 582(14), 1977-1986.

Gopalsrivastava, R., Haynes, J. I. and Piatigorsky, J. (1995) 'REGULATION OF THE MURINE ALPHA-B-CRYSTALLIN SMALL HEAT-SHOCK PROTEIN GENE IN CARDIAC-MUSCLE', *Molecular and Cellular Biology*, 15(12), 7081-7090.

Gourlay, C. W. and Ayscough, K. R. (2005) 'The actin cytoskeleton: a key regulator of apoptosis and ageing?', *Nature Reviews Molecular Cell Biology*, 6(7), 583-U5.

Graceffa, P. (2011) 'Hsp27-actin interaction', *Biochemistry research international*, 2011, 901572.

Graw, J. (1999a) 'Cataract mutations and lens development', *Progress in Retinal and Eye Research*, 18(2), 235-267.

Graw, J. (1999b) 'Cataract mutations and lens development', *Progress in Retinal and Eye Research*, 18(2), 235-267.

Graw, J. (2009a) 'Mouse models of cataract', *Journal of Genetics*, 88(4), 469-486.

Graw, J. (2009b) 'Mouse models of cataract', *Journal of Genetics*, 88(4), 469-486.

Graw, J. (2010a) 'EYE DEVELOPMENT' in Koopman, P., ed., *Organogenesis in Development*, San Diego: Elsevier Academic Press Inc, 343-386.

Graw, J. (2010b) 'EYE DEVELOPMENT' in Koopman, P., ed., *Organogenesis in Development*, San Diego: Elsevier Academic Press Inc, 343-386.

Gribbon, C., Dahm, R., Prescott, A. R. and Quinlan, R. A. (2002) 'Association of the nuclear matrix component NuMA with the Cajal body and nuclear speckle compartments during transitions in transcriptional activity in lens cell differentiation', *European Journal of Cell Biology*, 81(10), 557-566.

Grob, T. J., Novak, U., Maisse, C., Barcaroli, D., Luthi, A. U., Pirnia, F., Hugli, B., Graber, H. U., De Laurenzi, V., Fey, M. F., Melino, G. and Tobler, A. (2001) 'Human Delta Np73 regulates a dominant negative feedback loop for TAp73 and p53', *Cell Death and Differentiation*, 8(12), 1213-1223.

Gunawardane, L. S., Saito, K., Nishida, K. M., Miyoshi, K., Kawamura, Y., Nagami, T., Siomi, H. and Siomi, M. C. (2007) 'A slicer-mediated mechanism for repeat-associated siRNA 5 ' end formation in Drosophila', *Science*, 315(5818), 1587-1590.

Guo, Y., Liao, Y., Jia, C. Y., Ren, J. L., Wang, J. C. and Li, T. (2013) 'MicroRNA-182 Promotes Tumor Cell Growth by Targeting Transcription Elongation Factor A-like 7 in Endometrial Carcinoma', *Cellular Physiology and Biochemistry*, 32(3), 581-590.

Haase, A. D., Fenoglio, S., Muerdter, F., Guzzardo, P. M., Czech, B., Pappin, D. J., Chen, C. F., Gordon, A. and Hannon, G. J. (2010) 'Probing the initiation and effector phases of the somatic piRNA pathway in Drosophila', *Genes & Development*, 24(22), 2499-2504.

Halder, G., Callaerts, P. and Gehring, W. J. (1995) 'INDUCTION OF ECTOPIC EYES BY TARGETED EXPRESSION OF THE EYELESS GENE IN DROSOPHILA', *Science*, 267(5205), 1788-1792.

Hall, A. (2005) 'Rho GTPases and the control of cell behaviour', *Biochemical Society Transactions*, 33, 891-895.

Hansson, H. (1970) 'Scanning electron microscopy of the lens of the adult rat.', *Z Zellforsch Mikrosk Anat*, 107(2), 187-98.

Harding, C. V., Susan, S., and Murphy, H. (1976) 'Light and scanning electron microscopy of rabbit lens capsules with intraocular lenses.', *Ophthalmic Res.*, 8, 443-455.

Haubst, N., Berger, J., Radjendirane, V., Graw, J., Favor, J., Saunders, G. F., Stoykova, A. and Gotz, M. (2004) 'Molecular dissection of Pax6 function: the specific roles of the paired domain and homeodomain in brain development', *Development*, 131(24), 6131-6140.

HCFA, H. F. A. (1996) *Historical Data*, Green Book.

Heavner, W. and Pevny, L. (2012) 'Eye Development and Retinogenesis', *Cold Spring Harbor Perspectives in Biology*, 4(12), 17.

Hegedus, B., Dasgupta, B., Shin, J. E., Emnett, R. J., Hart-Mahon, E. K., Elghazi, L., Bernal-Mizrachi, E. and Gutmann, D. H. (2007) 'Neurofibromatosis-1 regulates neuronal and glial cell differentiation from neuroglial progenitors in vivo by both cAMP- and ras-dependent mechanisms', *Cell Stem Cell*, 1(4), 443-457.

Hell, J. W., Westenbroek, R. E., Breeze, L. J., Wang, K. K. W., Chavkin, C. and Catterall, W. A. (1996) 'N-methyl-D-aspartate receptor-induced proteolytic conversion of postsynaptic class C L-type calcium channels in hippocampal neurons', *Proceedings of the National Academy of Sciences of the United States of America*, 93(8), 3362-3367.

Henrion-Caude, A., Girard, M. and Amiel, J. (2012) 'MicroRNAs in Genetic Disease: Rethinking the Dosage', *Current Gene Therapy*, 12(4), 292-300.

Hess, H. H., Newsome, D. A., Knapka, J. J. and Westney, G. E. (1982) 'SLITLAMP ASSESSMENT OF AGE OF ONSET AND INCIDENCE OF CATARACTS IN PINK-EYED, TAN-HOODED RETINAL DYSTROPHIC RATS', *Current Eye Research*, 2(4), 265-269.

Hill, R. E., Favor, J., Hogan, B. L. M., Ton, C. C. T., Saunders, G. F., Hanson, I. M., Prosser, J., Jordan, T., Hastie, N. D. and Vanheyningen, V. (1991) 'MOUSE SMALL EYE RESULTS FROM MUTATIONS IN A PAIRED-LIKE HOMEOBOX-CONTAINING GENE', *Nature*, 354(6354), 522-525.

Hoffmann, A., Huang, Y. S., Suetsugu-Maki, R., Ringelberg, C. S., Tomlinson, C. R., Del Rio-Tsonis, K. and Tsonis, P. A. (2012) 'Implication of the miR-184 and miR-204 Competitive RNA Network in Control of Mouse Secondary Cataract', *Molecular Medicine*, 18(3), 528-538.

Hollenberg, M. J., Wyse, J. P. H. and Lewis, B. J. (1976) 'SURFACE MORPHOLOGY OF LENS FIBERS FROM EYES OF NORMAL AND MICROPHTHALMIC (BROWMAN) RATS', *Cell and Tissue Research*, 167(4), 425-438.

Honda, K., Yamada, T., Endo, R., Ino, Y., Gotoh, M., Tsuda, H., Yamada, Y., Chiba, H. and Hirohashi, S. (1998) 'Actinin-4, a novel actin-bundling protein associated with cell motility and cancer invasion', *Journal of Cell Biology*, 140(6), 1383-1393.

Hosokawa, M., Shoji, M., Kitamura, K., Tanaka, T., Noce, T., Chuma, S. and Nakatsuji, N. (2007) 'Tudor-related proteins TDRD1/MTR-1, TDRD6 and TDRD7/TRAP: Domain composition, intracellular localization, and function in male germ cells in mice', *Developmental Biology*, 301(1), 38-52.

Huang, L., Yappert, M. C., Miller, J. J. and Borchman, D. (2007) 'Thyroxine ameliorates oxidative stress by inducing lipid compositional changes in human lens epithelial cells', *Investigative Ophthalmology & Visual Science*, 48(8), 3698-3704.

Hughes, A. E., Bradley, D. T., Campbell, M., Lechner, J., Dash, D. P., Simpson, D. A. and Willoughby, C. E. (2011) 'Mutation Altering the miR-184 Seed Region Causes Familial Keratoconus with Cataract', *American Journal of Human Genetics*, 89(5), 628-633.

Huntington, J. A. (2011) 'Serpin structure, function and dysfunction', *Journal of Thrombosis and Haemostasis*, 9, 26-34.

Huot, J., Houle, F., Spitz, D. R. and Landry, J. (1996) 'HSP27 phosphorylation-mediated resistance against actin fragmentation and cell death induced by oxidative stress', *Cancer Research*, 56(2), 273-279.

Ionides, A., Francis, P., Berry, V., Mackay, D., Bhattacharya, S., Shiels, A. and Moore, A. (1999) 'Clinical and genetic heterogeneity in autosomal dominant cataract', *British Journal of Ophthalmology*, 83(7), 802-808.

Ireland, M., Lieska, N. and Maisel, H. (1983) 'LENS ACTIN - PURIFICATION AND LOCALIZATION', *Experimental Eye Research*, 37(4), 393-408.

Ireland, M. and Maisel, H. (1983a) 'IDENTIFICATION OF NATIVE ACTIN-FILAMENTS IN CHICK LENS FIBER CELLS', *Experimental Eye Research*, 36(4), 531-536.

Ireland, M. and Maisel, H. (1983b) 'IDENTIFICATION OF NATIVE ACTIN-FILAMENTS IN CHICK LENS FIBER CELLS', *Experimental Eye Research*, 36(4), 531-536.

Ireland, M. and Maisel, H. (1984a) 'A CYTOSKELETAL PROTEIN UNIQUE TO LENS FIBER CELL-DIFFERENTIATION', *Experimental Eye Research*, 38(6), 637-645.

Ireland, M. and Maisel, H. (1984b) 'A CYTOSKELETAL PROTEIN UNIQUE TO LENS FIBER CELL-DIFFERENTIATION', *Experimental Eye Research*, 38(6), 637-645.

Iwig, M., Glaesser, D. and Bethge, M. (1981) 'CELL SHAPE-MEDIATED GROWTH-CONTROL OF LENS EPITHELIAL-CELLS GROWN IN CULTURE', *Experimental Cell Research*, 131(1), 47-55.

Jalan-Sakrikar, N., Bartlett, R. K., Baucum, A. J. and Colbran, R. J. (2012) 'Substrate-selective and Calcium-independent Activation of CaMKII by alpha-Actinin', *Journal of Biological Chemistry*, 287(19), 15275-15283.

Jamieson, R. V., Perveen, R., Kerr, B., Carette, M., Yardley, J., Heon, E., Wirth, M. G., van Heyningen, V., Donnai, D., Munier, F. and Black, G. C. M. (2002) 'Domain disruption and mutation of the bZIP transcription factor, MAF, associated with cataract, ocular anterior segment dysgenesis and coloboma', *Human Molecular Genetics*, 11(1), 33-42.

Janga, S. C. (2012) 'From specific to global analysis of posttranscriptional regulation in eukaryotes: posttranscriptional regulatory networks', *Briefings in Functional Genomics*, 11(6), 505-521.

Jean, D., Ewan, K. and Gruss, P. (1998) 'Molecular regulators involved in vertebrate eye development', *Mechanisms of Development*, 76(1-2), 3-18.

Jia, Y. F., Wu, S. L., Isenberg, J. S., Dai, S. J., Sipes, J. M., Field, L., Zeng, B. X., Bandle, R. W., Ridnour, L. A., Wink, D. A., Ramchandran, R., Karger, B. L. and Roberts, D. D. (2010) 'Thiolutin inhibits endothelial cell adhesion by perturbing Hsp27 interactions with components of the actin and intermediate filament cytoskeleton', *Cell Stress & Chaperones*, 15(2), 165-181.

Jin, C. F., Jiang, J., Wang, W. and Yao, K. (2010) 'Identification of a MIP mutation that activates a cryptic acceptor splice site in the 3 ' untranslated region', *Molecular Vision*, 16(241-42), 2253-2258.

Jin, Z. B., Hirokawa, G., Gui, L., Takahashi, R., Osakada, F., Hiura, Y., Takahashi, M., Yasuhara, O. and Iwai, N. (2009) 'Targeted deletion of miR-182, an abundant retinal microRNA', *Molecular Vision*, 15(52-53), 523-533.

Jonckheere, A. I., Hogeveen, M., Nijtmans, L. G. J., van den Brand, M. A. M., Janssen, A. J. M., Diepstra, J. H. S., van den Brandt, F. C. A., van den Heuvel, L. P., Hol, F. A., Hofste, T. G. J., Kapusta, L., Dillmann, U., Shamdeen, M. G., Smeitink, J. A. M. and Rodenburg, R. J. T. (2008) 'A novel mitochondrial ATP8 gene mutation in a patient with apical hypertrophic cardiomyopathy and neuropathy', *Journal of Medical Genetics*, 45(3), 129-133.

Jonckheere, A. I., Smeitink, J. A. M. and Rodenburg, R. J. T. (2012) 'Mitochondrial ATP

synthase: architecture, function and pathology', *Journal of Inherited Metabolic Disease*, 35(2), 211-225.

Joy, A., Mohammed, T. A. and Al-Ghoul, K. J. (2010) 'Abnormal fiber end migration in Royal College of Surgeons rats during posterior subcapsular cataract formation', *Molecular Vision*, 16(159), 1453-1466.

Karali, M., Peluso, I., Gennarino, V. A., Bilio, M., Verde, R., Lago, G., Dolle, P. and Banfi, S. (2010) 'miRNeye: a microRNA expression atlas of the mouse eye', *Bmc Genomics*, 11, 14.

Kawaoka, S., Izumi, N., Katsuma, S. and Tomari, Y. (2011) '3 ' End Formation of PIWI-Interacting RNAs In Vitro', *Molecular Cell*, 43(6), 1015-1022.

Kedersha, N. and Anderson, P. (2007) 'Mammalian stress granules and processing bodies' in Lorsch, J., ed., *Translation Initiation: Cell Biology, High-Throughput Methods, and Chemical-Based Approaches*, San Diego: Elsevier Academic Press Inc, 61-+.

Kedersha, N. and Anderson, P. (2009) 'Regulation of Translation by Stress Granules and Processing Bodies' in Hershey, J. W. B., ed., *Translational Control in Health and Disease*, San Diego: Elsevier Academic Press Inc, 155-185.

Keene, J. D. (2007) 'RNA regulons: coordination of post-transcriptional events', *Nature Reviews Genetics*, 8(7), 533-543.

Kerimoglu, C., Agis-Balboa, R. C., Kranz, A., Stilling, R., Bahari-Javan, S., Benito-Garagorri, E., Halder, R., Burkhardt, S., Stewart, A. F. and Fischer, A. (2013) 'Histone-Methyltransferase MLL2 (KMT2B) Is Required for Memory Formation in Mice', *Journal of Neuroscience*, 33(8), 3452-3464.

Khanna, K. K. and Jackson, S. P. (2001) 'DNA double-strand breaks: signaling, repair and the cancer connection', *Nature Genetics*, 27(3), 247-254.

Kilic, F. and Trevithick, J. R. (1995) 'VITAMIN-C REDUCES CYTOCHALASIN-D CATARACTOGENESIS', *Current Eye Research*, 14(10), 943-949.

Kilpinen, H. and Barrett, J. C. (2013) 'How next-generation sequencing is transforming complex disease genetics', *Trends in Genetics*, 29(1), 23-30.

Kim, J. I., Li, T. S., Ho, I. C., Grusby, M. J. and Glimcher, L. H. (1999) 'Requirement for the c-Maf transcription factor in crystallin gene regulation and lens development', *Proceedings of the National Academy of Sciences of the United States of America*, 96(7), 3781-3785.

King, C. R. and Piatigorsky, J. (1984) 'ALTERNATIVE SPLICING OF ALPHA-A-CRYSTALLIN RNA - STRUCTURAL AND QUANTITATIVE-ANALYSES OF THE MESSENGER-RNAS FOR THE ALPHA-A2-CRYSTALLIN AND ALPHA-AINS-CRYSTALLIN POLYPEPTIDES', *Journal of Biological Chemistry*, 259(3), 1822-1826.

Kirino, Y., Kim, N., de Planell-Saguer, M., Khandros, E., Chiorean, S., Klein, P. S., Rigoutsos, I., Jongens, T. A. and Mourelatos, Z. (2009) 'Arginine methylation of Piwi proteins catalysed by dPRMT5 is required for Ago3 and Aub stability', *Nature Cell Biology*, 11(5), 652-U478.

Kozak, M. (1991) 'AN ANALYSIS OF VERTEBRATE MESSENGER-RNA SEQUENCES - INTIMATIONS OF TRANSLATIONAL CONTROL', *Journal of Cell Biology*, 115(4), 887-903.

Kozmik, Z., Czerny, T. and Busslinger, M. (1997) 'Alternatively spliced insertions in the paired domain restrict the DNA sequence specificity of Pax6 and Pax8', *Embo Journal*, 16(22), 6793-6803.

Kumari, S. S., Varadaraj, M., Yerramilli, V. S., Menon, A. G. and Varadaraj, K. (2012) 'Spatial expression of aquaporin 5 in mammalian cornea and lens, and regulation of Its localization by phosphokinase A', *Molecular Vision*, 18(99-102), 957-967.

Kuroyanagi, H. (2009) 'Fox-1 family of RNA-binding proteins', *Cellular and Molecular Life Sciences*, 66(24), 3895-3907.

Kuszak, J., Alcala, J. and Maisel, H. (1980) 'THE SURFACE-MORPHOLOGY OF EMBRYONIC AND ADULT CHICK LENS-FIBER CELLS', *American Journal of Anatomy*, 159(4), 395-410.

Kuszak, J. R., Al-Ghoul, K. J., Novak, L. A., Peterson, K. L., Herbert, K. L. and Sivak, J. G. (1999) 'The internalization of posterior subcapsular cataracts (PSCs) in Royal College of Surgeons (RCS) rats. II. The inter-relationship of optical quality and structure as a function of age', *Molecular vision*, 5, 7-7.

Kuszak, J. R., Macsai, M. S. and Rae, J. L. (1983) 'STEREO SCANNING ELECTRON-MICROSCOPY OF THE CRYSTALLINE LENS', *Scanning Electron Microscopy*, 1415-1426.

Kuszak, J. R., Peterson, K. L. and Brown, H. G. (1996) 'Electron microscopic observations of the crystalline lens', *Microscopy Research and Technique*, 33(6), 441-479.

Kuszak, J. R. and Rae, J. L. (1982) 'SCANNING ELECTRON-MICROSCOPY OF THE FROG LENS', *Experimental Eye Research*, 35(5), 499-519.

Kuszak, J. R., Zoltoski, R. K. and Sivertson, C. (2004a) 'Fibre cell organization in crystalline lenses', *Experimental Eye Research*, 78(3), 673-687.

Kuszak, J. R., Zoltoski, R. K. and Tiedemann, C. E. (2004b) 'Development of lens sutures', *International Journal of Developmental Biology*, 48(8-9), 889-902.

Lachke, S. A., Alkuraya, F. S., Kneeland, S. C., Ohn, T., Aboukhalil, A., Howell, G. R., Saadi, I., Cavallesco, R., Yue, Y. Z., Tsai, A. C. H., Nair, K. S., Cosma, M. I., Smith, R. S., Hodges, E., AlFadhli, S. M., Al-Hajeri, A., Shamseldin, H. E., Behbehani, A., Hannon, G. J., Bulyk, M. L., Drack, A. V., Anderson, P. J., John, S. W. M. and Maas, R. L. (2011) 'Mutations in the RNA Granule Component TDRD7 Cause Cataract and Glaucoma', *Science*, 331(6024), 1571-1576.

Lachke, S. A., Ho, J. W. K., Kryukov, G. V., O'Connell, D. J., Aboukhalil, A., Bulyk, M. L., Park, P. J. and Maas, R. L. (2012) 'iSyTE: Integrated Systems Tool for Eye Gene Discovery', *Investigative Ophthalmology & Visual Science*, 53(3), 1617-1627.

Ladopoulos, V., Hofemeister, H., Hoogenkamp, M., Riggs, A. D., Stewart, A. F. and Bonifer, C. (2013) 'The Histone Methyltransferase KMT2B Is Required for RNA Polymerase II Association and Protection from DNA Methylation at the MagohB CpG Island Promoter', *Molecular and Cellular Biology*, 33(7), 1383-1393.

Lampi, K. J., Ma, Z. X., Hanson, S. R. A., Azuma, M., Shih, M., Shearer, T. R., Smith, D. L., Smith, J. B. and David, L. L. (1998) 'Age-related changes in human lens crystallins identified by two-dimensional electrophoresis and mass spectrometry', *Experimental Eye Research*, 67(1), 31-43.

Lavail, M. M., Sidman, R. L. and Gerhardt, C. O. (1975) 'CONGENIC STRAINS OF RCS RATS WITH INHERITED RETINAL DYSTROPHY', *Journal of Heredity*, 66(4), 242-244.

Lavoie, J. N., Hickey, E., Weber, L. A. and Landry, J. (1993) 'MODULATION OF ACTIN MICROFILAMENT DYNAMICS AND FLUID-PHASE PINOCYTOSIS BY PHOSPHORYLATION OF HEAT-SHOCK PROTEIN-27', *Journal of Biological Chemistry*, 268(32), 24210-24214.

Le Thomas, A., Rogers, A. K., Webster, A., Marinov, G. K., Liao, S. E., Perkins, E. M., Hur, J. K., Aravin, A. A. and Toth, K. F. (2013) 'Piwi induces piRNA-guided transcriptional silencing and establishment of a repressive chromatin state', *Genes & Development*, 27(4), 390-399.

Ledee, D. R., Chen, J., Tonelli, L. H., Takase, H., Gery, I. and Zelenka, P. S. (2004) 'Differential expression of splice variants of chemokine CCL27 mRNA in lens, cornea, and retina of the normal mouse eye', *Molecular Vision*, 10(79-80), 663-667.

Lee, A., Fischer, R. S. and Fowler, V. M. (2000) 'Stabilization and remodeling of the membrane skeleton during lens fiber cell differentiation and maturation', *Developmental Dynamics*, 217(3), 257-270.

Lee, J. H., Shimojo, M., Chai, Y. G. and Hersh, L. B. (2000) 'Studies on the interaction of REST4 with the cholinergic repressor element-1/neuron restrictive silencer element', *Molecular Brain Research*, 80(1), 88-98.

Leung, A. K. L. and Sharp, P. A. (2010) 'MicroRNA Functions in Stress Responses', *Molecular Cell*, 40(2), 205-215.

Li, C. J., Vagin, V. V., Lee, S. H., Xu, J., Ma, S. M., Xi, H. L., Seitz, H., Horwich, M. D., Syrzycka, M., Honda, B. M., Kittler, E. L. W., Zapp, M. L., Klattenhoff, C., Schulz, N., Theurkauf, W. E., Weng, Z. P. and Zamore, P. D. (2009) 'Collapse of Germline piRNAs in the Absence of Argonaute3 Reveals Somatic piRNAs in Flies', *Cell*, 137(3), 509-521.

Li, Y. and Piatigorsky, J. (2009) 'Targeted Deletion of Dicer Disrupts Lens Morphogenesis, Corneal Epithelium Stratification, and Whole Eye Development', *Developmental Dynamics*, 238(9), 2388-2400.

Licatalosi, D. D. and Darnell, R. B. (2010) 'APPLICATIONS OF NEXT-GENERATION SEQUENCING RNA processing and its regulation: global insights into biological networks', *Nature Reviews Genetics*, 11(1), 75-87.

Lim, A. K. and Kai, T. (2007) 'Unique germ-line organelle, nuage, functions to repress selfish genetic elements in Drosophila melanogaster', *Proceedings of the National Academy of Sciences of the United States of America*, 104(16), 6714-6719.

Lis, H. and Sharon, N. (1998) 'Lectins: Carbohydrate-specific proteins that mediate cellular recognition', *Chemical Reviews*, 98(2), 637-674.

Little, J. T. and Jurica, M. S. (2008) 'Splicing factor SPF30 bridges an interaction between the prespliceosome protein U2AF35 and tri-small nuclear ribonucleoprotein protein hPrp3', *Journal of Biological Chemistry*, 283(13), 8145-8152.

Liu, H., Cao, Y. D., Ye, W. X. and Sun, Y. Y. (2010) 'Effect of microRNA-206 on cytoskeleton remodelling by downregulating Cdc42 in MDA-MB-231 cells', *Tumori*,

96(5), 751-755.

Liu, H. P., Wang, J. Y. S., Huang, Y., Li, Z. Z., Gong, W. M., Lehmann, R. and Xu, R. M. (2010) 'Structural basis for methylarginine-dependent recognition of Aubergine by Tudor', *Genes & Development*, 24(17), 1876-1881.

Liu, K., Chen, C., Guo, Y. H., Lam, R., Bian, C. B., Xu, C., Zhao, D. Y., Jin, J., MacKenzie, F., Pawson, T. and Min, J. R. (2010) 'Structural basis for recognition of arginine methylated Piwi proteins by the extended Tudor domain', *Proceedings of the National Academy of Sciences of the United States of America*, 107(43), 18398-18403.

Lo, W. K., Shaw, A. P. and Wen, X. J. (1997) 'Actin filament bundles in cortical fiber cells of the rat lens', *Experimental Eye Research*, 65(5), 691-701.

Loren, C. E., Schrader, J. W., Ahlgren, U. and Gunhaga, L. (2009) 'FGF signals induce Caprin2 expression in the vertebrate lens', *Differentiation*, 77(4), 386-394.

Lovicu, F. J. and McAvoy, J. W. (2005) 'Growth factor regulation of lens development', *Developmental Biology*, 280(1), 1-14.

Lu, J. Y., Mohammed, T. A., Donohue, S. T. and Al-Ghoul, K. J. (2008) 'Distribution of basal membrane complex components in elongating lens fibers', *Molecular Vision*, 14(140), 1187-1203.

Lunde, B. M., Moore, C. and Varani, G. (2007) 'RNA-binding proteins: modular design for efficient function', *Nature Reviews Molecular Cell Biology*, 8(6), 479-490.

Lyon, M. F., Bogani, D., Boyd, Y., Guillot, P. and Favor, J. (2000) 'Further genetic analysis of two autosomal dominant mouse eye defects, Ccw and Pax6(coop)', *Molecular Vision*, 6(25), 199-203.

MA, B., AI, D., VN, Y., IV, B. and J., B. (2004) 'Lipid peroxidation and cataracts: N-acetylcarnosine as a therapeutic tool to manage age-related cataracts in human and in canine eyes', *Drugs in R&D*, 5(3), 125-39.

Ma, H., Fukiage, C., Azuma, M. and Shearer, T. R. (1998) 'Cloning and expression of mRNA for calpain Lp82 from rat lens: Splice variant of p94', *Investigative Ophthalmology & Visual Science*, 39(2), 454-461.

Ma, H., Shih, M., Fukiage, C., Azuma, M., Duncan, M. K., Reed, N. A., Richard, I., Beckmann, J. S. and Shearer, T. R. (2000) 'Influence of specific regions in Lp82 calpain on protein stability, activity, and localization within lens', *Investigative Ophthalmology & Visual Science*, 41(13), 4232-4239.

Ma, S. M., Liu, G. D., Sun, Y. and Xie, J. Y. (2007) 'Relocalization of the polypyrimidine tract-binding protein during PKA-induced neurite growth', *Biochimica Et Biophysica Acta-Molecular Cell Research*, 1773(6), 912-923.

Mackay, D. S., Bennett, T. M., Culican, S. M. and Shiels, A. (2014) 'Exome sequencing identifies novel and recurrent mutations in GJA8 and CRYGD associated with inherited cataract', *Human Genomics*, 8, 8.

Magin, A., Lietz, M., Cibelli, G. and Thiel, G. (2002) 'RE-1 silencing transcription factor-4 (REST4) is neither a transcriptional repressor nor a de-repressor', *Neurochemistry International*, 40(3), 195-202.

Malone, C. D., Brennecke, J., Dus, M., Stark, A., McCombie, W. R., Sachidanandam, R. and Hannon, G. J. (2009) 'Specialized piRNA Pathways Act in Germline and Somatic Tissues of the Drosophila Ovary', *Cell*, 137(3), 522-535.

Mardis, E. R. (2008) 'The impact of next-generation sequencing technology on genetics', *Trends in Genetics*, 24(3), 133-141.

Matsushita, M., Tanaka, S., Nakamura, N., Inoue, H. and Kanazawa, H. (2004) 'A novel kinesin-like protein, KIF1B beta 3 is involved in the movement of lysosomes to the cell periphery in non-neuronal cells', *Traffic*, 5(3), 140-151.

Matsushita, M., Yamamoto, R., Mitsui, K. and Kanazawa, H. (2009) 'Altered Motor Activity of Alternative Splice Variants of the Mammalian Kinesin-3 Protein KIF1B', *Traffic*, 10(11), 1647-1654.

Mattila, P. K. and Lappalainen, P. (2008) 'Filopodia: molecular architecture and cellular functions', *Nature Reviews Molecular Cell Biology*, 9(6), 446-454.

McCabe, K. L. and Bronner-Fraser, M. (2009) 'Molecular and tissue interactions governing induction of cranial ectodermal placodes', *Developmental Biology*, 332(2), 189-195.

Mendez, M. G., Kojima, S. I. and Goldman, R. D. (2010) 'Vimentin induces changes in cell shape, motility, and adhesion during the epithelial to mesenchymal transition', *Faseb Journal*, 24(6), 1838-1851.

Menko, A. S. (2002) 'Lens epithelial cell differentiation', *Experimental Eye Research*, 75(5), 485-490.

Miao, A. Z., Zhang, X. Y., Jiang, Y. X., Chen, Y. H., Fang, Y. W., Ye, H. F., Chu, R. Y. and Lu, Y. (2012) 'Proteomic analysis of SRA01/04 transfected with wild-type and mutant

HSF4b identified from a Chinese congenital cataract family', *Molecular Vision*, 18(73-74), 694-704.

Mills, M. A., Yang, N., Weinberger, R. P., Vander Woude, D. L., Beggs, A. H., Easteal, S. and North, K. N. (2001) 'Differential expression of the actin-binding proteins, alpha-actinin-2 and-3, in different species: implications for the evolution of functional redundancy', *Human Molecular Genetics*, 10(13), 1335-1346.

Miron, T., Vancompernolle, K., Vandekerckhove, J., Wilchek, M. and Geiger, B. (1991) 'A 25-KD INHIBITOR OF ACTIN POLYMERIZATION IS A LOW-MOLECULAR MASS HEAT-SHOCK PROTEIN', *Journal of Cell Biology*, 114(2), 255-261.

Mitchison, T. J. and Cramer, L. P. (1996) 'Actin-based cell motility and cell locomotion', *Cell*, 84(3), 371-379.

Mogilner, A. and Oster, G. (2003) 'Polymer motors: Pushing out the front and pulling up the back', *Current Biology*, 13(18), R721-R733.

Molitoris, B. A., Harrington, J. T., Perrone, R., Jaber, B., Herman, I. M., Balakrishnan, V. S., Pahari, D. K. and Levey, A. S. (2004) 'Actin cytoskeleton in ischemic acute renal failure', *Kidney International*, 66(2), 871-883.

Monastirli, A., Vourekas, A., Badavanis, G., Pasmatzi, E., Sagriotis, A., Drainas, D., Pavlidou, D., Georgiou, S., Sakkis, T., Mantagos, S., Kourounis, G., Varakis, J., Stamatiou, G. and Tsambaos, D. (2005) 'Hsp27 expression coincides with epidermal stratification during human epidermal morphogenesis', *Acta Dermato-Venereologica*, 85(5), 389-393.

Moreno-Dominguez, A., El-Yazbi, A. F., Zhu, H. L., Colinas, O., Zhong, X. Z., Walsh, E. J., Cole, D. M., Kargacin, G. J., Walsh, M. P. and Cole, W. C. (2014) 'Cytoskeletal Reorganization Evoked by Rho-associated kinase- and Protein Kinase C-catalyzed Phosphorylation of Cofilin and Heat Shock Protein 27, Respectively, Contributes to Myogenic Constriction of Rat Cerebral Arteries', *Journal of Biological Chemistry*, 289(30), 20939-20952.

Mousa, G. Y. and Trevithick, J. R. (1977a) 'DIFFERENTIATION OF RAT LENS EPITHELIAL-CELLS IN TISSUE-CULTURE .2. EFFECTS OF CYTOCHALASINS-B AND CYTOCHALASINS-D ON ACTIN ORGANIZATION AND DIFFERENTIATION', *Developmental Biology*, 60(1), 14-25.

Mousa, G. Y. and Trevithick, J. R. (1977b) 'DIFFERENTIATION OF RAT LENS EPITHELIAL-CELLS IN TISSUE-CULTURE .2. EFFECTS OF CYTOCHALASINS-B AND CYTOCHALASINS-D ON ACTIN ORGANIZATION

AND DIFFERENTIATION', *Developmental Biology*, 60(1), 14-25.

Mousa, G. Y. and Trevithick, J. R. (1979a) 'ACTIN IN THE LENS - CHANGES IN ACTIN DURING DIFFERENTIATION OF LENS EPITHELIAL-CELLS INVIVO', *Experimental Eye Research*, 29(1), 71-81.

Mousa, G. Y. and Trevithick, J. R. (1979b) 'ACTIN IN THE LENS - CHANGES IN ACTIN DURING DIFFERENTIATION OF LENS EPITHELIAL-CELLS INVIVO', *Experimental Eye Research*, 29(1), 71-81.

Mullen, R. J. and Lavail, M. M. (1976) 'INHERITED RETINAL DYSTROPHY - PRIMARY DEFECT IN PIGMENT EPITHELIUM DETERMINED WITH EXPERIMENTAL RAT CHIMERAS', *Science*, 192(4241), 799-801.

N, A., M, D. F. and P., L. 'Regulation of K-cl cotransport: From function to genes'.

Nakagawa, S. (2004) 'The role of Wnt signaling in eye organogenesis', *Seikagaku*, 76(12), 1573-1576.

Nishiguchi, S., Wood, H., Kondoh, H., Lovell-Badge, R. and Episkopou, V. (1998) 'Sox1 directly regulates the gamma-crystallin genes and is essential for lens development in mice', *Genes & Development*, 12(6), 776-781.

Norose, K., Lo, W. K., Clark, J. I., Sage, E. H. and Howe, C. C. (2000) 'Lenses of SPARC-null mice exhibit an abnormal cell surface-basement membrane interface', *Experimental Eye Research*, 71(3), 295-307.

Nowak, R. B. and Fowler, V. M. (2012) 'Tropomodulin 1 Constrains Fiber Cell Geometry during Elongation and Maturation in the Lens Cortex', *Journal of Histochemistry & Cytochemistry*, 60(6), 414-427.

Obazawa, H. (1967) 'Electron microscopic studies on the lens nucleus in cataract. I. Normal and senile cataractous lens', *Nippon Ganka Gakkai zasshi*, 71(7), 1019-28.

Okten, Z. and Schliwa, M. (2007) 'Molecular motors - A step dissected', *Nature*, 450(7170), 625-626.

Otey CA, P. F., Burridge K. (1990) 'An interaction between alpha-actinin and the beta 1 integrin subunit in vitro', *The Journal of Cell Biology*, 111(2), 721-9.

Otey, C. A., Vasquez, G. B., Burridge, K. and Erickson, B. W. (1993) 'MAPPING OF THE ALPHA-ACTININ BINDING-SITE WITHIN THE BETA-1 INTEGRIN CYTOPLASMIC DOMAIN', *Journal of Biological Chemistry*, 268(28), 21193-21197.

Pellizzoni, L., Kataoka, N., Charroux, B. and Dreyfuss, G. (1998) 'A novel function for SMN, the spinal muscular atrophy disease gene product, in pre-mRNA splicing', *Cell*, 95(5), 615-624.

Perng, M. D. and Quinlan, R. A. (2005) 'Seeing is believing! The optical properties of the eye lens are dependent upon a functional intermediate filament cytoskeleton', *Experimental Cell Research*, 305(1), 1-9.

Piatigorsky, J. (1981) 'LENS DIFFERENTIATION IN VERTEBRATES - A REVIEW OF CELLULAR AND MOLECULAR-FEATURES', *Differentiation*, 19(3), 134-153.

Pollard, T. D. and Borisy, G. G. (2003) 'Cellular motility driven by assembly and disassembly of actin filaments', *Cell*, 112(4), 453-465.

Quinlan, R. A., Sandilands, A., Procter, J. E., Prescott, A. R., Hutcheson, A. M., Dahm, R., Gribbon, C., Wallace, P. and Carter, J. M. (1999) 'The eye lens cytoskeleton', *Eye*, 13, 409-416.

Rafferty, N. S. and Scholz, D. L. (1985) 'ACTIN IN POLYGONAL ARRAYS OF MICROFILAMENTS AND SEQUESTERED ACTIN BUNDLES (SABS) IN LENS EPITHELIAL-CELLS OF RABBITS AND MICE', *Current Eye Research*, 4(6), 713-718.

Rafferty, N. S., Zigman, S., McDaniel, T. and Scholz, D. L. (1993) 'NEAR-UV RADIATION DISRUPTS FILAMENTOUS ACTIN IN LENS EPITHELIAL-CELLS', *Cell Motility and the Cytoskeleton*, 26(1), 40-48.

Ramaekers, F., Jap, P., Mungyer, G. and Bloemendal, H. (1982) 'MICROFILAMENT ASSEMBLY DURING LENS CELL ELONGATION INVITRO', *Current Eye Research*, 2(3), 169-181.

Ramaekers, F. C. S., Boomkens, T. R. and Bloemendal, H. (1981) 'CYTOSKELETAL AND CONTRACTILE STRUCTURES IN BOVINE LENS CELL-DIFFERENTIATION', *Experimental Cell Research*, 135(2), 454-461.

Ramaswami, M., Taylor, J. P. and Parker, R. (2013) 'Altered Ribostasis: RNA-Protein Granules in Degenerative Disorders', *Cell*, 154(4), 727-736.

Rao, P. V. and Maddala, R. (2006a) 'The role of the lens actin cytoskeleton in fiber cell elongation and differentiation', *Seminars in Cell & Developmental Biology*, 17(6), 698-711.

Rao, P. V. and Maddala, R. (2006b) 'The role of the lens actin cytoskeleton in fiber cell elongation and differentiation', *Seminars in Cell & Developmental Biology*, 17(6), 698-711.

Rao, P. V. and Maddala, R. (2009) 'Abundant Expression of Ponsin, a Focal Adhesion Protein, in Lens and Downregulation of Its Expression by Impaired Cytoskeletal Signaling', *Investigative Ophthalmology & Visual Science*, 50(4), 1769-1777.

Ro-Choi, T. S. (1999) 'Nuclear snRNA and nuclear function (Discovery of 5 ' cap structures in RNA)', *Critical Reviews in Eukaryotic Gene Expression*, 9(2), 107-158.

Rorbach, J. and Minczuk, M. (2012) 'The post-transcriptional life of mammalian mitochondrial RNA', *Biochemical Journal*, 444, 357-373.

Roucou, X. (2009) 'Prion protein and RNA: a view from the cytoplasm', *Frontiers in Bioscience*, 14, 5157-5164.

Saika, S., Ohmi, S., Tanaka, S., Ohnishi, Y., Yamanaka, A. and Ooshima, A. (1997) 'Light and scanning electron microscopy of rabbit lens capsules with intraocular lenses', *Journal of Cataract and Refractive Surgery*, 23(5), 787-794.

Sanchez, A. G., Valle-Casuso, J. C., Medina, J. M. and Tabernero, A. (2012) 'HIF-1 and c-Src mediate increased glucose uptake induced by endothelin-1 and connexin43 in astrocytes', *Febs Journal*, 279, 289-289.

Sanchez-Diaz, P. and Penalva, L. O. F. (2006) 'Post-transcription meets post-genomic: the saga of RNA binding proteins in a new era', *RNA biology*, 3(3), 101-9.

Sauka-Spengler, T. and Bronner-Fraser, M. (2008) 'A gene regulatory network orchestrates neural crest formation', *Nature Reviews Molecular Cell Biology*, 9(7), 557-568.

Savage, S. A. and Bertuch, A. A. (2010) 'The genetics and clinical manifestations of telomere biology disorders', *Genetics in Medicine*, 12(12), 753-764.

Scheiblin, D. A., Gao, J. Y., Caplan, J. L., Simirskii, V. N., Czymmek, K. J., Mathias, R. T. and Duncan, M. K. (2014) 'Beta-1 integrin is important for the structural maintenance and homeostasis of differentiating fiber cells', *International Journal of Biochemistry & Cell Biology*, 50, 132-145.

Schleiff, E., Shore, G. C. and Goping, I. S. (1997) 'Human mitochondrial import receptor, Tom20p. Use of glutathione to reveal specific interactions between Tom20-glutathione S-transferase and mitochondrial precursor proteins', *Febs Letters*, 404(2-3), 314-318.

Schoenwaelder, S. M. and Burridge, K. (1999) 'Bidirectional signaling between the cytoskeleton and integrins', *Current Opinion in Cell Biology*, 11(2), 274-286.

Schoumacher, M., Goldman, R. D., Louvard, D. and Vignjevic, D. M. (2010) 'Actin, microtubules, and vimentin intermediate filaments cooperate for elongation of invadopodia', *Journal of Cell Biology*, 189(3), 541-556.

Sellers, J. R. (2000) 'Myosins: a diverse superfamily', *Biochimica Et Biophysica Acta-Molecular Cell Research*, 1496(1), 3-22.

Shaham, O., Gueta, K., Mor, E., Oren-Giladi, P., Grinberg, D., Xie, Q., Cvekl, A., Shomron, N., Davis, N., Keydar-Prizant, M., Raviv, S., Pasmanik-Chor, M., Bell, R. E., Levy, C., Avellino, R., Banfi, S., Conte, I. and Ashery-Padan, R. (2013) 'Pax6 Regulates Gene Expression in the Vertebrate Lens through miR-204', *Plos Genetics*, 9(3), 15.

Shi, Y. R., Barton, K., De Maria, A., Petrash, J. M., Shiels, A. and Bassnett, S. (2009) 'The stratified syncytium of the vertebrate lens', *Journal of Cell Science*, 122(10), 1607-1615.

Shiels, A., Bennett, T. M. and Hejtmancik, J. F. (2010) 'Cat-Map: putting cataract on the map', *Molecular Vision*, 16(215-19), 2007-2015.

Shukla, G. C. and Padgett, R. A. (2004) 'U4 small nuclear RNA can function in both the major and minor spliceosomes', *Proceedings of the National Academy of Sciences of the United States of America*, 101(1), 93-98.

Sivertson, C. R., Zoltoski, R. K. and Kuszak, J. R. (2003) 'Quantification of variable mature fiber length as a function of lens suture type and age', *Investigative Ophthalmology & Visual Science*, 44, U326-U326.

Skouri-Panet, F., Michiel, M., Ferard, C., Duprat, E. and Finet, S. (2012) 'Structural and functional specificity of small heat shock protein HspB1 and HspB4, two cellular partners of HspB5: Role of the in vitro hetero-complex formation in chaperone activity', *Biochimie*, 94(4), 975-984.

Smith, A. N., Miller, L. A. D., Song, N., Taketo, M. M. and Lang, R. A. (2005) 'The duality of beta-catenin function: A requirement in lens morphogenesis and signaling suppression of lens fate in periocular ectoderm', *Developmental Biology*, 285(2), 477-489.

Somlyo, A. P. and Somlyo, A. V. (2003) 'Ca2+ sensitivity of smooth muscle and nonmuscle myosin II: Modulated by G proteins, kinases, and myosin phosphatase', *Physiological*

Reviews, 83(4), 1325-1358.

Stamenovic, D., Fredberg, J. J., Wang, N., Butler, J. P. and Ingber, D. E. (1996) 'A microstructural approach to cytoskeletal mechanics based on tensegrity', *Journal of Theoretical Biology*, 181(2), 125-136.

Sussman, M. A., McAvoy, J. W., Rudisill, M., Swanson, B., Lyons, G. E., Kedes, L. and Blanks, J. (1996) 'Lens tropomodulin: Developmental expression during differentiation', *Experimental Eye Research*, 63(2), 223-232.

Tanaka, T., Hosokawa, M., Vagin, V. V., Reuter, M., Hayashi, E., Mochizuki, A. L., Kitamura, K., Yamanaka, H., Kondoh, G., Okawa, K., Kuramochi-Miyagawa, S., Nakano, T., Sachidanandam, R., Hannon, G. J., Pillai, R. S., Nakatsuji, N. and Chuma, S. (2011) 'Tudor domain containing 7 (Tdrd7) is essential for dynamic ribonucleoprotein (RNP) remodeling of chromatoid bodies during spermatogenesis', *Proceedings of the National Academy of Sciences of the United States of America*, 108(26), 10579-10584.

Tardieu, A. and Delaye, M. (1988) 'EYE LENS PROTEINS AND TRANSPARENCY - FROM LIGHT TRANSMISSION THEORY TO SOLUTION X-RAY STRUCTURAL-ANALYSIS', *Annual Review of Biophysics and Biophysical Chemistry*, 17, 47-70.

Taube, J. R., Gao, C. Y., Ueda, Y., Zelenka, P. S., David, L. L. and Duncan, M. K. (2002) 'General utility of the chicken beta B1-Crystallin promoter to drive protein expression in lens fiber cells of transgenic mice', *Transgenic Research*, 11(4), 397-410.

Taylor, V. L., AlGhoul, K. J., Lane, C. W., Davis, V. A., Kuszak, J. R. and Costello, M. J. (1996) 'Morphology of the normal human lens', *Investigative Ophthalmology & Visual Science*, 37(7), 1396-1410.

Terada, K., Kanazawa, M., Yano, M., Hanson, B., Hoogenraad, N. and Mori, M. (1997) 'Participation of the import receptor Tom20 in protein import into mammalian mitochondria: Analyses in vitro and in cultured cells', *Febs Letters*, 403(3), 309-312.

The Cell, A Molecular Approach, 2nd edition (2000), Sunderland (MA): Sinauer Associates.

Tojkander, S., Gateva, G. and Lappalainen, P. (2012) 'Actin stress fibers - assembly, dynamics and biological roles', *Journal of Cell Science*, 125(8), 1855-1864.

Tripathi, R. C. and Tripathi, B. J. (1983) 'LENS MORPHOLOGY, AGING, AND CATARACT', *Journals of Gerontology*, 38(3), 258-270.

Virtanen, I., Badley, R. A., Paasivuo, R. and Lehto, V. P. (1984) 'DISTINCT CYTOSKELETAL DOMAINS REVEALED IN SPERM CELLS', *Journal of Cell Biology*, 99(3), 1083-1091.

Vrensen, G. and Willekens, B. (1990) 'BIOMICROSCOPY AND SCANNING ELECTRON-MICROSCOPY OF EARLY OPACITIES IN THE AGING HUMAN LENS', *Investigative Ophthalmology & Visual Science*, 31(8), 1582-1591.

Walcott, S. and Sun, S. X. (2010) 'A mechanical model of actin stress fiber formation and substrate elasticity sensing in adherent cells', *Proceedings of the National Academy of Sciences of the United States of America*, 107(17), 7757-7762.

Walker, J. and Menko, A. S. (2009) 'Integrins in lens development and disease', *Experimental Eye Research*, 88(2), 216-225.

Wang, N. and Ingber, D. E. (1994) 'CONTROL OF CYTOSKELETAL MECHANICS BY EXTRACELLULAR-MATRIX, CELL-SHAPE, AND MECHANICAL TENSION', *Biophysical Journal*, 66(6), 2181-2189.

Wang, N., Naruse, K., Stamenovic, D., Fredberg, J. J., Mijailovich, S. M., Toric-Norrelykke, I. M., Polte, T., Mannix, R. and Ingber, D. E. (2001) 'Mechanical behavior in living cells consistent with the tensegrity model', *Proceedings of the National Academy of Sciences of the United States of America*, 98(14), 7765-7770.

Wang, Y. Q., Guo, R. D., Guo, R. M., Sheng, W. and Yin, L. R. (2013) 'MicroRNA-182 promotes cell growth, invasion, and chemoresistance by targeting programmed cell death 4 (PDCD4) in human ovarian carcinomas', *Journal of Cellular Biochemistry*, 114(7), 1464-1473.

Ware, S. M., El-Hassan, N., Kahler, S. G., Zhang, Q., Ma, Y. W., Miller, E., Wong, B., Spicer, R. L., Craigen, W. J., Kozel, B. A., Grange, D. K. and Wong, L. J. (2009) 'Infantile cardiomyopathy caused by a mutation in the overlapping region of mitochondrial ATPase 6 and 8 genes', *Journal of Medical Genetics*, 46(5), 308-314.

Watkins, N. J. and Bohnsack, M. T. (2012) 'The box C/D and H/ACA snoRNPs: key players in the modification, processing and the dynamic folding of ribosomal RNA', *Wiley Interdisciplinary Reviews-Rna*, 3(3), 397-414.

WawersikvS, Purcell, P. and Maas, R. (2000) 'Pax6 and the genetic control of early eye development', *Results Probl Cell Differ*, 31, 15–36.

Weber, G. F. and Menko, A. S. (2006) 'Actin filament organization regulates the induction of lens cell differentiation and survival', *Developmental Biology*, 295(2), 714-729.

Weis, W. I. and Drickamer, K. (1996) 'Structural basis of lectin-carbohydrate recognition', *Annual Review of Biochemistry*, 65, 441-473.

Wigle, J. T., Chowdhury, K., Gruss, P. and Oliver, G. (1999) 'Prox1 function is crucial for mouse lens-fibre elongation', *Nature Genetics*, 21(3), 318-322.

Williams, S. C., Altmann, C. R., Chow, R. L., Hemmati-Brivanlou, A. and Lang, R. A. (1998) 'A highly conserved lens transcriptional control element from the Pax-6 gene', *Mechanisms of Development*, 73(2), 225-229.

Woo, M. K. and Fowler, V. M. (1994) 'IDENTIFICATION AND CHARACTERIZATION OF TROPOMODULIN AND TROPOMYOSIN IN THE ADULT-RAT LENS', *Journal of Cell Science*, 107, 1359-1367.

Woo, M. K., Lee, A., Fischer, R. S., Moyer, J. and Fowler, V. M. (2000) 'The lens membrane skeleton contains structures preferentially enriched in spectrin-actin or tropomodulin-actin complexes', *Cell Motility and the Cytoskeleton*, 46(4), 257-268.

Yamashiro, S., Gokhin, D. S., Kimura, S., Nowak, R. B. and Fowler, V. M. (2012) 'Tropomodulins: Pointed-end capping proteins that regulate actin filament architecture in diverse cell types', *Cytoskeleton*, 69(6), 337-370.

Yang, J., Luo, L. X., Liu, X. L., Rosenblatt, M. I., Qu, B., Liu, Y. H. and Liu, Y. Z. (2010) 'Down regulation of the PEDF gene in human lens epithelium cells changed the expression of proteins vimentin and alpha B-crystallin', *Molecular Vision*, 16(12-13), 105-112.

Yang, J. C. and Xu, X. L. (2012) 'alpha-Actinin2 is required for the lateral alignment of Z discs and ventricular chamber enlargement during zebrafish cardiogenesis', *Faseb Journal*, 26(10), 4230-4242.

Yao, K., Ye, P. P., Zhang, L., Tan, J., Tang, X. J. and Zhang, Y. D. (2008) 'Epigallocatechin gallate protects against oxidative stress-induced mitochondria-dependent apoptosis in human lens epithelial cells', *Molecular Vision*, 14(26-28), 217-223.

Yeung, T., Georges, P. C., Flanagan, L. A., Marg, B., Ortiz, M., Funaki, M., Zahir, N., Ming, W. Y., Weaver, V. and Janmey, P. A. (2005) 'Effects of substrate stiffness on cell morphology, cytoskeletal structure, and adhesion', *Cell Motility and the Cytoskeleton*, 60(1), 24-34.

Zelenka, P. S. (2004) 'Regulation of cell adhesion and migration in lens development', *International Journal of Developmental Biology*, 48(8-9), 857-865.

Zhang, H. T., Ghai, P., Wu, H., Wang, C. H., Field, J. and Zhou, G. L. (2013) 'Mammalian Adenylyl Cyclase-associated Protein 1 (CAP1) Regulates Cofilin Function, the Actin Cytoskeleton, and Cell Adhesion', *Journal of Biological Chemistry*, 288(29), 20966-20977.

Zhang, W., Cui, H. and Wong, L. J. C. (2014) 'Application of Next Generation Sequencing to Molecular Diagnosis of Inherited Diseases' in Tang, N. L. S. and Poon, T., eds., *Chemical Diagnostics: from Bench to Bedside*, Berlin: Springer-Verlag Berlin, 19-45.

Zhao, H. T., Yang, T. Y., Madakashira, B. P., Thiels, C. A., Bechtle, C. A., Garcia, C. M., Zhang, H., Yu, K., Ornitz, D. M., Beebe, D. C. and Robinson, M. L. (2008) 'Fibroblast growth factor receptor signaling is essential for lens fiber cell differentiation', *Developmental Biology*, 318(2), 276-288.

Zheng, C., Wu, M., He, C. Y., An, X. J., Sun, M., Chen, C. L. and Ye, J. (2014) 'RNA granule component TDRD7 gene polymorphisms in a Han Chinese population with age-related cataract', *Journal of International Medical Research*, 42(1), 153-163.

Zigler, J. S., Bodaness, R. S., Gery, I. and Kinoshita, J. H. (1983) 'EFFECTS OF LIPID-PEROXIDATION PRODUCTS ON THE RAT LENS IN ORGAN-CULTURE - A POSSIBLE MECHANISM OF CATARACT INITIATION IN RETINAL DEGENERATIVE DISEASE', *Archives of Biochemistry and Biophysics*, 225(1), 149-156.

Zigler, J. S. and Hess, H. H. (1985) 'CATARACTS IN THE ROYAL-COLLEGE-OF-SURGEONS RAT - EVIDENCE FOR INITIATION BY LIPID-PEROXIDATION PRODUCTS', *Experimental Eye Research*, 41(1), 67-76.

CURATED GENE LIST FROM TDRD7-/- MOUSE MUTANTS

Table 4. List of genes that are differentially regulated with significant FDR-values and a fold change of 1.5 and over. These genes are also over 10 counts using both counts per million and RPKM.

mgi_symbol	Fold-change (FC)	FDR-corrected Pvalue
mt-Atp8	2.4	3.5E-23
Eif2s3y	1.9	3.1E-04
Krcc1	1.7	3.0E-07
Idi1	1.7	3.2E-22
Gcg	1.7	1.9E-07
Lsm5	1.6	4.6E-04
Rpl39	1.6	3.2E-12
Med21	1.6	8.4E-14
Rnf113a1	1.6	5.6E-12
Tceb1	1.6	1.8E-11
mt-Nd6	1.5	2.4E-12
Cetn3	1.5	3.8E-13
mt-Nd3	1.5	2.4E-10
Nr2f6	1.5	3.9E-07
Uchl3	1.5	1.2E-05
Casp7	1.5	6.1E-10
Tbca	1.4	2.6E-10
Scoc	1.4	3.2E-11
Gm1673	-1.5	3.6E-06
Cxx1a	-1.5	1.9E-03
Pabpn1	-1.5	1.9E-05
Actn2	-1.5	4.2E-05
Pkdcc	-1.5	9.9E-08
Lpin1	-1.5	5.1E-09
Gltp	-1.5	6.7E-10
Snx22	-1.6	5.8E-15
Gpsm2	-1.6	2.9E-17
Metrn	-1.6	6.6E-05
Dcakd	-1.6	3.2E-07
Hspb6	-1.7	6.1E-08
Rpl13	-1.7	4.4E-03
Rpl17	-1.8	6.3E-05

Hspb1	-1.9	1.1E-07
Aarsd1	-1.9	3.4E-03
Avp	-2.1	6.2E-13

COMPARISION OF RPKM AND COUNTS PER MILLION FOR CURATED GENE LIST

Table 5. RPKM and counts per million within the curated list of genes shown in appendix A. Each gene listed has at least 10 RPKM.

mgi_symbol	FDR-corrected Pvalue	C1-RPKM	C2-RPKM	T2-RPKM	T3-RPKM	C1-CPM	C2-CPM	T2-CPM	T3-CPM
mt-Atp8	3.5E-23	628.72	582.47	1146.60	1636.40	143.98	136.86	281.56	383.37
Eif2s3y	3.1E-04	8.71	10.04	21.71	12.09	17.95	21.24	47.99	25.48
Krcc1	3.0E-07	33.55	32.45	50.05	57.02	4.15	4.07	6.68	7.12
Idi1	3.2E-22	14.39	14.42	24.09	24.33	38.43	39.17	66.53	63.47
Gcg	1.9E-07	27.61	37.33	48.64	56.67	35.05	48.63	66.21	73.60
Lsm5	4.6E-04	6.00	7.07	9.13	12.56	2.87	3.64	4.79	5.83
Rpl39	3.2E-12	367.82	396.20	493.93	579.16	172.86	200.27	281.90	316.66
Med21	8.4E-14	28.73	29.39	40.84	48.14	35.34	37.09	53.92	60.62
Rnf113a1	5.6E-12	82.23	80.37	110.55	138.28	112.43	112.75	162.09	193.42
Tceb1	1.8E-11	19.75	21.96	29.51	33.46	21.15	24.13	33.89	36.66
mt-Nd6	2.4E-12	543.52	491.45	706.35	838.13	316.67	293.77	441.28	499.55
Cetn3	3.8E-13	25.90	25.43	34.89	39.78	29.04	29.26	41.95	45.64
mt-Nd3	2.4E-10	480.82	439.23	604.58	727.39	187.83	176.05	253.25	290.70
Nr2f6	3.9E-07	9.19	9.19	7.12	7.38	14.50	14.45	10.11	9.80
Uchl3	1.2E-05	10.57	12.03	14.54	17.74	10.98	12.73	16.01	18.44
Casp7	6.1E-10	37.56	38.37	49.02	57.69	99.09	103.86	138.68	155.68
Tbca	2.6E-10	94.62	101.70	131.81	143.80	53.36	58.92	79.70	82.70
Scoc	3.2E-11	21.75	21.33	29.11	32.64	45.81	46.24	64.96	67.80
Gm1673	3.6E-06	16.25	15.90	11.07	10.32	12.13	12.18	8.86	7.88
Cxx1a	1.9E-03	13.45	14.34	10.50	9.55	5.35	5.87	4.18	3.46
Pabpn1	1.9E-05	26.97	26.32	22.00	18.59	27.19	28.62	21.57	16.39

Actn2	4.2E-05	9.77	7.15	5.19	5.85	40.50	30.44	23.09	24.84
Pkdcc	9.9E-08	4.44	4.46	2.81	2.94	12.18	12.56	8.27	8.25
Lpin1	5.1E-09	9.41	10.58	6.62	6.01	60.47	69.78	45.65	39.53
Gltp	6.7E-10	9.55	9.42	6.16	5.75	18.84	19.06	13.04	11.60
Snx22	5.8E-15	84.47	77.71	49.59	45.19	143.40	137.85	95.21	86.22
Gpsm2	2.9E-17	11.83	11.22	6.89	7.54	46.02	44.80	28.60	29.88
Metrn	6.6E-05	9.93	9.41	6.63	6.53	6.68	6.67	4.71	3.83
Dcakd	3.2E-07	14.61	14.77	11.22	11.03	13.46	13.25	9.42	7.66
Hspb6	6.1E-08	10.47	9.55	6.45	5.18	16.02	15.00	10.59	8.11
Rpl13	4.4E-03	324.30	322.71	272.34	193.35	10.42	9.58	7.85	4.11
Rpl17	6.3E-05	301.66	313.13	308.69	330.10	37.41	40.14	27.48	15.80
Hspb1	1.1E-07	407.78	514.32	275.58	214.61	217.58	280.36	156.66	109.76
Aarsd1	3.4E-03	12.39	11.70	9.32	9.57	1.62	1.54	0.69	0.93
Avp	6.2E-13	14.15	12.07	6.40	5.78	9.17	8.02	4.42	3.83

IACUC APPROVAL

University of Delaware
Institutional Animal Care and Use Committee
Request to Amend an Animal Use Protocol

RECEIVED
MAY 20 2014
IACUC CK

Title of Protocol: Investigate the function of genes associated with animal development using mouse and chicken	
AUP Number: 1226-2014-A	**← (4 digits only)**
Principal Investigator: Salil A. Lachke	

Requested Changes

I am requesting a change to: ***(Check all that apply)***

- ☐ Animal Species *(Complete Section 1)*
- ☒ Animal Numbers *(Complete Section 2)*
- ☐ Animal Procedures *(Complete Section 3)*
- ☐ Therapeutic or Experimental Agents *(Complete Section 4)*
- ☐ Pain Category *(Complete Section 5)*
- ☐ Use of Biological Material, Hazardous Agents or Radiation *(Complete Sections 4 & 6)*
- ☐ Other *(Specify)* Click here to enter text.

(Complete Section 7)

Changes MUST NOT be initiated until IACUC approval is granted

Official Use Only

IACUC Approval Signature: Glenn Tallman, DVM

Date of Approval: 5/29/2014